行政院國家科學委員會專題研究計畫　成果報告

以具基因特異性之蛋白體學方法研究訊息傳導

計畫類別：個別型計畫
計畫編號：NSC92-3112-B-002-003-
執行期間：92 年 05 月 01 日至 93 年 04 月 30 日
執行單位：國立臺灣大學醫學院臨床醫學研究所

計畫主持人：周祖述

報告類型：完整報告
報告附件：出席國際會議研究心得報告及發表論文
處理方式：本計畫可公開查詢

中　華　民　國 93 年 9 月 4 日

TABLE OF CONTENTS

Progress Report

1. Response to previous reviewers' critiques

Please describe the previous reviewers' critiques and how based on the critiques, you made modifications to specific aims, experimental design, or resource allocation etc.

1) In aim1, Dr. Jou propose to use the dual regulatory expressing system (Ecdysone and tetracycline inducible system) ……using constitutively active Rac1 and dominant negative IkB as a study pair. This aim is well thought through, and several alternative approaches were described. One minor comment is that the limitation of 2-D gel is not discussed, and the new ICAT and /or 2-D LC system is not mentioned as alternative approaches.

We have set up a collaboration with Dr. Chung-Lin Liao in Academia Sinica using ICAT as an alternative approach to 2DGE for identifying candidates in relaying the signaling from Rac1 to NFkB (please see the following section).

2) In aim 2, Dr. Jou proposed to construct stable cell lines,…… However, it is hard to know whether these candidates are biologically relevant. This is an intrinsic problem for all proteomic approaches.

With those candidate genes identified by microarray assay, we would then use quantitative RT-PCR and Western blotting analysis to confirm the roles they play in Rho family proteins signaling.

3) and 4) In aim 3, Dr. Jou proposed to perform proteomic approaches to discover target molecules linking RhoA family small GTPases after differentially expressing RhoA/Rac1/Cdc42 mutant genes….. With very good controls and carefully designed experiments, he should be able to produce very interesting results. In aim 4, Dr. Jou proposed to apply these systems to study medically important issues. ……..

These arms of the project is still undergoing.

2. Specific Aims

Our primary goal, which has not been modified so far, is to generate double inducible gene expression system in a simplistic and efficient way, and apply this system for dissecting signalling transduction pathways involving Ras related small GTPases using experimental approaches, such as DNA microarray and proteomic studies, based upon comparison of global differences in gene expression profiles.

Specific Aim I. Using the dual regulatory expressing system (Ecdysone and tetracycline inducible system) already set up in HEK293 cell lines to demonstrate the feasibility of conjugating this double regulated expression system with proteomic studies for dissecting complex signalling transduction pathways; using constitutively active Rac1 and dominant negative IkB as a study pair.

We would like to catagorize the downstream signaling molecules of Rac1, according to the global gene expression patterns, into three groups:
Group X- molecules downstream of Rac1and upstream of NFkB
Group Y- molecules downstream of NFkB and further downstream of Rac1
Group Z- molecules downstream of Rac1and unrelated to NFkB signaling pathway

Specific Aim II. Construct stable cell lines, using inducible expression systems set up in MDCK cells, expressing candidate genes identified during the experimental approaches aimed at specific aim I to confirm the finding and also explore the relevant biological meaning

Specific Aim III. Performing proteomic approaches to discover target molecules linking RhoA family small GTPases after differentially expressing RhoA/Rac1/Cdc42 mutant genes in either dual regulatory HEK293 or MDCK cells.

Specific Aim IV. Apply the achievement that would be made to characterize genes involved in hepatocellular oncogensis after successfully carrying out the researches mentioned for specific aim I to III.

> **Specific Aim IV(A).** Construct dual regulatory cell lines in differentiated rat liver cell line, WB, and transformed hepatic cell line, such as HepG2, Hep3B, and Huh7.
>
> **Specific Aim IV(B).** Generate stable cell lines expressing viral genes or other oncogenesis-related candidate genes in cell line set up under Specific Aim IV (A), and then apply comparative proteomic studies to dissect the signalling pathways leading to hepato-oncogenesis .

3. Progress Summary

To pursue **specific aim 1** of our proposal, we had used the following three different approaches in the past 8 months:

(a) **Two-dimensional gel electrophoresis (2-DGE) analysis**- both
(1a) conventional and
(1b) DIGE (Difference Gel Electrophoresis), which is using the commercially available CyDye system (Amersham/Pharmacia) to differentially label different protein samples, to resolve our samples in gel.

(b) **Isotope-Coded Affinity Tag (ICAT) technique**- a collaboration between Dr. Chung-Lin Liao's group in the Institute of Chemistry in the Academia Sinica.

(c) DNA Microarray analysis

Before we present our data in the later section, we would like to first define our experimental settings and use **E1~E4** as the abbreviations to facilitate communication.

The lysates or mRNAs from HEK293 cells differentially expressing either constitutive Rac1 (Rac1V12) or dominant negative IkB(IkB-DN) mutant were collected in the following settings:

Experimental condition 1 (**E1**)- neither Rac1V12 nor IkB-DN was expressed (**Basal condition**)
Experimental condition 2 (**E2**)- Only Rac1V12 was induced (**all group X, Y, and Z protein expressions should be elicited**)
Experimental condition 4 (**E4**)- Both Rac1V12 and IkB-DN were expressed (**group Y proteins should return to near basal condition, group Z should not be affected, while group X proteins might be further changed**)
Experimental condition (E3) was not performed, because it was not related to our goal, in which only IkB-DN was expressed, and therefore group Y proteins might be down-regulated.

Two-dimensional gel electrophoresis (2-DGE) analysis

While we were using the conventional 2DGE to resolve the protein lysates from experimental condition 1, 2, and 4 (**E1, E2, and E4**), we met some problems at first including inadequate sonication of the cell pellets or inadequate use of protease inhibitors, just to name a few of them. We eventually solved out what would be the most optimal condition to get the proteins well separated on 2D gel and stained by Sybro Ruby staining for protein quantification (Fig. 1).

In the meantime, we also tried the DIGE system advocated by Amersham/Pharmacia. Although we could see many differentially labeled spots on the gels, but many are just artifacts caused by so-called reflection errors (the single arrows in Fig. 2A, 2B, and 2C), which are characterized by the double-vision like, vertically overlapped images. We noticed they were happening no matter which combination of protein samples were subjected for the DIGE analysis. There were also some other types of differentially labeled spots visible on the gel, which were well separated and horizontally arranged (the double arrows in Fig. 2A, 2B, and 2C). Initially, we thought these might be the ones which we sought to pursue. However, we found they were still happening without any correlation to the ways how protein samples were combined; i.e., no matter whether Rac1V12 or dominant negative IkB was induced or not, they were there. Furthermore, we also found if we expressed different pair of transgenes, such as Rac1V12 and RhoAV14, they were still there with the same kind of labeling pattern (data not shown). We were puzzled by this finding and decided to isolate the protein spots for mass spectrometrical analysis to make sure the identities of those mysterious proteins.

Due to the intrinsic problems associated with DIGE, we decided to take conventional approach for 2DGE despite it is tedious and challenging to get three gels (E1, E2, and E4 on three separate gels) run at the same condition. Nevertheless, we did catagorize the differential expression pattern under these three different conditions (E1, E2, and E4) into group X, Y, and Z patterns. The examples are given in Fig. 3.

We have so far identified 7, 7, and 5 spots with group X, Y, and Z expression patterns, respectively, and would be analyzed by MS them when we get enough proteins.

Isotope-Coded Affinity Tag (ICAT) technique

Collaborating with Dr. Chung-Lin Liao in the Institute of Chemistry, Academia Sinica (Genomics/Proteomics Center), we also had our protein samples undergo ICAT approach. Dr. Liao developed a new ICAT reagent, which labels the NH2- group, instead of SH-group, of proteins. This results in higher chance of labeling in proteins containing few cysteines. After trypsinization of the protein samples prepared in E1, E2, and E4 conditions, the peptides were differentially labeled with hydrogen (D0, light) or deuterium (D4, heavy) containing reagents, and undergoing multiple dimensional liquid chromatography (MDLC) and MS analysis. Initial protein identification revealed about one thousand proteins in the samples, and further manual MS spectrum inspection, which took totally three weeks' effort because there was no commercially available software could reliably substitute this part of work, confirmed about 200 peptide pairs between E1/E2 and E2/E4 experimental conditions. A selective list of proteins and their quantification ratios in E2/E1 and E4/E2 conditions are shown in **Table 1** and **Table 2**.

So far, we haven't identified a protein significantly increasing in E2 vs. E1 conditions, and also in E4 vs. E2 conditions. Our hypothesis for this phenomenon would be discussed later after we presented the data from our microarray analysis.

DNA Microarray analysis

We initially performed microarray assays at our own lab using the protocol and DNA arrays from the Third Core Laboratory in National Taiwan University Hospital, which is also sponsored by the
National Research Program in Genomic Medicine. However, we got inconsistent data which were difficult to analyze. Later, we shifted to glass type DNA array using fluorescent probe instead of alkaline phosphatase based colorimetric probe. We think we have finally got much more reliable data (Table 3A-C) because we could identify Rac1, the transgene regulated by the tetracycline inducible system, gene up-regulated in experimental condition E2 vs. E1, and the Rac1 mRNA level is the same between experimental condition E2 and E4 (group Z expression pattern in Table 3C). Furthermore, after we used several algorithms to analyze the expression pattern we got, we could get pretty nice clustering of the gene expression patterns (Fig. 4A and 4B).

There are many interesting genes and expression patterns from the microarray assay. Taking the genes classified as group X expression pattern for examples, **ARRH (RhoH)** is an atypical Rho family GTPase, which doesn't have endogenous GTPase activity and is demonstrated to have a dominant negative effect of the endogenous RhoA protein. It has been previously hypothesized that Rac1 has an antagoisitic effect on RhoA, but the detailed mechanism has been elusive. If RhoH is activated by Rac1, which might be the reason why Rac1 activation might downregulate RhoA activity.

Another gene belonging to group X expression pattern, **FNBP1 (formin binding protein 1)**, has been demonstrated to be a Cdc42 interacting partner and a GEF for Cdc42. This protein may act as a link between cdc42 signaling and regulation of the actin cytoskeleton. If FNBP1 is transcriptionally regulated by Rac1, this could provide a mechanistic basis for the interaction between Rac1 and Cdc42 on actin cytoskeleton.

Mismatch between the data from microarray and ICAT assays, and the possible solutions to reconcile these differences in the future

Although we are satisfied with the result coming out of microarray assay, the protein expression patterns between the result from microarray do not match with each other. Our explanation is that we overload the MS capacity with a protein sample of very high complexity. The ICAT reagent we used is different from the conventional one in that the former doesn't contain biotin modification and we therefore do not enrich the ICAT labeled tryptic peptides with streptavidin beads. Basically, all the proteins, after trypsin digestion, are entering the MDLC-MS analysis, and it is very likely that the MS spectra of low abundance proteins are masked by those of high abundance proteins. If the expression products of those genes identified by microarray are low in abundance, it is very likely they could be missed from our current ICAT assay.

To solve this problem, we are planning to fractionate our protein samples first into membranous, microsomal, cytosolic, nuclear, and cytoskeletal compartments, followed by reverse phase LC separation of the protein samples of each sub-fractionation before going to the ICAT procedure. Preliminary data from Dr. Liao's group show this might be helpful in decreasing the complexity of proteins going into the ICAT analysis.

In the meantime, we are going to isolate the protein complex by immunoprecipitating either the myc-epitope tagged Rac1V12 or the inhibitor of nuclear factor kappa B (IkB) under experimental conditions differentially expressing constitutively active Rac1V12 or dominant negative IkB. We hypothesize the associated signaling molecules to either Rac1V12 IkB would be different when the signaling pathways are manipulated by Rac1 and IkB mutant proteins. This might sound a desperate approach, but could be easily tested.

Specific Aim II. Construct stable cell lines, using inducible expression systems set up in MDCK cells, expressing candidate genes identified during the experimental approaches aimed at specific aim I to confirm the finding and also explore the relevant biological meaning

This part of the project awaits the identities of those candidate genes being disclosed after experiments related to **Specific Aim I** would be completed.

Specific Aim III. Performing proteomic approaches to discover target molecules linking RhoA family small GTPases after differentially expressing RhoA/Rac1/Cdc42 mutant genes in either dual regulatory HEK293 or MDCK cells.

To search for possible connections between different members of Rho family GTPases, we have focused in the past one year on the connections between Cdc42 and Rac1. We had then demonstrated a signaling cascade ignaling cascade **Cdc42 → Rac1 → PI3K** in modulating detachment induced apoptosis (anoikis). This part of work has been written up as a submitted manuscript, and now the manuscript has been revised and re-evaluated by *Experimental Cell Research* (please refer to the manuscript attached in appendix 2).

Specific Aim IV(A). Construct dual regulatory cell lines in differentiated rat liver cell line, WB, and transformed hepatic cell line, such as HepG2, Hep3B, and Huh7.

We have so far generated Tetracycline inducible expression system in three of the above three cell lines, using the strategy we have recently published (Am J Physiol Cell Physiol 2003; 285:C711-719). Taking the Huh7 cell line as example, after three rounds of positive FACS based selection and one round of negative selection, we have enriched inducible clones with an inducibility of about **100 folds**.

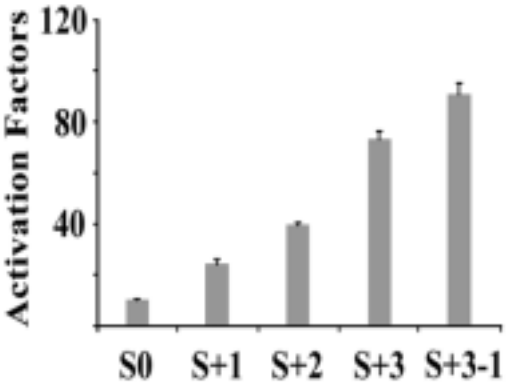

For HepG2 and Hep3B, after similar approaches, we have inducible cell populations with inducibility of about **60** and **80 folds**.

As for the differentiated WB cell line, we would conduct similar selection scheme very soon. Once we finish establishing tetraycline controlled expression system in all these four cell lines, we would set up ecdysone inducible expression system in them to complete the making of dual regulatory expression systems in four cell lines.

While we were generating the dual regulatory expression system, we accidentally found doxycycline, previously thought to be an inert chemical compound, might differentially regulate the expression level of reverse type tetracycline regulated tranactivator (rtTA). We studied the mechanistic basis of this phenomenon and wrote up a manuscript which had been submitted to *Journal of Gene Medicine* (please appendix 3).

Table 1 **Proteins identified to be up-regulated in E2 vs E1 condition by ICAT analysis**

Mascot No.	Accession No.	Protein Name	E2/E1
23	gi|4885375	H1 histone family, member 2; histone H1d [Homo sapiens]	1.541
373	gi|27498927	similar to CG5882-PA [Homo sapiens]	1.474
422	gi|4506583	replication protein A1, 70kDa; replication protein A1 (70kD) [Homo sapiens]	1.429
396	gi|37538778	similar to dJ753D5.2 (novel protein similar to RPS17 (40S ribosomal protein S17)) [Homo sapiens]	1.426
186	gi|444021	sub2.3 [Homo sapiens]	1.409
947	gi|6424942	ALG-2 interacting protein 1 [Homo sapiens]	1.397
506	gi|243123	cytochrome c oxidase subunit VIIa='liver-type' isoform {EC 1.9.3.1} [human, skeletal muscle, Peptid	1.394
360	gi|4506681	ribosomal protein S11; 40S ribosomal protein S11 [Homo sapiens]	1.383
559	gi|9022435	ribosomal protein S3; RPS3 [Homo sapiens]	1.378
233	gi|6841566	HSPC173 [Homo sapiens]	1.370
448	gi|4757900	calreticulin precursor; Sicca syndrome antigen A (autoantigen Ro; calreticulin); autoantigen Ro [Ho	1.370
474	gi|5032087	splicing factor 3a, subunit 1, 120kDa; pre-mRNA splicing factor SF3a (120 kDa subunit) [Homo sapien	1.336
471	gi|36142	ribosomal protein homologous to yeast S24 [Homo sapiens]	1.335
230	gi|478813	nonhistone chromosomal protein HMG-1 - human	1.318
183	gi|14250148	Ribosomal protein L3 [Homo sapiens]	1.313
8	gi|1136741	KIAA0002 [Homo sapiens]	1.298
623	gi|5901922	CDC37 homolog [Homo sapiens]	1.293
122	gi|2136253	TCP1 ring complex protein TRiC5 - human	1.281
194	gi|1203969	filamin [Homo sapiens]	1.278
46	gi|4507677	tumor rejection antigen (gp96) 1; Tumor rejection antigen-1 (gp96); glucose regulated protein, 94 k	1.276
28	gi|28614	aldolase A [Homo sapiens]	1.273
295	gi|178663	medium tumor antigen-associated 61-kD protein	1.272
84	gi|7433799	fatty-acid synthase (EC 2.3.1.85) (version 2) - human	1.267
75	gi|115206	C-1-tetrahydrofolate synthase, cytoplasmic (C1-THF synthase) [Includes: Methylenetetrahydrofolate d	1.262
192	gi|423123	tpr protein - human	1.250
141	gi|553640	ribosomal protein S13 [Homo sapiens]	1.249
539	gi|20987810	MRPS27 protein [Homo sapiens]	1.214
18	gi|5174735	tubulin, beta, 2 [Homo sapiens]	1.213
147	gi|5174447	guanine nucleotide binding protein (G protein), beta polypeptide 2-like 1; protein homologous to ch	1.206

Table 2 **Proteins identified to be up-regulated in E4 vs E2 condition by ICAT analysis**

Mascot No.	Accession No.	Protein Name	4H/2L ratio
102	gi|37542903	similar to 60 kDa heat shock protein, mitochondrial precursor (Hsp60) (60 kDa chaperonin) (CPN60) (	8.29
350	gi|37538336	KIAA1856 protein [Homo sapiens]	2.99
1090	gi|14591909	ribosomal protein L5; 60S ribosomal protein L5 [Homo sapiens]	1.33
59	gi|4758756	nucleosome assembly protein 1-like 1; HSP22-like protein interacting protein; NAP-1 related protein	1.31
469	gi|2135244	chromosome segregation protein smc1 [similarity] - human	1.28
62	gi|6005854	repressor of estrogen receptor activity; B-cell associated protein [Homo sapiens]	1.22
71	gi|7433799	fatty-acid synthase (EC 2.3.1.85) (version 2) - human	1.21
589	gi|4884564	vitamin D3 receptor interacting protein [Homo sapiens]	1.21
41	gi|180555	creatine kinase-B	1.19
93	gi|105294	alternative splicing factor ASF-2 - human	1.18
142	gi|20521660	KIAA0788 protein [Homo sapiens]	1.14
186	gi|438069	thiol-specific antioxidant protein [Homo sapiens]	1.14
177	gi|2559008	chaperonin containing t-complex polypeptide 1, delta subunit; CCT-delta [Homo sapiens]	1.10
79	gi|4503297	DEAH (Asp-Glu-Ala-His) box polypeptide 9 isoform 1; DEAD/H (Asp-Glu-Ala-Asp/His) box polypeptide 9	1.08
90	gi|4506607	ribosomal protein L18; 60S ribosomal protein L18 [Homo sapiens]	1.07
513	gi|8923579	hypothetical protein FLJ20625 [Homo sapiens]	1.07
805	gi|4759196	symplekin [Homo sapiens]	1.06
841	gi|25136577	ELYS transcription factor-like protein TMBS62 [Homo sapiens]	1.04
96	gi|4506671	ribosomal protein P2; 60S acidic ribosomal protein P2; acidic ribosomal phosphoprotein P2 [Homo sap	1.04
249	gi|4506691	ribosomal protein S16; 40S ribosomal protein S16 [Homo sapiens]	1.02
74	gi|9802306	DNA-binding protein TAXREB107 [Homo sapiens]	1.00
170	gi|5031635	cofilin 1 (non-muscle) [Homo sapiens]	1.00
49	gi|337424	poly(ADP-ribose) synthetase	0.99
8	gi|7106439	tubulin, beta 5 [Mus musculus]	0.99
254	gi|135538	T-complex protein 1, alpha subunit (TCP-1-alpha) (CCT-alpha)	0.99
313	gi|136066	TRIOSEPHOSPHATE ISOMERASE (TIM)	0.99
220	gi|4506209	proteasome 26S ATPase subunit 2; proteasome 26S subunit, ATPase, 2; mammalian suppressor of sgv-1 o	0.98
305	gi|1431788	Chain A, Cyclophilin A Complexed With Cyclosporin A (Nmr, 22 Structures)	0.98
456	gi|36142	ribosomal protein homologous to yeast S24 [Homo sapiens]	0.98
283	gi|18848326	Similar to GDP dissociation inhibitor 2 [Homo sapiens]	0.97

Table 3A. Genes displaying group X expression pattern (expression ratio under E2/E1 experimental conditions is more than 2, while expression ratio under E4/E2 experimental conditions is more than 1.45) by DNA microarray assay

CLID	NAME	E2-E1	E4-E2
IMAGE:704274	transcriptional regulating protein 132	20.549	2.540
IMAGE:1306637	tumor protein D52	2.382	2.227
IMAGE:1285720	formin binding protein 1	2.133	1.925
IMAGE:454475	phosphorylase kinase, alpha 2 (liver)	2.035	1.557
IMAGE:302591	ras homolog gene family, member H	8.846	1.491
IMAGE:1307809	Similar to interferon-gamma receptor alpha chain	2.208	1.467

Table 3B. Genes displaying group Y expression pattern (expression ratio under E2/E1 experimental conditions is more than 2, while expression ratio under E4/E2 experimental conditions is less than 0.5) by DNA microarray assay

CLID	NAME	E2-E1	E4-E2
IMAGE:809901	collagen, type XV, alpha 1	19.213	0.032
IMAGE:789369	inhibitor of DNA binding 4, dominant negative helix-loop-helix protein	8.462	0.083
IMAGE:196992	aldo-keto reductase family 1, member C1	8.369	0.077
IMAGE:1309018	uncharacterized hypothalamus protein HCDASE	7.863	0.062
IMAGE:430038	FYN binding protein (FYB-120/130)	6.797	0.141
IMAGE:669310	mitogen-activated protein kinase-activated protein kinase 5	6.440	0.259
IMAGE:712341	ribonuclease 6 precursor	5.996	0.128
IMAGE:323181	fibroblast activation protein, alpha	5.856	0.241
IMAGE:21655	5'-nucleotidase, ecto (CD73)	5.680	0.181
IMAGE:223176	MAX dimerization protein 1	5.389	0.206
IMAGE:2477598	secretory leukocyte protease inhibitor	5.216	0.499
IMAGE:1271368	SH3-domain binding protein 1	4.803	0.368
IMAGE:784928	sushi-repeat protein	4.721	0.372
IMAGE:461727	phenylalanine hydroxylase	4.624	0.151
IMAGE:1302646	chromosome 13 open reading frame 9	4.579	0.363
IMAGE:814251	signaling lymphocytic activation molecule family member 1	4.569	0.460
IMAGE:753346	aminolevulinate, delta-, synthase 2	4.341	0.477
IMAGE:1240974	Rho GDP dissociation inhibitor (GDI) beta	4.284	0.360
IMAGE:2448778	cathepsin F	4.067	0.265
IMAGE:2508044	haptoglobin	4.059	0.241
IMAGE:1287536	zinc finger protein, subfamily 1A, 1 (Ikaros)	4.006	0.250
IMAGE:1470151	GRB2-associated binding protein 2	3.926	0.168

Table 3B. Continued

CLID	NAME	E2-E1	E4-E2
IMAGE:74537	alpha-fetoprotein	3.880	0.208
IMAGE:204541	asialoglycoprotein receptor 1	3.853	0.266
IMAGE:685022	diacylglycerol kinase, epsilon 64kDa	3.829	0.395
IMAGE:712278	c-fos	3.769	0.245
IMAGE:428083	basic transcription factor 2	3.630	0.368
IMAGE:487418	filamin A, alpha (actin binding protein 280)	3.620	0.274
IMAGE:2028959	dopa decarboxylase (aromatic L-amino acid decarboxylase)	3.615	0.371
IMAGE:1335809	hypoxia-inducible factor 1, alpha subunit	3.470	0.394
IMAGE:243174	serine (or cysteine) proteinase inhibitor, clade F (alpha-2 antiplasmin member 2	3.425	0.392
IMAGE:2353365	deoxyribonuclease I-like 1	3.371	0.290
IMAGE:704815	Inhibitor of DNA binding 2	3.274	0.239
IMAGE:70692	serine (or cysteine) proteinase inhibitor, clade B (ovalbumin)	3.182	0.247
IMAGE:284022	Rho guanine nucleotide exchange factor (GEF) 10	3.141	0.423
IMAGE:565319	mal, T-cell differentiation protein 2	3.076	0.301
IMAGE:324492	matrix metalloproteinase 3	3.072	0.433
IMAGE:612576	3-oxoacid CoA transferase	3.055	0.402
IMAGE:2449395	aldo-keto reductase family 1, member C2	3.044	0.310
IMAGE:825645	activation-induced cytidine deaminase	3.013	0.392
IMAGE:1534853	centaurin, beta 1	3.008	0.394
IMAGE:325145	pentaxin-related gene, rapidly induced by IL-1 beta	2.932	0.456
IMAGE:2449786	tumor necrosis factor receptor superfamily, member 18	2.882	0.393
IMAGE:50604	**androgen-induced 1	2.834	0.425
IMAGE:1241180	zinc finger protein, subfamily 1A, 1 (Ikaros)	2.670	0.299
IMAGE:1334310	CGI-109 protein	2.661	0.332
IMAGE:50503	integrin, beta 2	2.650	0.232
IMAGE:840844	heat shock 70kDa protein 5	2.623	0.264
IMAGE:1656636	UDP glycosyltransferase 2 family, polypeptide B4	2.583	0.312
IMAGE:704084	centaurin, delta 1	2.567	0.341
IMAGE:487429	collagen, type VI, alpha 1	2.491	0.271
IMAGE:212188	apolipoprotein H (beta-2-glycoprotein I)	2.485	0.283
IMAGE:1306275	mutL homolog 3 (E. coli)	2.224	0.328
IMAGE:2298080	kynureninase (L-kynurenine hydrolase)	2.213	0.345
IMAGE:1681489	serine (or cysteine) proteinase inhibitor, clade E (nexin, plasminogen activator inhibitor type 1), member 1	2.210	0.326
IMAGE:31093	cadherin 13, H-cadherin (heart)	2.155	0.205
IMAGE:1241157	tripartite motif-containing 22	2.151	0.338
IMAGE:668182	zinc finger protein 193	2.120	0.326
IMAGE:768443	microsomal glutathione S-transferase 1	2.104	0.326
IMAGE:2458975	inhibin, beta A (activin A, activin AB alpha polypeptide)	2.089	0.227

Table 3C. Genes displaying group Z expression pattern (expression ratio under E2/E1 experimental conditions is more than 2, while expression ratio under E4/E2 experimental conditions is between 0.5 and 1.45) by DNA microarray assay

CLID	NAME	E2-E1	E4-E2
IMAGE:1369976	ecotropic viral integration site 2A	9.547	0.564
IMAGE:143523	collagen, type V, alpha 1	5.049	1.438
LCP:138	methionine-tRNA synthetase	4.800	1.217
IMAGE:2117981	47-kD autosomal chronic granulomatous disease protein	4.332	1.250
IMAGE:703774	**mitogen-activated protein kinase 8 interacting protein 3	4.332	0.699
IMAGE:1338277	RAC1	4.190	0.812
IMAGE:2491247	solute carrier family 21 (organic anion transporter), member 9	3.761	0.692
IMAGE:827132	ras-related C3 botulinum toxin substrate 2	3.489	1.426
IMAGE:781105	AHA1, activator of heat shock 90kDa protein ATPase homolog 2 (yeast)	3.437	1.154
IMAGE:825590	xylosyltransferase	3.401	1.301
IMAGE:1307643	phosphatidylinositol transfer protein, membrane-associated 1	3.265	0.529
IMAGE:712279	kelch-like 6 (Drosophila	3.211	0.641
LCP:1	deoxynucleotidyltransferase, terminal	3.180	1.053
IMAGE:284263	myelin-associated oligodendrocyte basic protein	3.134	0.777
IMAGE:1019777	butyrylcholinesterase	3.130	0.851
IMAGE:704154	epidermodysplasia verruciformis 1	3.065	1.113
IMAGE:563574	FSHD region gene 1	2.986	0.527
IMAGE:701572	NADP-dependent retinol dehydrogenase/reductase	2.963	0.923
IMAGE:1184934	purinergic receptor P2Y, G-protein coupled, 8	2.914	0.723
IMAGE:683257	EST from selenoprotein P promoter region	2.866	0.954
IMAGE:358842	runt-related transcription factor 3	2.805	1.171
IMAGE:685210	T-cell activation GTPase activating protein	2.572	1.306
IMAGE:127636	**zuotin related factor 1	2.530	1.281
IMAGE:686274	peptidylprolyl isomerase (cyclophilin)-like 2	2.519	1.163
IMAGE:1543346	transketolase-like 1	2.474	1.221

CLID	NAME	E2-E1	E4-E2
IMAGE:701018	transcription factor Dp-2 (E2F dimerization partner 2)	2.302	1.340
IMAGE:1306711	ceroid-lipofuscinosis, neuronal 6, late infantile, variant	2.299	1.324
IMAGE:260200	myeloid cell nuclear differentiation antigen	2.201	1.401
IMAGE:80915	succinate dehydrogenase complex, subunit A	2.124	1.437
IMAGE:1286006	centrosomal kinesin-like protein	2.108	1.442
IMAGE:1670870	unc-93 homolog B1 (C. elegans)	2.062	1.429

Figure 1

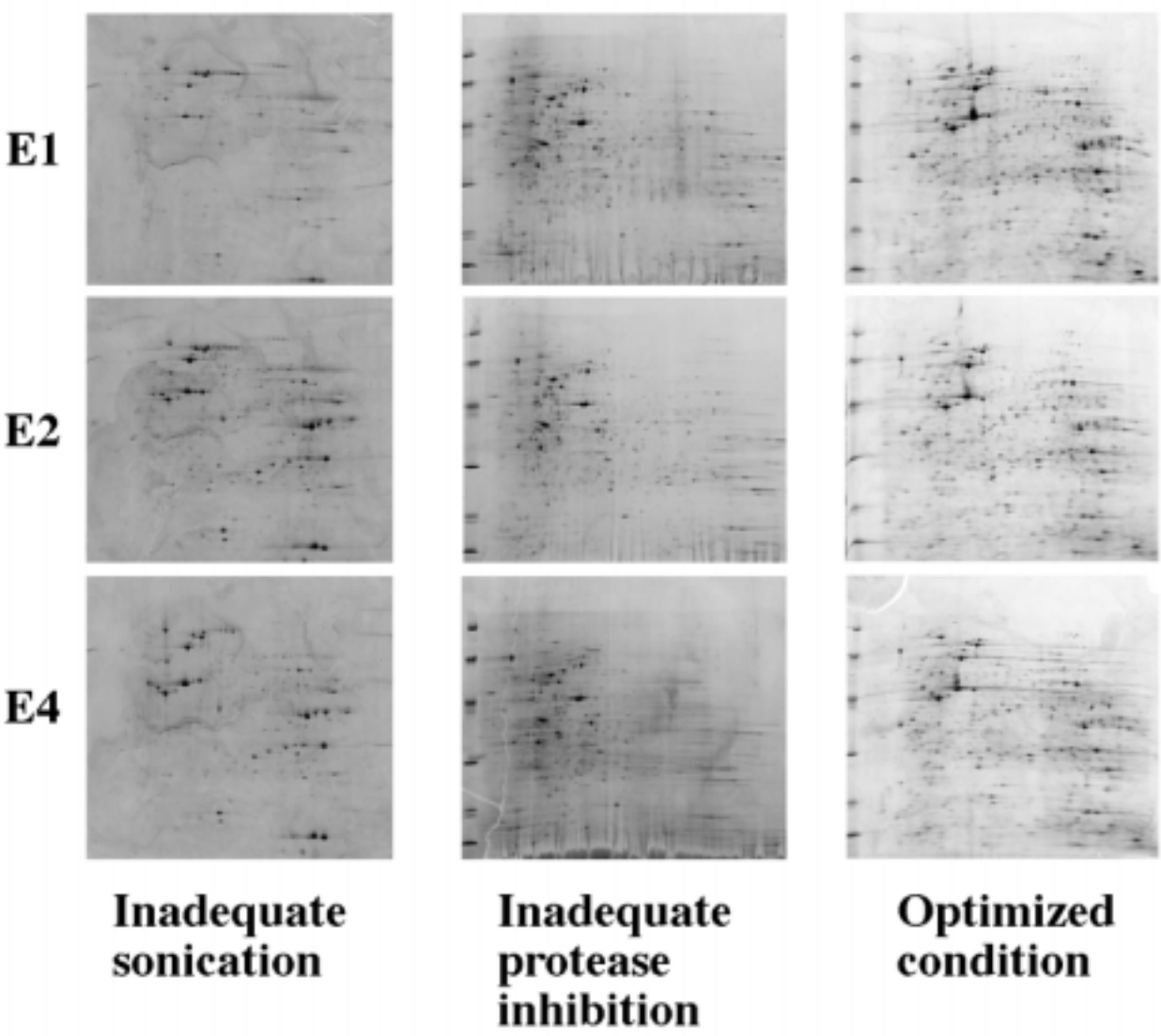
E1
E2
E4
Inadequate sonication
Inadequate protease inhibition
Optimized condition

Figure 2A

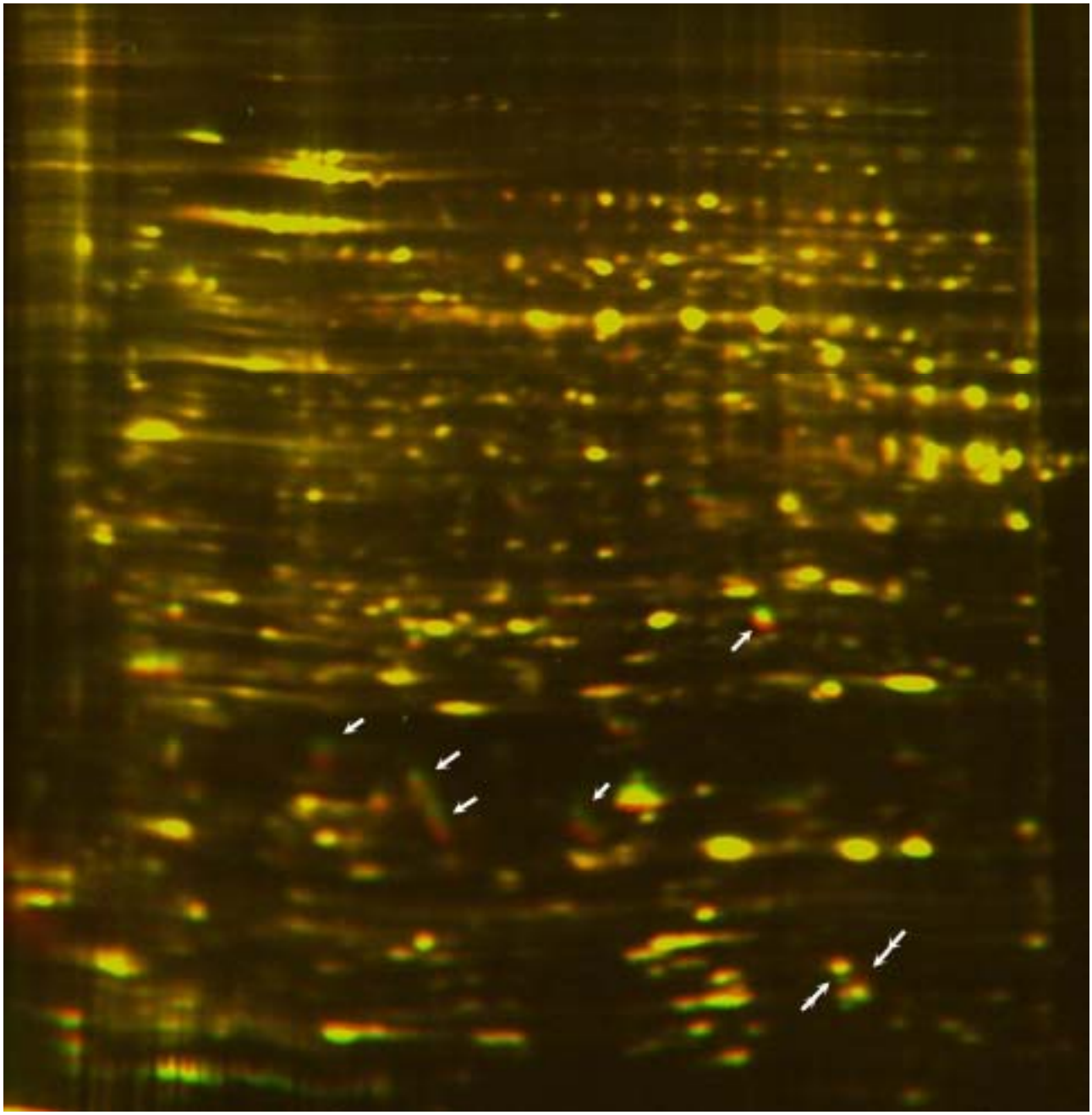

E1 lysate- neither Rac1V12 nor IkB-DN was expressed, labeled in red

E2 lysate- Only Rac1V12 was induced, labeled in green

Figure 2B

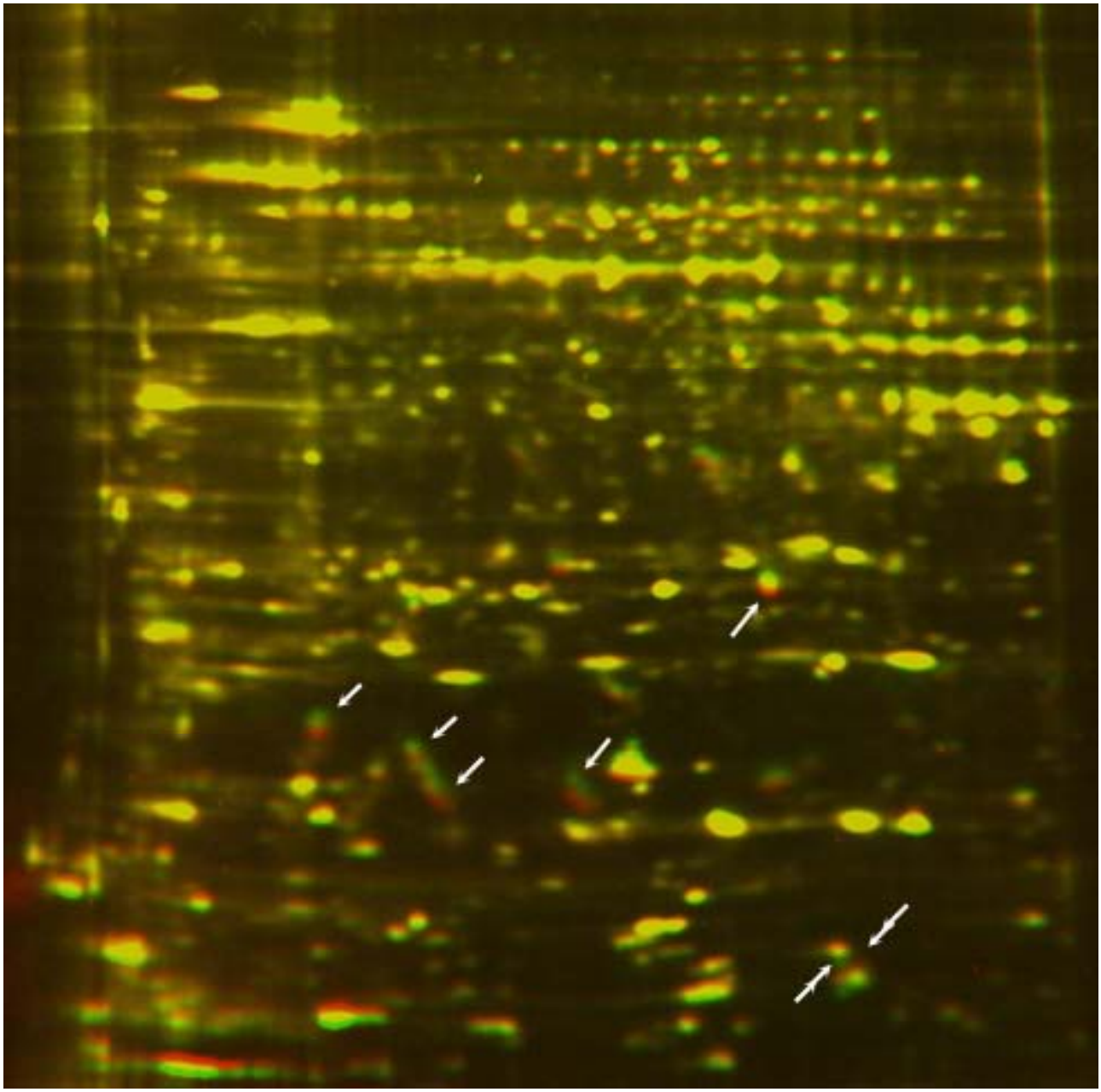

E2 lysate- Only Rac1V12 was induced, labeled in red

E4 lysate- Both Rac1V12 and IkB-DN were expressed, labeled in green

Figure 2C

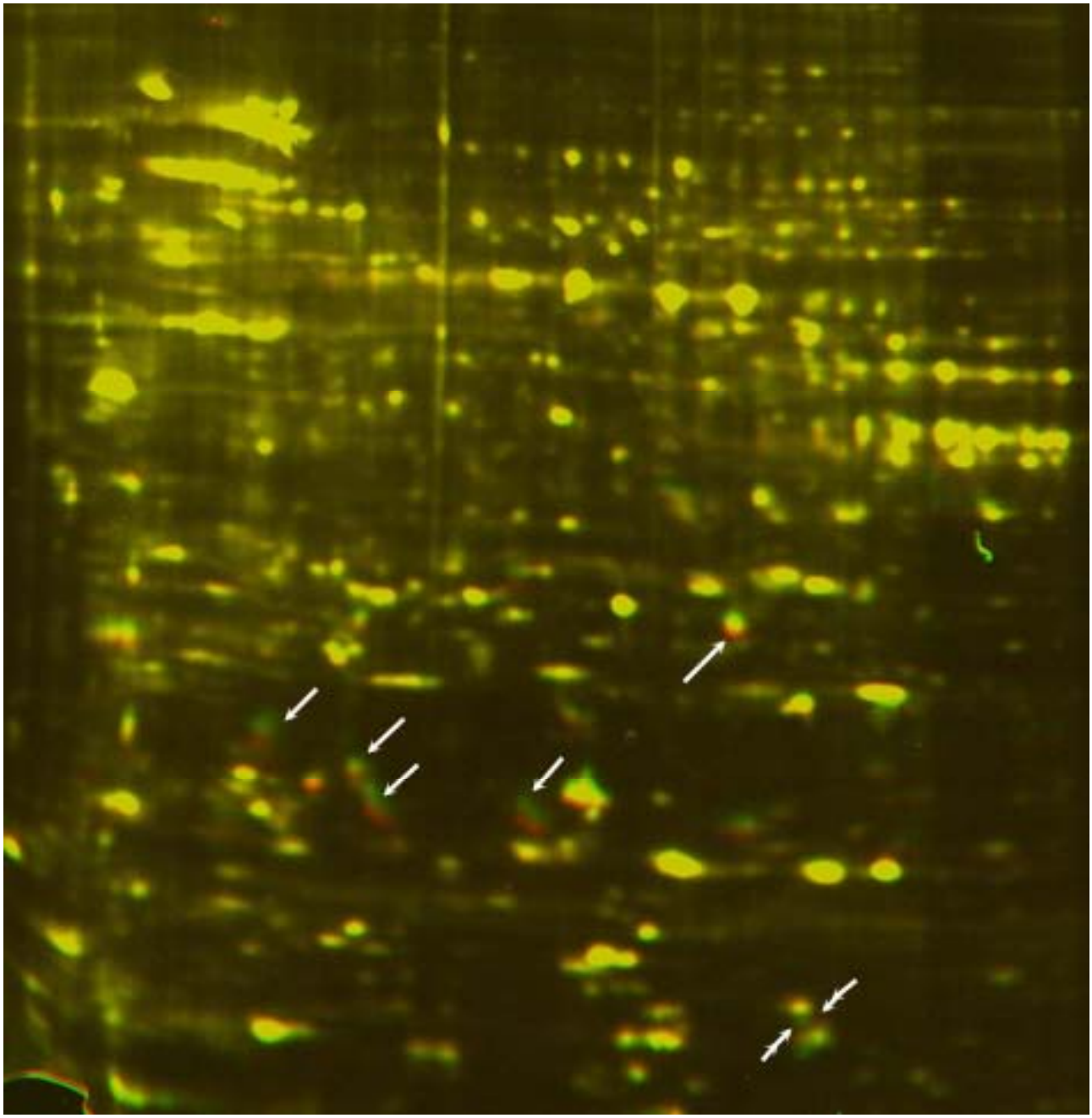

E1 lysate- neither Rac1V12 nor IkB-DN was expressed, labeled in red
E4 lysate- Both Rac1V12 and IkB-DN were expressed, labeled in green

Figure 3 **Examples of differential expression classified as group X, Y, Z expression**

patterns; the left upper quadrant in each composite image shows the quantified intensities of the index spots as a histogram in the order of E1, E2, and E4. The gels were stained with Sybro Ruby stain, scanned by Typhoon 9200 (Amersham/Pharmacia) and quantified by using the PDQuest7.1.1 software (Bio-Rad).

Group X expression pattern

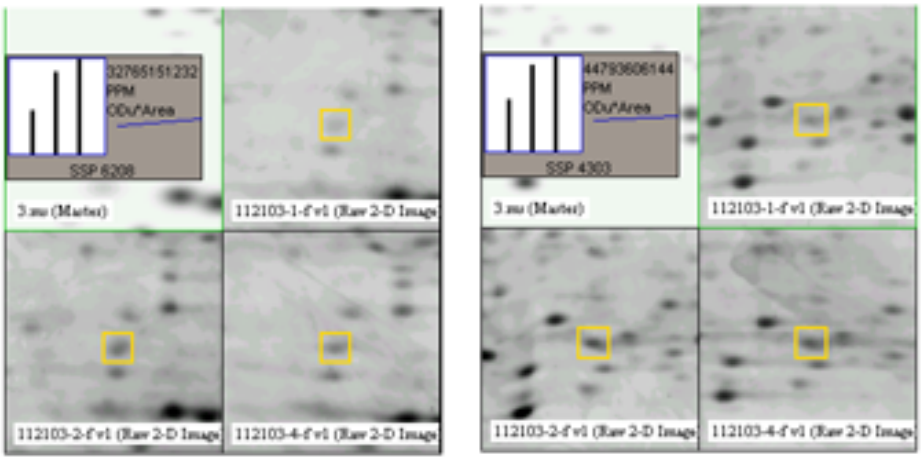

Group Y expression pattern

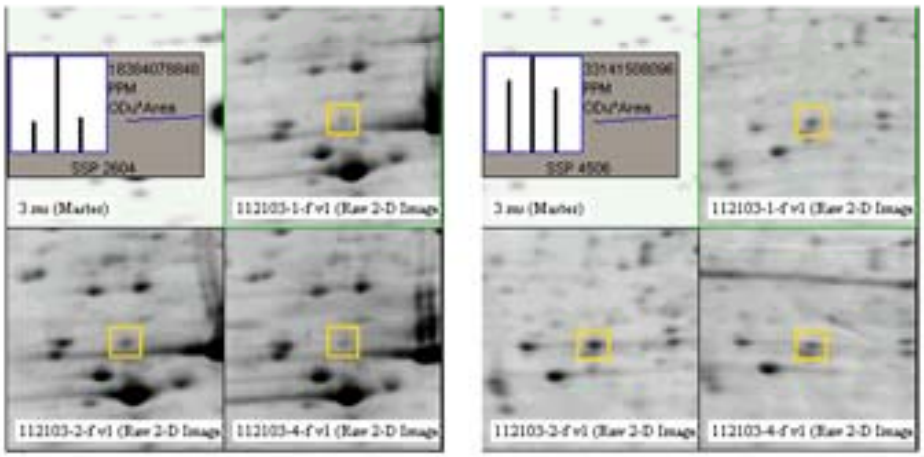

Group Z expression pattern

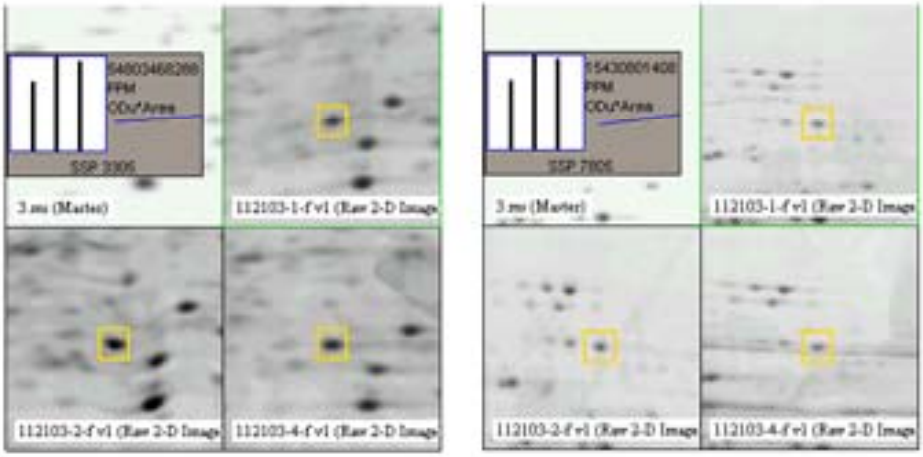

Figure 4A **Hierarchical clustering result of group X (red), Y (green) , and Z (blue) genes.**

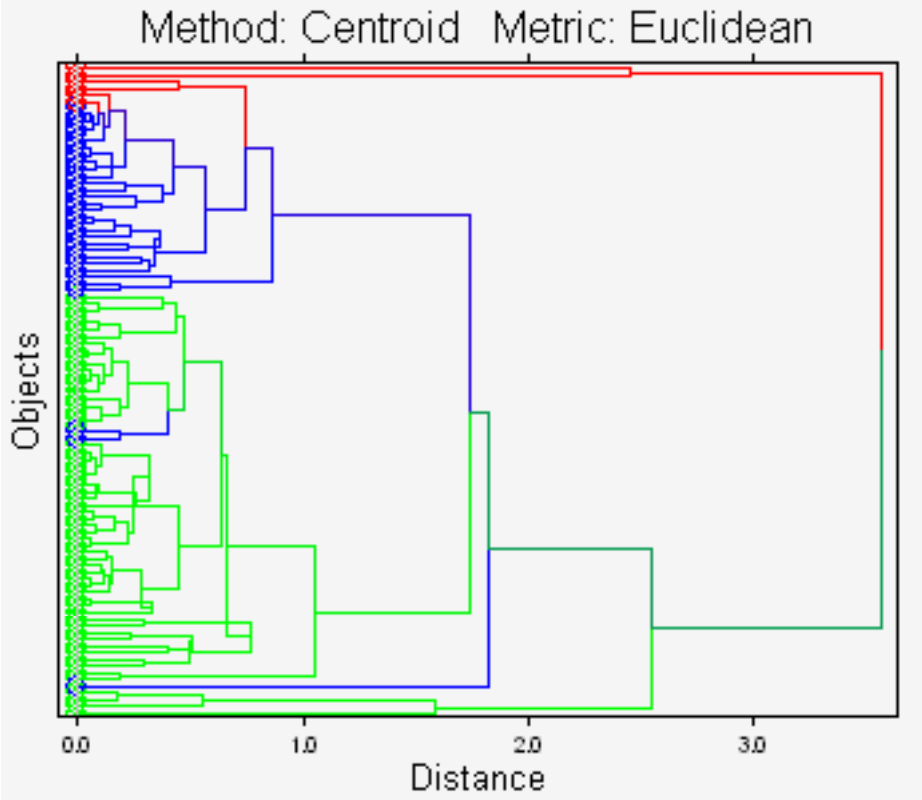

Figure 4B **Non-hierarchical clustering result of group X (yellow), Y (blue), and Z (red) genes.**

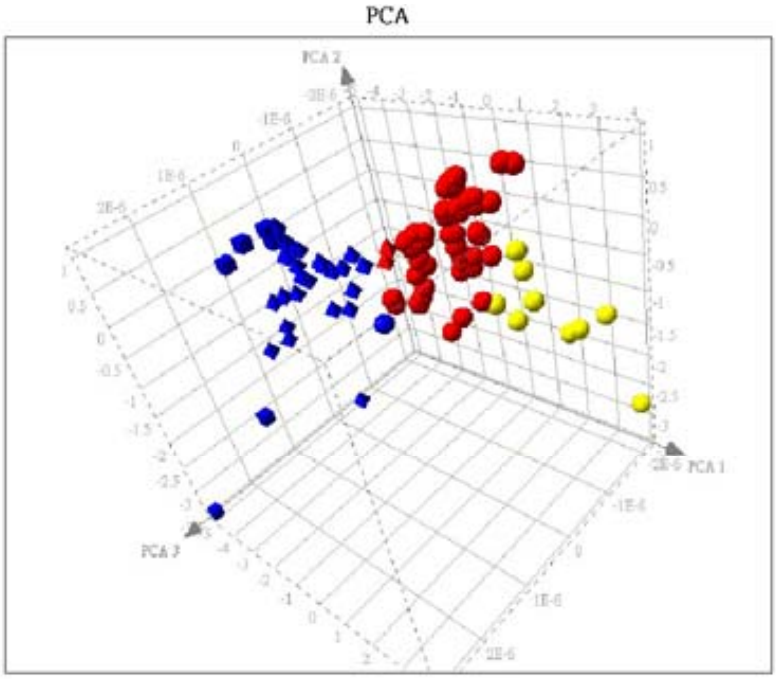

4. Projected Timeline & Brief Summary of Plans for Next Year

Specific Aim I. (From 2004-01-01 to 2004-4-30)

Using the combined approaches by conventional 2DGE, ICAT, and microarray assay to dissect the complex signalling transduction pathways linking constitutively active Rac1 and nuclear factor kappa B (NFkB), we would eventually track down the possible candidates.

As we found the complexity of our protein samples might be too high for the ICAT assay, we plain to sub-fractionate the protein samples according to their distribution in different cellular compartment, and the fractionated protein samples would be further separated by reverse phase liquid chromatography. We would use quantitative real-time RT-PCR and western blotting analysis to confirm the expression patterns of several candidate genes we identified by microarray, notably those involved in Rho family protein signalling, such as RhoH and FNBP1(formin binding protein 1). We also plan to summarize our microarray data in a small methodology paper.

Specific Aim II. (From 2004-5-01 to 2004-08-31)

Construct stable cell lines, using inducible expression systems set up in MDCK cells, expressing candidate genes identified during the experimental approaches aimed at specific aim I to confirm the finding and also explore the relevant biological meaning

Specific Aim III. (From 2004-01-01 to 2004-12-31)

Given the experience we obtained in the past 8 months or so, we think we could start using the combined proteomic and microarray approach to discover target molecules linking Rho family small GTPases after differentially expressing RhoA/Rac1/Cdc42 mutant genes in either dual regulatory HEK293 or MDCK cells. Since we have already written up a manuscript, which is under second revision after being sent to *Experimental Cell Research*, describing the signaling cascade **Cdc42 → Rac1 → PI3K** in modulating detachment-induced apoptosis (anoikis) (please refer to the manuscript in appendix 2). We would propably start from the constitutively active Cdc42 and dominant negative Rac1 double mutant cells first.

Specific Aim IV. (From 2004-01-01 to 2004-06-30)

Specific Aim IV(A). Finish constructing dual regulatory cell lines in differentiated rat liver cell line and transformed hepatic cell line, such as HepG2, Hep3B, and Huh7.

5. Personnel

Summarize the **personnel involved in the project during the grant period**. List the personnel in accordance to the following categories: (1) senior investigators, including visitors; (2) postdoctoral fellows; (3) graduate students; (4) technicians or research assistants. Specify for each individual the period of involvement and the percentage commitment of effort.

Name		Position Title	Education Degree	% of personal effort on this project	Job Description or Responsibilities
In Chinese	In English				
周祖述	Tzuu-Shuh Jou	Assistant Professor (Principal Investigator)	MD;Ph.D	50% (with another NSC sponsored project at hand)	Coordinating the works and planning the experiments associated with this project Writing proposals, manuscripts, and rebuttals for the publication
鄭子琳	Tzu-Ling Cheng	1st year technician	Master degree	100%	DNA plasmid constrtuction, Cell Culturing, and Making stable clones . cell biology and biochemical assay; carrying the project related to the submitted paper No-1
鄭心遠	Hsin-Yuan Cheng	1st year technician	Master degree	100%	cell biology and biochemical assay; carrying the project related to the submitted paper No-2
蔡舒聿	Su-Yu Tsai	1st year technician	Master degree	100%	Protein extraction, Running 2D gel FACS sorting
林育誼	Yu-Yi Lin	3rd Year Resident in internal medicine	M.D.	50%	Microarray assay and data analysis

6. Publications and/or Patents

6a. Publications

List the title and complete references (author(s), journal or book, year, page number) of all publications **directly resulting from studies supported by the project (i.e., with citation of this grant in the acknowledgement section)**. List the publications for the project in accordance to the following categories: (1) manuscripts published and accepted for publications; (2) manuscripts submitted; and (3) conference proceedings. Provide one copy of each publication not previously reported to the National Science Council in the Appendix.

1.

Lai JF, Juang SH, Hung YM, Cheng HY, Cheng TL, Mostov KE, Jou TS. Related Articles, Links

An ecdysone and tetracycline dual regulatory expression system for studies on Rac1 small GTPase-mediated signaling.
Am J Physiol Cell Physiol. 2003 Sep;285(3):C711-9. Epub 2003 May 07.

2. Tzu-Ling Cheng, Marc Symons, Tzuu-Shuh Jou

Regulation of Anoikis by Cdc42 and Rac1

(Submitted to Experimental Cell Research, revised and resubmitted)

3. Jen-Feng Lai, Hsin-Yuan Cheng, Tzu-Ling Cheng, Yu-Yu Lin, Li-Chieh Chen, Mau-Ting Lin, Tzuu-Shuh Jou

Doxycycline and Tetracycline Regulated Transcriptional Silencer Enhance the Expression Level and Transactivating Performance of rtTA

(Submitted to Journal of Gene Medicine).

Appendix 1

Lai JF, Juang SH, Hung YM, Cheng HY, Cheng TL, Mostov KE, Jou TS. An ecdysone and tetracycline dual regulatory expression system for studies on Rac1 small GTPase-mediated signaling. Am J Physiol Cell Physiol. 2003 Sep;285(3):C711-9. Epub 2003 May 07 (To save pages, please log onto http://ajpcell.physiology.org/cgi/content/full/285/3/C711 for full reprint).

Appendix 2 (Submitted to Experimental Cell Research, revised and resubmitted).

Regulation of Anoikis by Cdc42 and Rac1

Tzu-Ling Cheng, Marc Symons*, Tzuu-Shuh Jou§

Department of Internal Medicine, National Taiwan University Hospital and National Taiwan University College of Medicine
No. 7, Chung-Shan S. Road
Taipei, 100 Taiwan

* Center for Oncology and Cell Biology, North Shore-LIJ Research Institute, 350 Community Drive, 11030, Manhasset, NY, USA

§To whom reprint should be addressed.
Tel: 8862-23123456 ext.7258
Fax: 8862-23709820
E-mail: jouts@med.mc.ntu.edu.tw

Manuscript Information: 41 pages of text, and 8 figures in the paper.

Running Title: Cdc42 modulates anoikis

ABSTRACT

Ras family small GTPases play a critical role in malignant transformation, and Rho subfamily members contribute significantly to this process. Anchorage-independent growth and the ability to avoid detachment-induced apoptosis (anoikis) are hallmarks of transformed epithelial cells. In this study, we have demonstrated that constitutive activation of Cdc42 inhibits anoikis in Madin Darby canine kidney (MDCK) epithelial cells. We showed that activated Cdc42 ~~could~~ stimulates the ERK, JNK and p38 MAPK pathways in suspension condition; however, inhibition of these signalling does not affect Cdc42-stimulated cell survival. However, we demonstrated that i~~I~~nhibition of phosphatidylinositol 3-kinase (PI3K) pathway ~~however~~ abolishes~~d~~ the protective effect of Cdc42 on anoikis. Taking advantage of a double regulatory expression system, we also showed that Cdc42-stimulated cell survival in suspension condition is, at least in part, mediated by Rac1. ~~The consequence of Rac1 activation initiates a~~We also provide evidence for a positive ~~regulatory~~ feedback loop ~~between~~ involving Rac1 and PI3K. In addition, we show that the survival functions of both constitutively active Cdc42 and Rac1 GTPases are abrogated by Latrunculin B, an actin filament-depolymerizing agent, implying an important role for the actin cytoskeleton in mediating survival signaling activated by Cdc42 and Rac1. Together, our results ~~suggest~~ indicate a role for Cdc42 in anchorage-independent survival of epithelial cells. We also propose ~~conclude~~ that this survival function depends on a positive feedback loop involving Rac1 and PI3K.

Key Words: Anoikis, apoptosis, Rac1, Cdc42, PI3 kinase, Akt

INTRODUCTION

The interaction between cells and the surrounding matrix is a major determinant of cellular behavior, modulating gene expression, cell growth and differentiation, cell migration, and overall tissue architecture [1]. Anchorage-dependent survival is also an important consequence of cell-matrix interaction [2]. Epithelial cells, endothelial cells, and muscle cells undergo programmed cell death when they are deprived of the contact with extracellular matrix [3].

Apoptosis induced by disruption of the interaction between epithelial cells and extracellular matrix has been termed as "anoikis", which means homelessness in Greek [4]. Anoikis plays an essential role in regulating tissue homeostasis in normal epithelial tissues. When keratinocytes and colonic epithelial cells migrate from the dividing basal layer toward the outer lining layer [5], the cells lose the ability to divide and eventually exofoliate from the monolayer. Anoikis also regulates involution of mammary glands [6], and is an important step in the first cavitation of embryogenesis [7]. Anoikis also modulates many pathological conditions. An important characteristic of transformed cells is the loss of anchorage-dependent growth control, thereby disrupting an essential surveillance mechanism that prevents cells from colonizing elsewhere when they are detached from their normal residence [8]-[9]. The capability of escaping anoikis regulation is thus a critical step in oncogenesis.

Initially identified as major players relaying the signalling from lipid and growth factor components in serum to actin cytoskeleton organization, Rho family GTPases have been demonstrated to regulate a large number of biological processes in response to cell-cell and cell-substratum adhesion [10, 11]. Rho family members regulate distinct actin cytoskeleton-based structures; namely, Cdc42 induces filopodia, Rac1 stimulates lamellipodia formation, while RhoA regulates the formation of stress fibers and focal adhesions [12-14]. There is considerable cross talk between members of the Rho family, the details of which appear to depend on the cell type and observation conditions [15]. Notably however, in most circumstances, Cdc42 appears to act upstream of Rac1 [14].

Rho family GTPases play an important role in cell transformation [16]. Expression of constitutively active (hydrolysis-defective) Rac1 in Rat1 fibroblasts induces serum- and anchorage-independent growth and is tumorigenic in nude mice [17]. Cdc42 regulates anchorage-independent growth and dominant negative Cdc42 N17 inhibits Ras focus formation and anchorage-independent growth [18]. We have also shown that constitutively active Rac1 protects MDCK cells from anoikis, while dominant negative Rac1 potentiates anoikis in MDCK cells [19]. In this paper, we address the role of Cdc42 in the regulation of anoikis, and examine its connection to survival signalling that is stimulated by Rac1.

Experimental procedures

Plasmids

Coding sequences expressing constitutively active and dominant negative Cdc42 were amplified by PCR using pCMVneoMYC-Cdc42V12 and pCMVneoMYC-Cdc42N17 (gifts of Dr. Arie Abo and Matt Hart, Onyx Pharmaceuticals) as a template respectively. The PCR primers were designed so that the amplified products were tagged with a 5' EcoRI and a 3' XhoI site. The PCR products were cloned into the EcoRI and XhoI restricted pCMV-Tag2B (Stratagene) to tag a FLAG epitope at their amino terminals, and resulted in two intermediate plasmids, pCF-Cdc42V12 and pCF-Cdc42N17. The FLAG-tagged Cdc42V12 coding sequence was released from pCF- Cdc42V12 by NotI and XhoI digestion, and cloned into similarly restricted vector, pIND(SP1), to generate pISF-Cdc42V12. By a similar strategy, pISF-Cdc42N17 was also made. pISF-Cdc42V12 and pISF-Cdc42N17 were confirmed to express FLAG-tagged constitutively active or dominant negative Cdc42 in an ecdysone responsive manner by immunoblotting and immunofluorescence after they were transiently transfected into MDCK and HEK293 cell clones which had been stably transfected with heterodimeric ecdysone receptors system [20]. pVgRXR (Invitrogen) is used to express the heterodimeric ecdysone receptors and confer zeocin (Invitrogen) resistance during drug selection. All the engineered plasmids were made according to standard molecular biological techniques and were confirmed by DNA nucleotide sequencing.

Stable cell lines construction

Madin-Darby canine kidney (MDCK) cells were grown in DMEM containing 10% fetal bovine serum at 37^{o}C in a humidified atmosphere containing 5% CO_2. Transfection was performed using lipofectamine 2000 reagent (Invitrogen) according to the manufacturer's instruction. Our ultimate goal is to establish dual regulatory cell lines expressing different small GTPase genes independently under tetracycline and ecdysone inducible systems. Therefore, we started with a well characterized MDCK cell line expressing dominant negative Rac1 (Rac1N17) gene under tetracycline repressible system [21, 22], and established ecdysone inducible expression system by zeocin selection and a FACS enrichment strategy [20] in this cell line which we named Rac1N17.1. We co-transfected 6 x 10^5 Rac1N17.1 cells in a p-35 well with 3.8 μg pISF-Cdc42V12 or pISF-Cdc42N17 respectively and 0.2 μg pUB-Bsd (Invitrogen), which carried blasticidin-S selection marker. Six hours after transfection, the cells were trypsinized and splitted onto 6 p-100 wells with the addition of 20 ng/ml of doxycycline to suppress the expression of the originally established (stably integrated) Rac1N17 transgene. The day after transfection, cell culture medium was replete with 10 μg/ml of blasticidin-S for selection of stably transfected clones. Individual candidate clones expressing FLAG-tagged Cdc42V12 or Cdc42N17 were identified by immunofluorescence and Western blotting using anti-FLAG antibody (M2) from Sigma. In parallel, empty pIND(SP1) vector was cotransfected and selected in the same way to establish mock transfectant control (used to generate data described in Figure 1C). To induce the transgene, MDCK clones expressing the mutant Cdc42 genes were added with the indicated

concentration of ponasterone (Stratagene), and an aliquot of cells were added with the same volume of vehicle (alcohol) as a control. To establish MDCK cell line expressing constitutively active PI3K mutant in the background of tetracycline repressible Rac1N17 transgene, we followed the same transfection and selection protocol as described above except we co-transfected 6 x 10^5 Rac1N17.1 cells in a p-35 well with 3.8 μg plasmid expressing CMV promoter driven PI3K constitutively active mutant (p110*) and 0.2 μg pVgRXR (Invitrogen), which carried zeocin selection marker.

Antibodies and inhibitors

Immunoblotting was performed with one of the following primary antibodies: rabbit anti-Cdc42 and anti-p110 catalytic domain of PI3K (Santa Cruz), rabbit anti-total ERK p42/44, rabbit anti-phosphorylated ERK p42/44 (T202/Y204), rabbit anti-total and anti- phosphorylated JNK, rabbit anti-total and anti- phosphorylated JNK, anti- phosphorylated GSK-3 (the above antibodies were from Cell Signaling Technology), mouse anti Rac1 (UBI), anti-myc (purified from 9E10 hybridoma) or anti-FLAG tag (M2, Sigma). The secondary antibody used for Western blotting analyis was either an anti-rabbit or anti-mouse HRP-linked antibody at 1:3000 dilution (Amersham). The following small molecule inhibitors were dissolved in DMSO and used for dissecting Cdc42V12 mediated survival signalling pathway taken by suspended cells: MEK inhibitor U0126 (Promega), JNK inhibitor SP600125 (Tocris), p38 inhibitor SB203580, PI3K inhibitor LY294002 (Calbiochem), and Latrunculin B (Calbiochem). When above inhibitors were

used, the same volume of DMSO was also added to the control wells.

Western blot analysis

Adherent or suspended cells were washed in PBS, and cell extracts were prepared by lysing cells in boiling SDS sample buffer (2% SDS, 150 mM NaCl, 62.5 mM Tris-HCl (pH 6.8), 10% glycerol, 50 mM dithiothreitol, 0.01% bromophenol blue). The protein samples were separated by SDS-PAGE and transferred to nitrocellulose membrane (Schleicher & Schuell) and the membranes were blocked in 5% non-fat milk in PBST (0.1% Tween-20 in PBS) followed by immunoblotting analysis. Blots were developed with ECL reagent (Amersham-Pharmacia Biotech) for Western blotting analysis of total lysate or SuperSignal West Femto substrate (Pierce) for GST-PAK pull-down assay.

~~**P38 and PI 3-kinase activity assay**~~

~~Immobilized phospho p38 (Thr180/Tyr182) monoclonal antibody (Cell Signaling Technology) and immobilized phospho-Akt (Ser473) monoclonal antibody (1G1) (Cell Signaling Technology) were used to determine p38 and Akt activities of MDCK cells in suspension. Extracts were made from 6 x10^6 cells that were induced to express transgenes for 24 hours under adherent condition and further cultured in suspension for 2 hours. The cells were then extracted using lysis buffer (20 mM Tris pH 7.5, 150 mM NaCl, 1mM EDTA, 1mM EGTA, 1% Triton, 2.5 mM sodium pyrophosphate, 1 mM β-glycerol phosphsate, 1 mM Na_3VO_4, and 1 μg/ml leupeptin) supplied by the manufacturer. Immunoprecipitation of activated p38 and Akt were carried out~~

~~overnight and for 3 hours at 4°C respectively. Immunoprecipitates of activated Akt were washed twice with lysis buffer and twice with kinase buffer (25 mM Tris pH 7.5, 5 mM β-glycerol phosphsate, 2 mM DTT, 0.1 mM Na_3VO_4, and 10 mM $MgCl_2$). Then kinase reactions were carried out at 30°C for 30 minutes in the presence of 200 μM ATP and 1 μg of GSK-3 to assay PKB activity. Reactions were terminated by adding 2X SDS sample buffer and the boiled samples were loaded onto a SDS-PAGE gel. Immunoprecipitates of activated p38 were washed three times with lysis buffer and 2X SDS sample buffer was added before loading onto a SDS-PAGE gel. Western blotting analysis was processed as described above and incubated with rabbit anti-phosphorylated GSK-3 or anti-phosphorylated p38 antibody to assess the activities of Akt and p38 respectively.~~

p38 activity assay

Immobilized phospho-p38 (Thr180/Tyr182) monoclonal antibody (Cell Signaling Technology) was used to determine p38 activities of MDCK cells in suspension. Extracts were made from 6 $x10^6$ cells that were induced to express transgenes for 24 hours under adherent condition and further cultured in suspension for 2 hours. The cells were then extracted using lysis buffer (20 mM Tris pH 7.5, 150 mM NaCl, 1mM EDTA, 1mM EGTA, 1% Triton, 2.5 mM sodium pyrophosphate, 1 mM β-glycerol phosphsate, 1 mM Na_3VO_4, and 1 μg/ml leupeptin) supplied by the manufacturer. Immunoprecipitation of activated p38 was carried out overnight at 4°C. Immunoprecipitates of activated p38 were washed three times with lysis buffer and 2X SDS sample buffer was added before loading onto a SDS-PAGE gel. Western blotting analysis was processed as described above and incubated with rabbit anti-phosphorylated p38 antibody to

assess the activities of p38.

Akt activity assay

Immobilized phospho-Akt (Ser473) monoclonal antibody (1G1) (Cell Signaling Technology) was used to determine Akt activities of MDCK cells in suspension. Extracts were made from 6 x10^6 cells that were induced to express transgenes for 24 hours under adherent condition and further cultured in suspension for 2 hours. The cells were then extracted using lysis buffer (20 mM Tris pH 7.5, 150 mM NaCl, 1mM EDTA, 1mM EGTA, 1% Triton, 2.5 mM sodium pyrophosphate, 1 mM β-glycerol phosphsate, 1 mM Na_3VO_4, and 1 µg/ml leupeptin) supplied by the manufacturer. Immunoprecipitation of activated Akt were carried out for 3 hours at 4^{o}C. Immunoprecipitates of activated Akt were washed twice with lysis buffer and twice with kinase buffer (25 mM Tris pH 7.5, 5 mM β-glycerol phosphsate, 2 mM DTT, 0.1 mM Na_3VO_4, and 10 mM $MgCl_2$). Then kinase reactions were carried out at 30^{o}C for 30 minutes in the presence of 200 µM ATP and 1 µg of GSK-3. Reactions were terminated by adding 2X SDS sample buffer and the boiled samples were loaded onto a SDS-PAGE gel. Western blotting analysis was processed as described above and incubated with rabbit anti-phosphorylated GSK-3 to assess the activities of Akt.

Immunofluorescence m~~M~~icroscopy

The procedure for morphological studies was the same as the one published previously [21]. The mouse anti-FLAG antibody (M2, Sigma) was used at 1 ng/ml for indirect immunofluorescence.

Anoikis induction and DNA fragmentation assays.

Mutant GTPases expressing MDCK cells were induced to express transgenes by adding the indicated concentration of ponasterone (for ecdysone inducible transgenes) or removing doxycycline (for tetracycline repressible transgenes) for 24 hours as a monolayer and subsequently trypsinized and cultured in suspension on ultra low attachment plates (Costar) at a density of 5 $x10^4$ cells/ ml for 16-18 hours. Cells were then processed for assessing the level of DNA fragmentation using the Cell Death ELISA kit (quantifying histone-associated DNA fragments) using the protocol suggested by the manufacturer (Roche Molecular Biomedicals). Lysates assayed were equivalent to 2.5 $x10^4$ cells. Each condition contained at least four independent samples. Results were representative of at least three independent experiments, and shown as the means with S.E.M.

Cell survival assay

10,000 MDCK cells expressing Cdc42V12 and control cells in 200 µl of culture medium were maintained in suspension condition for 18 hours. Then, 40 µl of a modified MTT reagent, MTS (3-(4,5-dimethylthiazol-2-yl)-5-(3-carboxymethoxyphenyl)-2-(4-sulfophenyl)-2H-tetrazolium mixed with an electron coupling reagent (phenazine ethosulfate) from Promega, was added to the well with gentle pipetting. After incubation in the incubator at 37^{o}C for 60 minutes, absorbance at 490 nm was recorded. In the meantime, 10,000 control cells were detached from plastic dish and immediately processed for similar assay. Results were representative of three independent

experiments, and shown as the means with S.E.M

Rac1 activation assay

The procedure of preparing GST-PAK fusion protein and processing cellular lysates to perform the pull down assay is essentially as described before [23]. In brief, the p21-binding domain (PBD) of p21-activated kinase 1 (PAK1) was fused with glutathione-S-transferase to make a recombinant protein (GST-PBD). The GST-PBD fusion protein was then expressed, purified, and coupled to glutathione-sepharose beads (Amersham-Pharmacia Biotech). One twentieth of the clarified cell lysate was immunoblotted for the corresponding GTPase specific antibody to confirm the presence of equal loading, while the rest of the lysate was then incubated for 60 min at 4°C with 40μg GST-PBD coupled to glutathione-sepharose beads for pull down assay.

Results

~~*Constitutively active*~~*Regulation of anoikis by Cdc42* ~~*suppresses, while inhibition of Cdc42 activities enhances, MDCK cell anoikis*~~

We choose MDCK cells, which readily undergo apoptosis when cultured in suspension, for studying anoikis [4, 24]. In order to explore the role of Cdc42 in cell survival in anchorage independent conditions, we generated stable MDCK cell lines that expressed constitutively active Cdc42V12 or dominant negative Cdc42N17 under the control of an ecdysone-inducible promoter [25]. We selected several lines for each mutant transgene, and examined the effect of regulated expression of Cdc42V12 and Cdc42N17 on anoikis. Results were consistent among independent clones, and were presented here with those generated from a representative clone. Addition of ponasterone, a synthetic ecdysone analogue, induced expression of Cdc42V12 comparable to that of endogenous Cdc42 (Fig 1A). Interestingly, the endogenous Cdc42 expression appeared to be down-regulated by the over-expressed transgene, possibly reflecting a regulatory mechanism to keep the activation status of Cdc42 in check (Fig. 1A).

Expression of Cdc42V12 by addition of ponasterone reduces the extent of apoptosis in suspension conditions in a dose-dependent manner, as measured by the level of histone-associated DNA fragments (Fig. 1B). In contrast, addition of the same concentration of ponasterone did not have any effect on apoptosis in the parental cell line (Fig. 1B). To exclude the possibility of ponasterone effect on the generation and release of DNA-histone complex for the assay, we added

similar doses of ponasterone into the medium of wild type MDCK, and mock transfectant controls. No significant effect of ponasterone was observed on the anoikis of these cells (Fig. 1C), arguing for the specificity of the effect elicited by Cdc42 activation on anoikis regulation.

To confirm that Cdc42 significantly enhances the survival potential of MDCK cells in suspension, we determined the viability of control and Cdc42V12-expressing cells after keeping them in suspension culture for 18 hours. We used a modified MTT (3-(4,5-dimethylthiazol-2-yl)-2,5-diphenyl) assay to quantify cell survival. Whereas only 40% of the control cells survived in suspension conditions, up to 70% of the Cdc42V12-expressing cells remained viable (Fig. 1D).

In contrast to the effect of Cdc42V12 on anoikis, ponasterone-regulated expression of dominant negative Cdc42 very slightly, but reproducibly, increased apoptosis in suspension conditions (Fig. 1E~~D~~). Inhibition of Cdc42 activity under adherent condition, however, did not elicit any detectable difference in apoptosis in comparison to the control (Fig. 1E~~D~~). Since the endogenous Cdc42 activity significantly declines after substratum detachment (unpublished data), the marginal effect of Cdc42N17 on cell survival could result from the inhibition of the residual Cdc42 activity in the suspended cells. The effects of Cdc42V12 and Cdc42N17 on the survival of MDCK cells in suspension strongly indicate a regulatory role of Cdc42 small GTPase on anoikis

Cdc42 survival signaling is independent of p42/44 ERK activation

To investigate the signalling mechanisms that mediate Cdc42V12- stimulated cell survival under anchorage-independent situation, we first examined the contribution of MAPK cascades. Cdc42 and Rac1 have been demonstrated to synergize with Raf in activating ERKs [26, 27]. Recently, Cdc42 and Rac1 were shown to enhance association of ERK2 with MEK1 through the activity of PAK in a fibronectin-dependent manner [28]. Furthermore, several reports indicate activated ERK prevents anoikis [29, 30]; conversely, inhibition of Cdc42 activity has been shown to trigger anoikis in murine fibroblasts which depend on an activated ERK activity [31].

To determine the role of ERK in Cdc42-stimulated survival signaling, we examined ERK activity in attached and suspension conditions using the ecdysone-inducible Cdc42V12-expressing cells. In control cells, ERK activity decreased significantly after cell detachment, and subsequently gradually returned to baseline levels (Fig. 2A). At present, we do not know which mechanism governs the restoration of the ERK activity after cell detachment. Expression of Cdc42V12 did not significantly enhance ERK activiation in either attachment or suspension conditions (Fig. 2A). In line with these observations, inhibition of MEK by U0126 did not affect Cdc42-induced protection against anoikis, although ERK activation was nearly abolished by the inhibitor (Fig. 2B). These results indicate that ERK activity does not play a significant role in Cdc42-mediated survival of MDCK cells cultured in suspension (Fig. 2C).

Cdc42 survival signaling is independent of JNK/SAPK pathway

The role of JNK in anoikis regulation remains controversial. Whereas JNK activation has been shown to be required for the induction of anoikis in one study [32], this has been contradicted by another study [24]. To investigate the role of JNK activation in the inhibition of anoikis caused by Cdc42, we used SP600125, a reversible ATP-competitive inhibitor of JNK-1, -2, -3 [33]. Whereas SP600125 efficiently inhibited the Cdc42V12-induced JNK activation, indicated by the diminished autophosphorylation of JNK (Fig. 3A) [34], the protective effect of Cdc42V12 against anoikis was not affected (Fig. 3B). Notably, the application of SP600125 at 10 μM, which inhibits JNK activation significantly, didn't have any effect on Cdc42V12 expression (Fig. 3A). We therefore conclude the protective effect of Cdc42 on anoikis is independent of the JNK pathway activation.

Cdc42 survival signaling is independent of p38

The role of p38 in anoikis regulation has also been controversial in that both pro-apoptotic [35] and anti-apoptotic [36] effects have been reported. This controversy could reflect the observation that distinct members of the p38 subfamily of mitogen-activated protein kinases may have different functions in apoptosis [37], which needs further to be reconciled within different cellular contexts [38]. Since p38 has been implicated in Cdc42-mediated survival signalling in fibroblasts grown in suspension condition [36], we investigated the role of p38 in survival stimulated by Cdc42 in MDCK cells. We therefore used SB203580, a pyridinyl imidazole

compound specifically inhibiting p38 at micromolar concentration [39]. Since p38 can autophosphorylate [40, 41], we examined the extent of p38 activation with a polyclonal serum specific for phosphorylated p38, after immunoprecipitating the phosphorylated p38 with a mouse monoclonal antibody. In the presence of 10 μM SB203580, p38 activation was significantly suppressed, while Cdc42V12 expression still fully protected suspended MDCK cells from anoikis (Fig. 4A and 4B). We therefor conclude that although Cdc42V12 can stimulate p38 in the absence of cell attachment, p38 activation is dispensable for Cdc42-mediated MDCK cell survival in these conditions.

Cdc42 mediates survival signaling in MDCK cells cultured in suspension by activating PI3

We have shown that activated Rac1 protects MDCK cells against anoikis via activation of PI3K [19]. To investigate whether PI3K/Akt signalling also plays a role in Cdc42-mediated survival in suspension culture, we performed *in vitro* kinase assays for Akt, and observed that Cdc42V12 significantly stimulates Akt in suspended MDCK cells (Fig. 5A). Furthermore, LY294002, a pharmacological inhibitor of PI3K, strongly inhibited PI3K activity (Fig. 5A) as well as the protective effect of Cdc42V12 (Fig. 5B). These results provide strong evidence for a significant role for PI3K in the protective effect induced by Cdc42 activation in MDCK cells in suspension.

Cdc42 acts upstream of Rac1 in PI3K /AKT pathway

Since both Cdc42 and Rac1 can inhibit anoikis via activation of PI3K, we next addressed the question whether there is a signaling cascade from Cdc42 to Rac1 in suspended MDCK cells, similar to the one observed in fibroblasts [14]. We used a Rac1N17 and Cdc42V12 double expressing cell line and examined whether differential expression of these two transgenes could affect apoptosis of MDCK cells kept in suspension condition. Fig. 6A shows the morphologyies of this particular MDCK cell line under adherent conditions. When Cdc42V12 was induced, the cells tended to be flatter than uninduced controls (panel b and a in Fig. 6A). This Cdc42V12 cell line also displayed other morphological features similar to previously characterized MDCK cell lines that express constitutively active Rac1 [21] (panel f in Fig. 6A). These included the formation of lamellipodia and macropinocytotic vesicles [21]. Immunostaining of Cdc42V12-expressing MDCK cells showed a spectrum of morphological characteristics from cells displaying abundant filopodia to cells with broad lamellipodia (Fig. 6B). Between these two types of cellsextremes, we observed cells with long protrusions embedded in sheet-like structures similar to those fibroblasts reported to be microinjected with constitutively active Cdc42 recombinant protein [14]. The Cdc42V12 microinjected fibroblasts first developed filopodia followed by lamellipodia progressively growing between the pre-formed filopodia and finally coalescing into a web like structure enclosing the majoritiesy of the filopodia [14]. When Rac1N17 was induced in addition to the expression of Cdc42V12, the cells had an aggregated and contracted morphology similar to the one when Rac1N17 was singly induced (panels d and c in Fig. 6A and [21]). The Rac1N17-expressing cells, although having a different appearance from the control cells, are still

viable, provided they are attached to substratum or embedded in a three dimensional collagen gel. In addition, they can polarize marker proteins at specific membrane domains [21, 22].

The observations that induction of Cdc42V12 ~~induction~~ elicit~~ings~~ filipodia as well as lamellipodia, a hallmark feature for Rac1 activation, and that dominant negative Rac1 expression revert~~ings~~ these phenotypes, ~~in MDCK cells~~ prompted us to examine ~~the possibility that~~whether constitutively active Cdc42 could lead to activation of Rac1. GST-PAK fusion protein pull-down assay demonstrated that Rac1 activity was higher when Cdc42V12 was induced in attached and suspended MDCK cells (Fig. 6C). In addition, Cdc42 activated PI3K in a Rac1 dependent manner, as indicated by the observation that dominant negative Rac1 abolished Akt activation by Cdc42V12 (Fig. 6D). In addition, expression of Rac1N17 strongly inhibited the protective effect of Cdc42V12 against anoikis (Fig. 6E). These results suggest that Rac1 acts downstream of Cdc42 in survival signalling in MDCK cells cultured in suspension.

PI3K-mediated protection against anoikis requires Rac1

While the survival signals stimulated by Rac1 in suspended cells clearly depend on PI3K activity [19], there are many conditions where Rac1 functions downstream of PI3K [42-44]. To further address this issue, we generate MDCK cell lines stably expressing constitutively active PI3K activity in the background of a tetracycline repressible dominant negative Rac1 (Rac1N17) transgene. The constitutively active PI3K mutant (p110*) was made by fusion of the p110

catalytic sub-unit and the SH2 domain from the p85 regulatory sub-unit of PI3K. This chimeric protein was demonstrated to activate PI3K signaling pathways independent of growth factor stimulation [45]. Two independent MDCK clones were selected and demonstrated to express p110* by Western blotting analysis (upper panel in Fig. 7A). It should be noted that the fusion of p110 and the SH2 domain makes p110* migrate as a 140 kDa molecule on the PAGE, and also the rabbit antibody we used for Western Blot could not recognize the endogenous canine form of PI3K. Inducible expression of Rac1N17 did not affect the expression level of the CMV promoter driven p110*, while the endogenous Rac1 expression levels seemed to be down-regulated by the expression of Rac1N17 (Fig. 7A).

When these p110* expressing MDCK cells were cultured in suspension conditions, they were more resistant to anoikis than the mock control (Fig. 7B) which was consistent with a previous report [46]. This protective effect of constitutively active PI3K, however, was inhibited by the inducible expression of Rac1N17 (Fig. 7B). This result indicates Rac1 could also function downstream of PI3K in providing survival signals against anoikis.

Cdc42- and Rac1-mediated protection against anoikis requires an intact actin cytoskeleton

Since both Cdc42 and Rac1 play major roles in controlling the organization of the actin cytoskeleton, we examined whether the anoikis-preventive effect of Cdc42V12 and Rac1V12

depends on an intact actin cytoskeleton. Latrunculin B, a potent actin polymerization inhibitor, significantly inhibited the anoikis-protective effects of both Cdc42V12 and Rac1V12 (Fig. 8~~7~~B), suggesting an important role for Cdc42/Rac1-controlled actin polymerisation in survival signalling by Cdc42 and Rac1. Interestingly however, the activation of PI3K by both Cdc42 and Rac1 was not significantly affected by latrunculin B (Fig. 8A), indicating that an intact actin cytoskeleton is largely dispensable for the Cdc42- and Rac1-induced PI3K activation.

Discussion

We have examined the role of Cdc42 in apoptosis induced by cell detachment from the substratum. Our study shows that inducible expression of Cdc42V12 significantly inhibits anoikis in MDCK cells. Our results also strongly suggest ~~indicate~~ that Cdc42-induced protection against anoikis is mediated by the activation of Rac1~~,~~. In addition, our data support a model in which Rac1 and PI3K participate in~~which then initiates~~ a positive ~~regulatory~~ feedback loop ~~involving Rac1 and PI3K~~ to inhibit anoikis. Furthermore, our data suggest that both Cdc42 and Rac1-stimulated cell survival depends on an intact actin cytoskeleton.

Our previous [19] and present studies demonstrate that PI3K activity is critical for Rac1V12- and Cdc42V12-mediated protection against anoikis. These observations are in line with several studies showing that Rac1-regulated functions, including cell survival, can be inhibited by pharmacological inhibitors of PI3K [47-49]. In addition, similar to the results that we obtained in MDCK cells, expression of constitutively active Rac1 in hematopoietic cells can stimulate PKB in a PI3K-dependent fashion [50]. Interestingly however, a number of earlier reports had indicated that Rac1 could function downstream of PI3K [42-44]. It appears therefore that PI3K may function both upstream and downstream of Rac1 (reviewed in [51]). In several cases, this could be demonstrated in the same type of cells [50]. Based on these observations, a positive feedback loop between Rac1 and PI3K has been postulated to function in the establishment of front-to-back polarity during chemotaxis of leukocytes [52]. Recently direct evidence for such a feedback loop

has been provided [53, 54]. Our results indicate that similar reciprocal interaction between Rac1 and PI3K also plays a role in integrin-mediated survival signaling in epithelial cells.

Exactly how Cdc42/Rac1 activate PI3K remains to be clarified. The 85 kDa regulatory subunit (p85) of PI3K has been shown to bind GTP-loaded Cdc42Hs with the enzymatic activity of PI3K being activated though this association [55, 56]. Rac1 can also bind to the p85 subunit of PI3K in a GTP-dependent manner, although whether or not this leads to enhanced PI-3,4,5-P_3 generation *in vivo* remains to be established [51, 56, 57]. In addition, it is possible that Rac1 activates PI3K by recruiting PI3K to the plasma membrane. Our data indicate in MDCK epithelial cells, the stimulatory effect of Cdc42 on PI3K activity and cell survival upon matrix-detached situation requires Rac1 activity. This is in line with the recent observation that Rac1 plays a dominant role in establishing a positive feedback loop to asymmetrically accumulate actin polymer and PI-3,4,5-P_3 in migrating neutrophils [58]. Although cellular morphology of the Cdc42V12 expressing MDCK cells is affected by interfering Rac1 activity using dominant negative construct (Fig. 6A), the effect of Cdc42 expression on actin cytoskeleton organization may not solely depends on Rac1 activity since the Cdc42V12 expressing cells display unique structure such as filopodia, (Fig. 6B) which is absent from the Rac1V12 expressing cells [21].

The signaling elements that act downstream of PI3K in the Cdc42 and Rac1-stimulated survival pathway remain to be identified. However, the prominent role played by PKB in

PI3K-mediated cell survival strongly suggests that PKB could play an important role in the protection against anoikis that is stimulated by Cdc42 and Rac1.

Both Cdc42 and Rac1 are key regulators of actin cytoskeleton organization. Transformed cells that are capable of manifesting anchorage-independent growth, also show a dramatic reorganization of the actin cytoskeleton, suggesting that actin dynamics may play a critical role in regulating anoikis [8, 59]. Indeed, several pro-apoptotic regulators have been shown to be associated with the actin cytoskeleton and could regulate anoikis by serving as sensors of cytoskeletal integrity [60, 61]. For example, upon loss of cell attachment, the pro-apoptotic Bcl-2-family protein Bmf dissociates from actin/myosin-associated dynein light chain-2 (DLC-2), allowing it to neutralize Bcl-2 and to activate cytochrome C release from mitochondria [61].

The inhibitory effect of Latrunculin B on Cdc42- and Rac1-mediated protection against anoikis implies that the cell survival effect of Cdc42/Rac in suspension conditions requires an intact actin cytoskeleton. The effect of actin polymerization on regulating anoikis is specific since actin polymerization inhibitor cytochalasin B blocks the RacV12-stimulated rescue of anoikis while basal survival under matrix attached condition is not affected (Coniglio S and Symons M, unpublished result). Interestingly, the activation of PI3K/Akt by Cdc42V12 and Rac1V12 is not affected by actin depolymerization (Fig. 8). Since Akt is not known to regulate actin polymerisation, these findings suggest that Cdc42/Rac may protect cells against anoikis via two

independent pathways, one mediated by Akt, and another one mediated by actin reorganization. Although our data indicate that the pro-survival signals of Cdc42 are in large part mediated through Rac1, it is possible that the Cdc42 and Rac1 signals converged on the regulation of the actin cytoskeleton, which could serve as a gatekeeper for pro-apoptotic proteins of the Bcl-2-family. In accord with this hypothesis, we showed that actin-depolymerizing agents such as Latrunculin B inhibit the protective effect of both Cdc42 and Rac1.

At present, we do not know which signaling elements mediate Cdc42/Rac-stimulated actin polymerisation, but there are a number of likely candidates, such as cofilin and phosphatidylinositol 5-kinase (PI 5-kinase), which regulates PIP2 synthesis. By activating LIM-kinase, Rac1 could affect the actin-binding and -severing abilities of cofilin and promote actin polymerization [62, 63]. Rac1- stimulated PI 5-kinase activity could increase the level of PIP2, which may affect the functions of many actin-binding proteins, thereby stimulating actin polymerization by uncapping or facilitating actin filament nucleation [64, 65].

In addition to activating PI3K, expression of Cdc42V12 stimulates a number of other signaling pathways that have been implicated in the control of cell survival. These include the ERK, JNK and p38 MAPK cascades. In most studies, ERK activation appears to inhibit anoikis [29, 30]. In contrast, a moderate degree of ERK activation has been shown to be necessary for the apoptotic process in extracellular matrix detached fibroblast [31]. Our result using the specific MEK inhibitor U0126 indicates that the ERK does not significantly contribute to Cdc42-mediated

protection against anoikis (Fig.2C). Intriguingly, ERK activity showed a biphasic response after detachment from substratum in MDCK cells (Fig.2A). Whether this represents a substitution of different MEK subtypes complexed with ERK as reported previously in matrix-attached and detached cells [28] remains to be clarified.

The precise role of JNK in epithelial cell survival in suspension conditions remains to be elucidated. Both Cdc42 and Rac1 can activate PAK [66], which in turn can activate JNK [67]. Our results indicate that JNK is indeed activated by Cdc42V12. This activation however is dispensable for Cdc42-stimulated survival in suspended MDCK cells (Fig.3B).

In intestinal epithelial cells, it has been demonstrated that anoikis involves over-expression of Fas ligand, which depends on the activation of p38 [68]. In contrast, p38 activity seems to be protective in fibroblast cultured in suspension condition [36]. Taking advantage of suspended MDCK cells as a model system to study anoikis, we conclude that the activation of the p38 MAPK pathway is not required for Cdc42-V12 mediated cell survival. Thus, in summary, the three MAPK pathways, ERK, JNK, and p38, seem to be largely dispensable for Cdc42V12 mediated survival of MDCK cells in suspension conditions.

Malignant transformation is characterized by serum- and adhesion-independent cell growth, loss of contact inhibition and the ability to promote tumorigenesis in nude mice. Many of these

phenotypes are regulated by members of the Rho family [16]. Notably, Cdc42 and Rac1 are essential for oncogenic Ras induced anchorage-independent growth [17, 18]. This study and our previous results [19] provide a mechanism for the role of these small GTPases in anchorage-independence and malignant transformation. Future studies aimed at the eludicidation of the signalling pathways that mediate cell survival downstream of Cdc42 and Rac may suggest novel drug targets for cancer therapy.

ACKNOWLEDGEMENTS: This work was supported by the National Science Council, Taiwan, R.O.C. (NSC 92-3112-B-002-003), and a research grant from National Taiwan University Hospital (NTUH 92-S014) to TSJ. Support by the Picower Foundation to MS is also gratefully acknowledged

References

1 Adams J.C., Watt F.M. Regulation of development and differentiation by the extracellular matrix. *Development* 1993;**117:** 1183-1198.

2 Jacks T., Weinberg R.A. Taking the study of cancer cell survival to a new dimension. *Cell* 2002;**111:** 923-925.

3 Ruoslahti E., Reed J.C., Jacks T., Weinberg R.A. Anchorage dependence, integrins, and apoptosis. *Cell* 1994;**77:** 477-478.

4 Frisch S.M., Francis H. Disruption of epithelial cell-matrix interactions induces apoptosis. *J Cell Biol* 1994;**124:** 619-626.

5 Hall P.A., Coates P.J., Ansari B., Hopwood D. Regulation of cell number in the mammalian gastrointestinal tract: the importance of apoptosis. *J Cell Sci* 1994;**107:** 3569-3577.

6 Boudreau N., Sympson C.J., Werb Z., Bissell M.J. Suppression of ICE and apoptosis in mammary epithelial cells by extracellular matrix. *Science* 1995;**267:** 891-893.

7 Coucouvanis E., Martin G.R. Signals for death and survival: a two-step mechanism for cavitation in the vertebrate embryo. *Cell* 1995;**83:** 279-287.

8 Frisch S.M., Screaton R.A. Anoikis mechanisms. *Curr Opin Cell Biol* 2001;**13:** 555-562.

9 Stoker M., O'Neill C., Berryman S., Waxman V., Coucouvanis E., Martin G.R. Anchorage and growth regulation in normal and virus-transformed cells. *Int J Cancer* 1968;**3:** 683-693.

10 Etienne-Manneville S., Hall A. Rho GTPases in cell biology. *Nature* 2002;**420:** 629-635.

11 Braga V.M. Cell-cell adhesion and signalling. *Curr Opin Cell Biol* 2002;**14:** 546-556.

12 Ridley A.J., Paterson H.F., Johnston C.L., Diekmann D., Hall A. The small GTP-binding protein rac regulates growth factor-induced membrane ruffling. *Cell* 1992;**70:** 401-410.

13 Ridley A.J., Hall A. The small GTP-binding protein rho regulates the assembly of focal adhesions and actin stress fibers in response to growth factors. *Cell* 1992;**70:** 389-399.

14 Nobes C.D., Hall A. Rho, rac, and cdc42 GTPases regulate the assembly of multimolecular focal complexes associated with actin stress fibers, lamellipodia, and filopodia. *Cell* 1995;**81:** 53-62.

15 Bar-Sagi D., Hall A. Ras and Rho GTPases: a family reunion. *Cell* 2000;**103:** 227-238.

16 Sahai E., Marshall C.J. RHO-GTPases and cancer. *Nat Rev Cancer* 2002;**2:** 133-142.

17 Qiu R.G., Chen J., Kirn D., McCormick F., Symons M. An essential role for Rac in Ras transformation. *Nature* 1995;**374:** 457-459.

18 Qiu R.G., Abo A., McCormick F., Symons M. Cdc42 regulates anchorage-independent growth and is necessary for Ras transformation. *Mol Cell Biol* 1997;**17:** 3449-3458.

19 Coniglio S.J., Jou T.S., Symons M. Rac1 protects epithelial cells against anoikis. *J Biol Chem* 2001;**276:** 28113-28120.

20 Lai J.F., Juang S.H., Hung Y.M., *et al.* Establishment of Ecdysone and Tetracycline Dual Regulatory Expression System for Studies on Rac1 Small GTPase Mediated Signalling. *Am J Physiol Cell Physiol* 2003;**285:** C711-C719.

21 Jou T.S., Nelson W.J. Effects of regulated expression of mutant RhoA and Rac1 small

GTPases on the development of epithelial (MDCK) cell polarity. *J Cell Biol* 1998;**142:** 85-100.

22 O'Brien L.E., Jou T.S., Pollack A.L., *et al.* Rac1 orientates epithelial apical polarity through effects on basolateral laminin assembly. *Nat Cell Biol* 2001;**3:** 831-838.

23 Criss A.K., Ahlgren D.M., Jou T.S., McCormick B.A., Casanova J.E. The GTPase Rac1 selectively regulates Salmonella invasion at the apical plasma membrane of polarized epithelial cells. *J Cell Sci* 2001;**114:** 1331-1341.

24 Khwaja A., Downward J. Lack of correlation between activation of Jun-NH2-terminal kinase and induction of apoptosis after detachment of epithelial cells. *J Cell Biol* 1997;**139:** 1017-1023.

25 No D., Yao T.P., Evans R.M. Ecdysone-inducible gene expression in mammalian cells and transgenic mice. *Proc Natl Acad Sci U S A* 1996;**93:** 3346-3351.

26 Frost J.A., Steen H., Shapiro P., *et al.* Cross-cascade activation of ERKs and ternary complex factors by Rho family proteins. *Embo J* 1997;**16:** 6426-6438.

27 Leng J., Klemke R.L., Reddy A.C., Cheresh D.A. Potentiation of cell migration by adhesion-dependent cooperative signals from the GTPase Rac and Raf kinase. *J Biol Chem* 1999;**274:** 37855-37861.

28 Eblen S.T., Slack J.K., Weber M.J., Catling A.D. Rac-PAK signaling stimulates extracellular signal-regulated kinase (ERK) activation by regulating formation of MEK1-ERK complexes. *Mol Cell Biol* 2002;**22:** 6023-6033.

29 Le Gall M., Chambard J.C., Breittmayer J.P., Grall D., Pouyssegur J., Van Obberghen-Schilling E. The p42/p44 MAP kinase pathway prevents apoptosis induced by anchorage and serum removal. *Mol Biol Cell* 2000;**11:** 1103-1112.

30 Lehmann K., Janda E., Pierreux C.E., *et al.* Raf induces TGFbeta production while blocking its apoptotic but not invasive responses: a mechanism leading to increased malignancy in epithelial cells. *Genes Dev* 2000;**14:** 2610-2622.

31 Zugasti O., Rul W., Roux P., *et al.* Raf-MEK-Erk cascade in anoikis is controlled by Rac1 and Cdc42 via Akt. *Mol Cell Biol* 2001;**21:** 6706-6717.

32 Frisch S.M., Vuori K., Kelaita D., Sicks S. A role for Jun-N-terminal kinase in anoikis; suppression by bcl-2 and crmA. *J Cell Biol* 1996;**135:** 1377-1382.

33 Bennett B.L., Sasaki D.T., Murray B.W., *et al.* SP600125, an anthrapyrazolone inhibitor of Jun N-terminal kinase. *Proc Natl Acad Sci U S A* 2001;**98:** 13681-13686.

34 Tsuiki H., Tnani M., Okamoto I., *et al.* Constitutively active forms of c-Jun NH2-terminal kinase are expressed in primary glial tumors. *Cancer Res* 2003;**63:** 250-255.

35 Xia Z., Dickens M., Raingeaud J., Davis R.J., Greenberg M.E. Opposing effects of ERK and JNK-p38 MAP kinases on apoptosis. *Science* 1995;**270:** 1326-1331.

36 Lassus P., Roux P., Zugasti O., *et al.* Extinction of rac1 and Cdc42Hs signalling defines a novel p53-dependent apoptotic pathway. *Oncogene* 2000;**19:** 2377-2385.

37 Nemoto S., Xiang J., Huang S., Lin A. Induction of apoptosis by SB202190 through inhibition of p38beta mitogen-activated protein kinase. *J Biol Chem* 1998;**273:**

16415-16420.

38 Vachon P.H., Harnois C., Grenier A., *et al.* Differentiation state-selective roles of p38 isoforms in human intestinal epithelial cell anoikis. *Gastroenterology* 2002;**123:** 1980-1991.

39 Lee J.C., Laydon J.T., McDonnell P.C., *et al.* A protein kinase involved in the regulation of inflammatory cytokine biosynthesis. *Nature* 1994;**372:** 739-746.

40 Ge B., Gram H., Di Padova F., *et al.* MAPKK-independent activation of p38alpha mediated by TAB1-dependent autophosphorylation of p38alpha. *Science* 2002;**295:** 1291-1294.

41 Jiang Y., Li Z., Schwarz E.M., *et al.* Structure-function studies of p38 mitogen-activated protein kinase. Loop 12 influences substrate specificity and autophosphorylation, but not upstream kinase selection. *J Biol Chem* 1997;**272:** 11096-11102.

42 Rodriguez-Viciana P., Warne P.H., Khwaja A., *et al.* Role of phosphoinositide 3-OH kinase in cell transformation and control of the actin cytoskeleton by Ras. *Cell* 1997;**89:** 457-467.

43 Hawkins P.T., Eguinoa A., Qiu R.G., *et al.* PDGF stimulates an increase in GTP-Rac via activation of phosphoinositide 3-kinase. *Curr Biol* 1995;**5:** 393-403.

44 Reif K., Nobes C.D., Thomas G., Hall A., Cantrell D.A. Phosphatidylinositol 3-kinase signals activate a selective subset of Rac/Rho-dependent effector pathways. *Curr Biol* 1996;**6:** 1445-1455.

45 Hu Q., Klippel A., Muslin A.J., Fantl W.J., Williams L.T. Ras-dependent induction of

cellular responses by constitutively active phosphatidylinositol-3 kinase. *Science* 1995;**268:** 100-102.

46 Khwaja A., Rodriguez-Viciana P., Wennstrom S., Warne P.H., Downward J. Matrix adhesion and Ras transformation both activate a phosphoinositide 3-OH kinase and protein kinase B/Akt cellular survival pathway. *Embo J* 1997;**16:** 2783-2793.

47 Ruggieri R., Chuang Y.Y., Symons M. The small GTPase Rac suppresses apoptosis caused by serum deprivation in fibroblasts. *Mol Med* 2001;**7:** 293-300.

48 Keely P.J., Westwick J.K., Whitehead I.P., Der C.J., Parise L.V. Cdc42 and Rac1 induce integrin-mediated cell motility and invasiveness through PI(3)K. *Nature* 1997;**390:** 632-636.

49 D'Souza-Schorey C., Boettner B., Van Aelst L. Rac regulates integrin-mediated spreading and increased adhesion of T lymphocytes. *Mol Cell Biol* 1998;**18:** 3936-3946.

50 Genot E.M., Arrieumerlou C., Ku G., Burgering B.M., Weiss A., Kramer I.M. The T-cell receptor regulates Akt (protein kinase B) via a pathway involving Rac1 and phosphatidylinositide 3-kinase. *Mol Cell Biol* 2000;**20:** 5469-5478.

51 Welch H.C., Coadwell W.J., Stephens L.R., Hawkins P.T. Phosphoinositide 3-kinase-dependent activation of Rac. *FEBS Lett* 2003;**546:** 93-97.

52 Rickert P., Weiner O.D., Wang F., *et al.* Leukocytes navigate by compass: roles of PI3Kgamma and its lipid products. *Trends Cell Biol* 2000;**10:** 466-473.

53 Wang F., Herzmark P., Weiner O.D., Srinivasan S., Servant G., Bourne H.R. Lipid products

of PI(3)Ks maintain persistent cell polarity and directed motility in neutrophils. *Nat Cell Biol* 2002;**4:** 513-518.

54 Weiner O.D., Neilsen P.O., Prestwich G.D., Kirschner M.W., Cantley L.C., Bourne H.R. A PtdInsP(3)- and Rho GTPase-mediated positive feedback loop regulates neutrophil polarity. *Nat Cell Biol* 2002;**4:** 509-513.

55 Zheng Y., Bagrodia S., Cerione R.A. Activation of phosphoinositide 3-kinase activity by Cdc42Hs binding to p85. *J Biol Chem* 1994;**269:** 18727-18730.

56 Tolias K.F., Cantley L.C., Carpenter C.L. Rho family GTPases bind to phosphoinositide kinases. *J Biol Chem* 1995;**270:** 17656-17659.

57 Bokoch G.M., Vlahos C.J., Wang Y., Knaus U.G., Traynor-Kaplan A.E. Rac GTPase interacts specifically with phosphatidylinositol 3-kinase. *Biochem J* 1996;**315:** 775-779.

58 Srinivasan S., Wang F., Glavas S., *et al.* Rac and Cdc42 play distinct roles in regulating PI(3,4,5)P3 and polarity during neutrophil chemotaxis. *J Cell Biol* 2003;**160:** 375-385.

59 Pawlak G., Helfman D.M. Cytoskeletal changes in cell transformation and tumorigenesis. *Curr Opin Genet Dev* 2001;**11:** 41-47.

60 Puthalakath H., Huang D.C., O'Reilly L.A., King S.M., Strasser A. The proapoptotic activity of the Bcl-2 family member Bim is regulated by interaction with the dynein motor complex. *Mol Cell* 1999;**3:** 287-296.

61 Puthalakath H., Villunger A., O'Reilly L.A., *et al.* Bmf: a proapoptotic BH3-only protein regulated by interaction with the myosin V actin motor complex, activated by anoikis.

Science 2001;**293:** 1829-1832.

62 Arber S., Barbayannis F.A., Hanser H., *et al.* Regulation of actin dynamics through phosphorylation of cofilin by LIM-kinase. *Nature* 1998;**393:** 805-809.

63 Yang N., Higuchi O., Ohashi K., *et al.* Cofilin phosphorylation by LIM-kinase 1 and its role in Rac-mediated actin reorganization. *Nature* 1998;**393:** 809-812.

64 Hartwig J.H., Bokoch G.M., Carpenter C.L., *et al.* Thrombin receptor ligation and activated Rac uncap actin filament barbed ends through phosphoinositide synthesis in permeabilized human platelets. *Cell* 1995;**82:** 643-653.

65 Rosenblatt J., Mitchison T.J., Hartwig J.H., *et al.* Actin, cofilin and cognition. *Nature* 1998;**393:** 739-740.

66 Manser E., Leung T., Salihuddin H., Zhao Z.S., Lim L. A brain serine/threonine protein kinase activated by Cdc42 and Rac1. *Nature* 1994;**367:** 40-46.

67 Bagrodia S., Derijard B., Davis R.J., Cerione R.A. Cdc42 and PAK-mediated signaling leads to Jun kinase and p38 mitogen-activated protein kinase activation. *J Biol Chem* 1995;**270:** 27995-27998.

68 Rosen K., Shi W., Calabretta B., Filmus J. Cell detachment triggers p38 mitogen-activated protein kinase-dependent overexpression of Fas ligand. A novel mechanism of Anoikis of intestinal epithelial cells. *J Biol Chem* 2002;**277:** 46123-46130.

Figure Legends

Fig. 1. Cdc42 rescues MDCK cells from anoikis. (A) Inducible expression of Cdc42V12 in suspension cells. MDCK-Cdc42V12 cells were cultured in the presence of the indicated ponasterone (Pon) concentrations on tissue culture plastic for 24 hours and further in suspension for 18 hours (Susp). A control well of uninduced cells was cultured under adherent condition for a total of 42 hours (Att). The expression levels of Cdc42 transgenes in cell lysates were assessed by immunoblotting. The lower band corresponds to endogenous Cdc42, while the higher bands to FLAG epitope-tagged Cdc42V12. (B) Cdc42V12 represses DNA fragmentation in suspended MDCK cells. MDCK-Cdc42V12 cells (black bars) and their parental controls (white bars) were cultured in the indicated concentrations of ponasterone as a monolayer for 24 hours and 18 hours in suspension. DNA fragmentation was assayed as described in materials and methods. (C) Wild type MDCK cells (Left panel) and pooled mock transfectants of an empty plasmid, pIND (right panel) were cultured in the absence or presence of 5 μM ponasterone for 24 hours as a monolayer and 18 hours in suspension before being processed for DNA fragmentation assay. (D) MDCK-Cdc42V12 cells were cultured in the indicated concentrations of ponasterone on tissue culture plastic for 24 hours and were suspended for 0 (S_0) or 18 (S_{18}) hours in suspension. Cell survival was examined by a modified MTT assay as described in materials and methods. (E~~D~~) Inhibition of Cdc42 activity marginally enhances anoikis. MDCK-Cdc42N17 cells (black bars) and their parental controls (white bars) were cultured in ponasterone of the indicated concentrations for 24 hours as a monolayer and 18 hours in suspension (Susp), and DNA

fragmentation was assayed as described in materials and methods. The expression levels of Cdc42 transgenes were assayed by immunoblotting. The lower band corresponds to endogenous Cdc42, while the higher bands to FLAG epitope-tagged Cdc42-N17. Concomitant cultures were cultured in the indicated concentrations of ponasterone as a monolayer for a total of 42 hours (Att) before DNA fragmentation was measured for comparison.

Fig. 2. ERK activation does not contribute to the protective effect of Cdc42V12 on anoikis. (A) Cell lysates prepared from Cdc42V12 expressing cells (+) or their uninduced control (-) cultured as adherent culture for 42 hours (Att) or cultured as monolayer for 24 hours followed by culture in suspension (Susp) for 0 to 18 hours were assayed for ERK activation by immunoblotting with a phosphorylated ERK (P-ERK) specific antibody. Equal loading was assessed by immunoblotting the cell lysates with an anti-ERK antibody. Results shown are representative of three independent experiments. (B) Cdc42V12 expressing cells were treated with 0 or 4 μM U0126 in suspension culture for 18 hours and expression level of phosphorylated ERK (P-ERK), FLAG-tagged Cdc42V12 (Cdc42V12), and endogenous Cdc42 (Cdc42) proteins were examined by Western blotting analysis. Results shown are representative of three independent experiments. (C) Inhibition of ERK does not interfere with Cdc42-induced inhibition of anoikis. Cells were cultured in 0 or 5 μM ponasterone (Pon) on tissue culture plastic for 24 hours, followed by culture in suspension for 18 hours in 0 or 4 μM U0126 and measurement of DNA fragmentation was performed as described before.

Fig. 3. JNK/SAPK activation does not contribute to the protective effect of Cdc42V12 on anoikis. (A) Cells were cultured in 0 or 5 μM ponasterone (Pon) on tissue culture plastic for 24 hours, followed by culture in suspension for 2 hours in the indicated concentrations of SP600125. Expression levels of phosphorylated JNK (P-JNK), total JNK, FLAG-tagged Cdc42V12 (Cdc42V12), and endogenous Cdc42 (Cdc42) were examined by Western blotting analysis. Results shown are representative of three independent experiments. (B) Concomitant cultures as in the conditions of (A) were measured for DNA fragmentation.

Fig. 4. p38 activation does not contribute to the protective effect of Cdc42V12 on anoikis. (A) Cells were cultured in 0 or 5 μM ponasterone (Pon) on tissue culture plastic for 24 hours, followed by culture in suspension for 2 hours in the indicated concentrations of SB203580. Expression level of phosphorylated p38 (p-p38) was assessed by a rabbit serum after immunoprecipitation was performed with a mouse monoclonal antibody specific for phosphorylated p38. Expression levels of total p38, FLAG-tagged Cdc42V12 (Cdc42V12), and endogenous Cdc42 (Cdc42) in cell lysates were examined by Western blotting analysis. Results shown are representative of three independent experiments. (B) Concomitant cultures as in the conditions of (A) were measured for DNA fragmentation.

Fig. 5. Cdc42-stimulated inhibition of anoikis depends on PI3K activity. (A) Cdc42V12 activates Akt in MDCK cells in suspension via PI3K. Cells were cultured in 0 or 5 μM ponasterone (Pon) on tissue culture plastic for 24 hours, followed by culture in suspension for 2 hours in the indicated concentration of LY294002. Akt activity was analyzed by *in vitro* phosphorylation of GSK-3 after immunoprecipitating phosphorylated Akt as described in Materials and Methods. Expression levels of phosphorylated GSK3α/β (P-GSK3α/β), total Akt, FLAG-tagged Cdc42V12 (Cdc42V12), and endogenous Cdc42 (Cdc42) were examined by Western blotting analysis. Results shown are representative of three independent experiments. (B) Concomitant cultures as in the conditions of (A) were measured for DNA fragmentation as described before.

Fig. 6. Cdc42 acts upstream of Rac1 in PI3K/AKT signaling pathway. (A) The phase contrast images of Cdc42V12, Rac1N17, or Rac1V12 differentially expressing cells. A dual regulatory cell line (Cdc42V12/Rac1N17) was cultured in the absence or presence of 20ng/ml doxycycline or 5μM ponasterone for 48 hours to singly induce FLAG-tagged Cdc42V12 (b) or Myc-tagged Rac1N17 (c), doubly express both transgenes (d), or serve as an uninduced control (a). Another Tet-Off system regulated MDCK cell line (Rac1V12) was grown in the presence of 20ng/ml doxycycline as a control (e) or induced to express Myc-tagged Rac1V12 in the absence of doxycycline (f). The expression levels of the respective transgenes in conditions a, b, c, d, e, and f were assessed by Western blotting analysis which could also detect the endogenous Cdc42 and Rac1 proteins (*). (B) FLAG-tagged Cdc42V12 was induced in the presence of 5μM ponasterone

and immunofluorescence was processed using mouse anti-FLAG antibody (M2). Representative images were presented to demonstrate a spectrum of cell morphologies from typical filopodia to predominant lamellipodia and with intermediate phenotypes displaying filopodia like protrusions embedded in lamellipodia like structures (starting from left upper and clockwise). (C) Time course of endogenous Rac1 activity after inducible expression of Cdc42V12. Ecdysone regulated Cdc42V12 expressing cells were cultured in 0 (white column) or 5 μM (black column) ponasterone on tissue culture plastic for 24 hours and were suspended for 0, 2, 18 hours (S_0, S_2, S_{18}) or simply cultured as adherent culture (Att) for 42 hours. The activities of endogenous Rac1 were examined by GST-PAK pull down assay, and expressed in arbitrary unit (a.u.). The graph represents the means and S.E.Ms from three separate experiments~~Inducible expression of Cdc42V12 increases endogenous Rac1 activity. Ecdysone system regulated Cdc42V12 expressing cells were cultured in 0 (control) or 5 μM (Cdc42V12) ponasterone on tissue culture plastic for 24 hours and were suspended for 0, 2, 18 hours (S_0, S_2, S_{18}) or simply cultured as adherent culture (Att) for 42 hours. The activities of endogenous Rac1 were examined by GST-PAK pull down assay. Double arrowhead represented the activated Rac1 in the pull-down material while Rac1 expression levels were examined in the initial total lysates as a sign of equal loading (single arrowhead)~~. (D) Inducible expression of Rac1N17 blocks AKT activity, which is activated by Cdc42V12. A Cdc42V12 and Rac1N17 dual regulatory cell line was cultured in 0 or 5 μM ponasterone either with or without 20ng/ml doxycycline on tissue culture plastic for 24 hours, followed by culture in suspension for 2 hours to induce Cdc42V12 or Rac1N17 expression. The

Akt activity was analyzed by *in vitro* phosphorylation of GSK-3, as described in Materials and Methods. (E) Concomitant cultures as in the conditions of (D) were kept in suspension for 18 hours and DNA fragmentation was measured as described before. Results are representative of three independent experiments.

Fig. 7. PI3K-stimulated inhibition of anoikis depends on Rac1 activity. (A) MDCK cell line expressing Myc-epitope tagged dominant negative Rac1 (Rac1N17) under tetracycline repressible system was stably transfected with a constitutively active PI3K mutant (p110*). The expression patterns of the transgenes were analyzed by Western blotting of total lysates from a mock transfected control and two selected PI3K mutants cultured in the presence or absence of 20 ng/ml doxycycline (Dox) to suppress or induce the Rac1N17 respectively. Upper panel shows the blot using a rabbit antiserum for p110 catalytic domain of PI3K, while the lower panel was from another blot using a mouse anti-Rac1 monoclonal antibody. (B) Constitutively active PI3K activity represses anoikis, which is mediated through Rac1. MDCK cell lines expressing p110* and the mock control were cultured in the presence (white bars) or absence (black bars) of 20 ng/ml doxycycline (Dox) to suppress or induce Rac1N17 mutant activity respectively. Cells were kept as a monolayer for 24 hours first and 18 hours later in suspension to induce anoikis. DNA fragmentation was assayed as described in materials and methods. Results shown are representative of three independent experiments.

Fig. 8. Actin cytoskeleton organization modulates PI3K/AKT activated survival signaling against anoikis. (A) The Cdc42V12 and Rac1V12 mediated Akt activation was not inhibited by Latrunculin B (LB). Cdc42V12 or Rac1V12 was induced by 5 μM ponasterone or de-repressed without 20ng/ml doxycycline on tissue culture plastic for 24 hours respectively in two different MDCK cell lines, followed by culture in suspension for 2 hours with or without 0.5μM LB. AKT activity was analyzed by *in vitro* phosphorylation of GSK-3, as described in Materials and Methods. Expression levels of phosphorylated GSK3α/β, total Akt, FLAG-tagged Cdc42V12 (Cdc42V12), endogenous Cdc42 (Cdc42), myc-tagged Rac1V12 (Rac1V12), and endogenous Rac1 (Rac1) were examined by Western blotting analysis. Results are representative of three independent experiments. (B) Concomitant culture was cultured as in the condition of (A) except the cells were suspended for 18 hours before DNA fragmentation was assessed as described before.

Figure 1

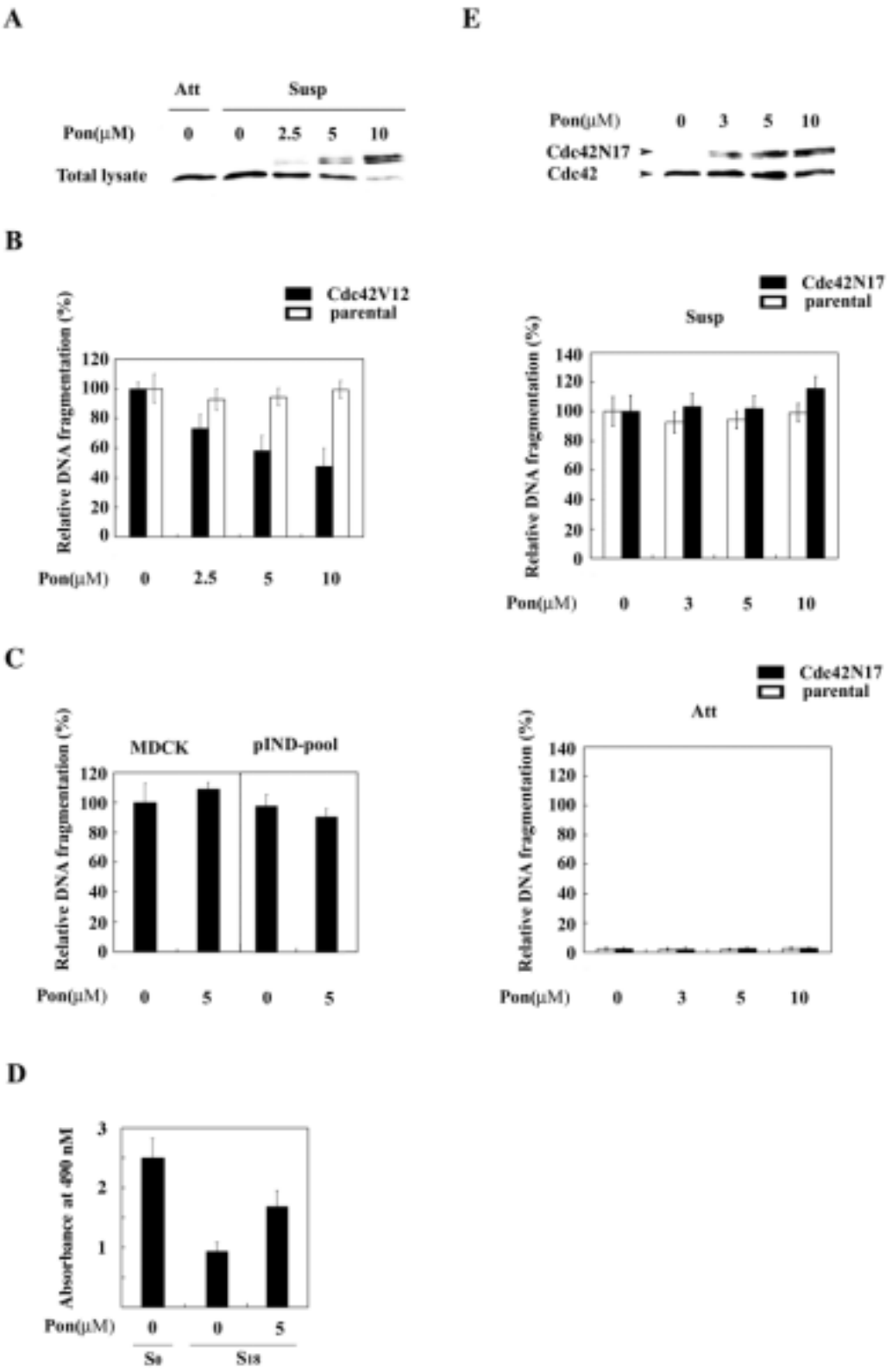
A
Att
Susp
Pon(μM) 0 0 2.5 5 10
Total lysate
E
Pon(μM) 0 3 5 10
Cdc42N17
Cdc42
B
Cdc42V12
parental
Relative DNA fragmentation (%)
120
100
80
60
40
20
0
Pon(μM) 0 2.5 5 10
Cdc42N17
parental
Susp
Relative DNA fragmentation (%)
140
120
100
80
60
40
20
0
Pon(μM) 0 3 5 10
C
MDCK
pIND-pool
Relative DNA fragmentation (%)
120
100
80
60
40
20
0
Pon(μM) 0 5 0 5
Cdc42N17
parental
Att
Relative DNA fragmentation (%)
140
120
100
80
60
40
20
0
Pon(μM) 0 3 5 10
D
Absorbance at 490 nM
3
2
1
Pon(μM) 0 0 5
S0
S18

Figure 2

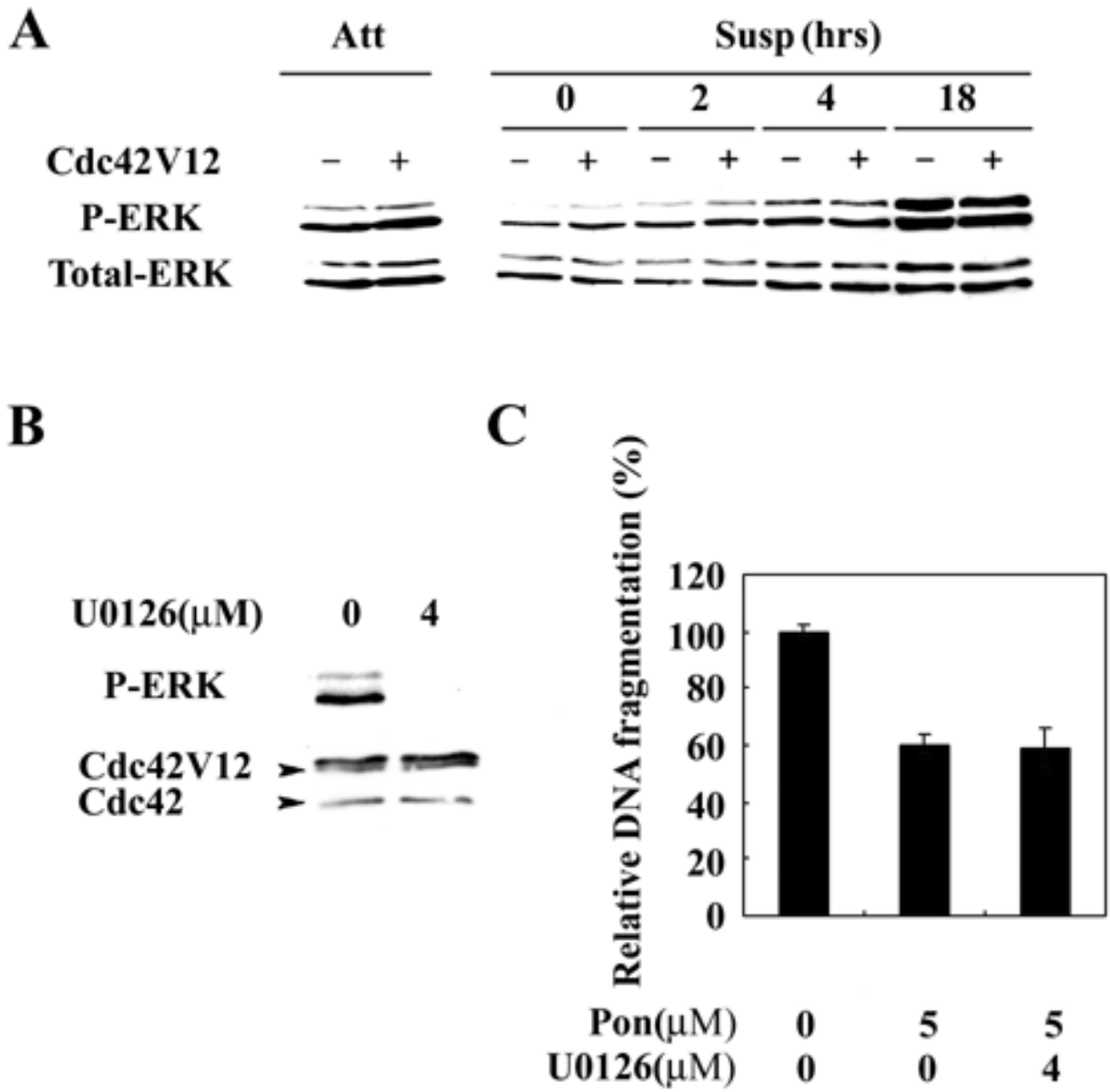
A
Att
Susp (hrs)
0
2
4
18
Cdc42V12
P-ERK
Total-ERK
B
U0126(μM)
0
4
P-ERK
Cdc42V12
Cdc42
C
Relative DNA fragmentation (%)
120
100
80
60
40
20
0
Pon(μM)
U0126(μM)

Figure 3

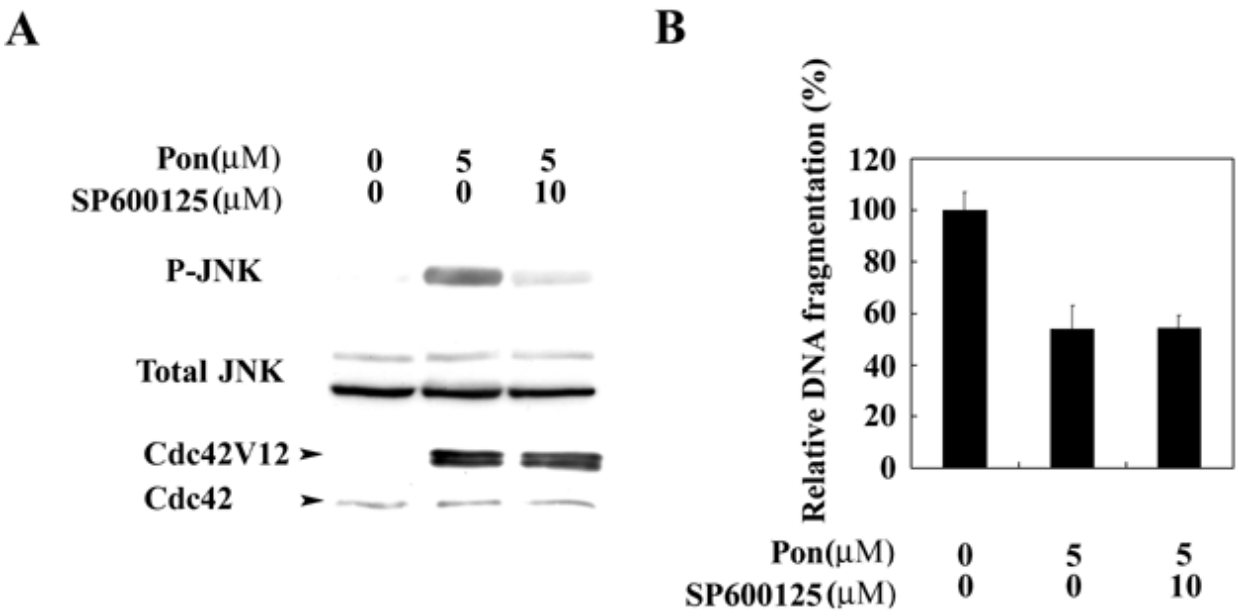
A
Pon(μM) 0 5 5
SP600125(μM) 0 0 10
P-JNK
Total JNK
Cdc42V12
Cdc42
B
Relative DNA fragmentation (%)
120
100
80
60
40
20
0
Pon(μM) 0 5 5
SP600125(μM) 0 0 10

Figure 4

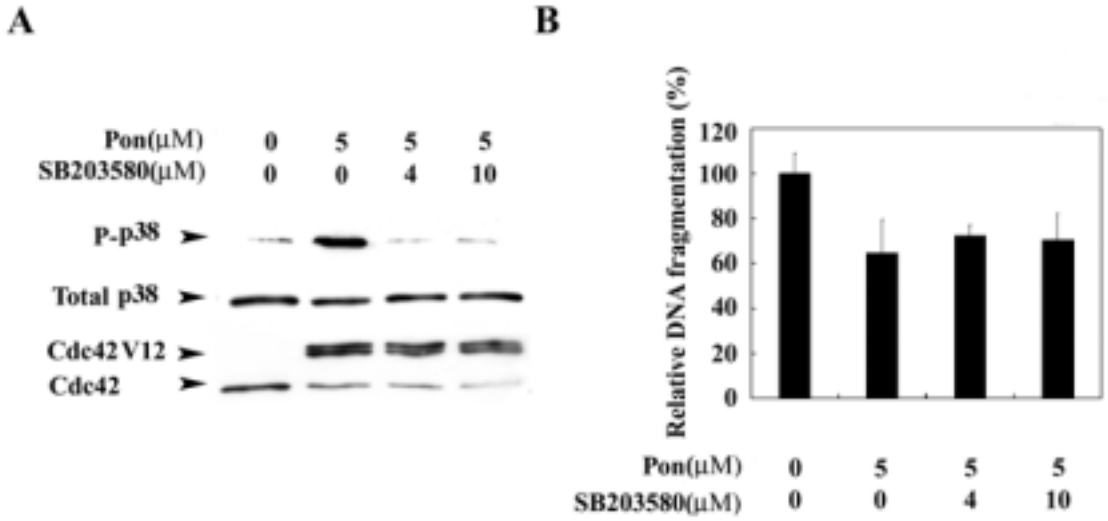
A
Pon(μM) 0 5 5 5
SB203580(μM) 0 0 4 10
P-p38
Total p38
Cdc42V12
Cdc42
B
Relative DNA fragmentation (%)
120
100
80
60
40
20
0
Pon(μM) 0 5 5 5
SB203580(μM) 0 0 4 10

Figure 5

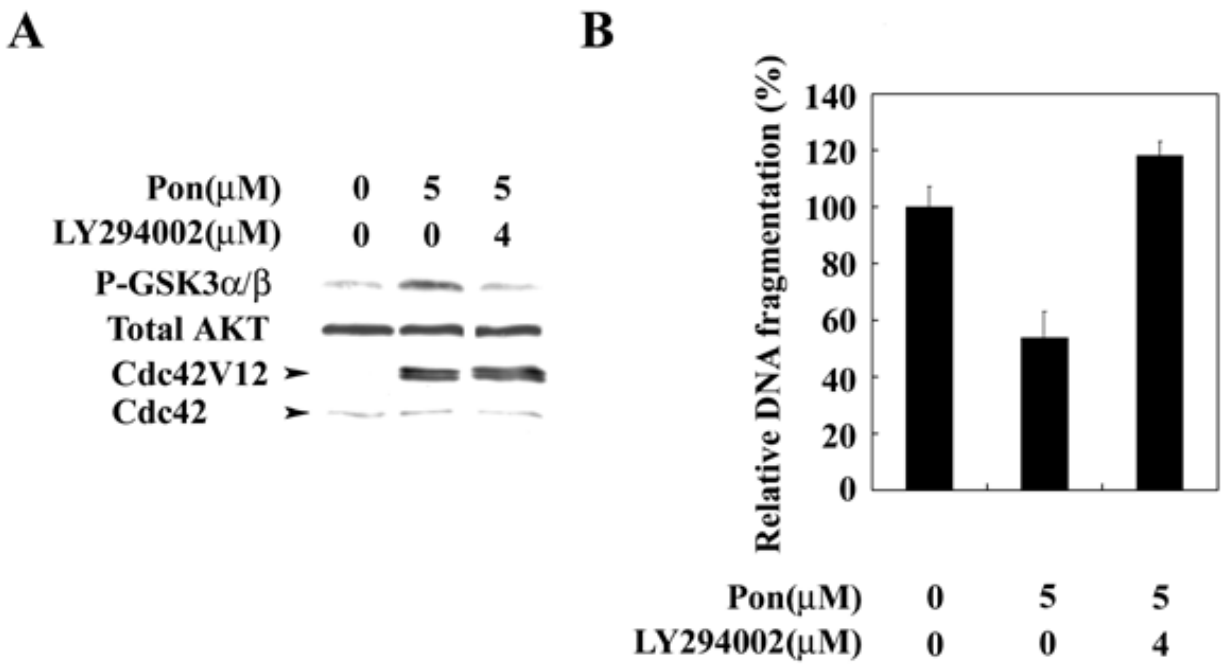
A
Pon(μM) 0 5 5
LY294002(μM) 0 0 4
P-GSK3α/β
Total AKT
Cdc42V12
Cdc42
B
Relative DNA fragmentation (%)
140
120
100
80
60
40
20
0
Pon(μM) 0 5 5
LY294002(μM) 0 0 4

Figure 6

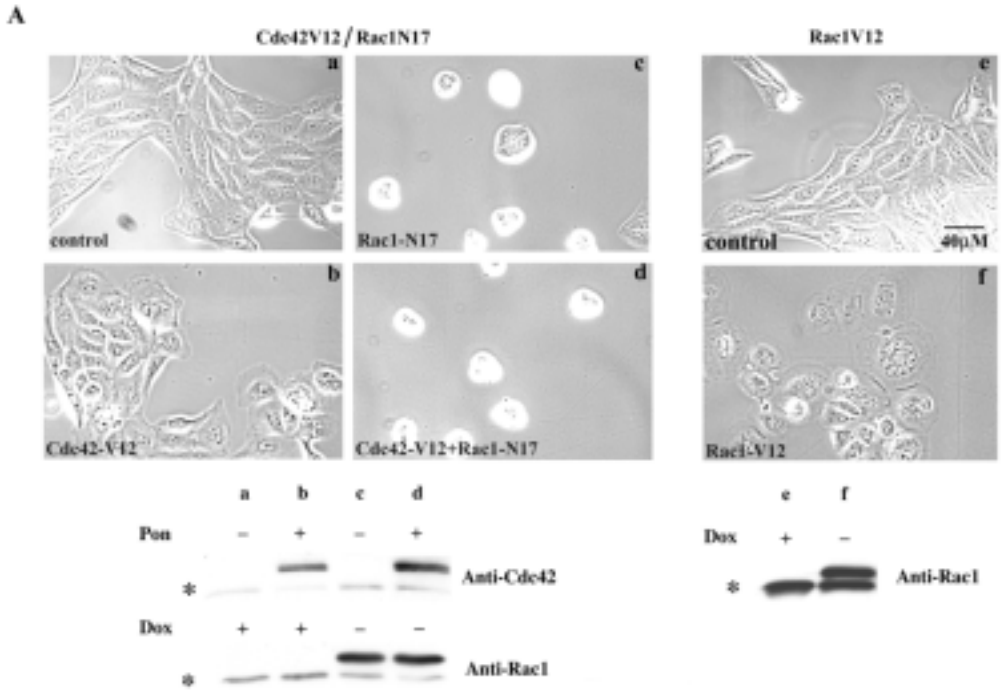
A
Cdc42V12 / Rac1N17
Rac1V12
a
c
e
control
Rac1-N17
control
40μM
b
d
f
Cdc42-V12
Cdc42-V12+Rac1-N17
Rac1-V12
a b c d
Pon – + – +
Anti-Cdc42
Dox + + – –
Anti-Rac1
e f
Dox + –
Anti-Rac1

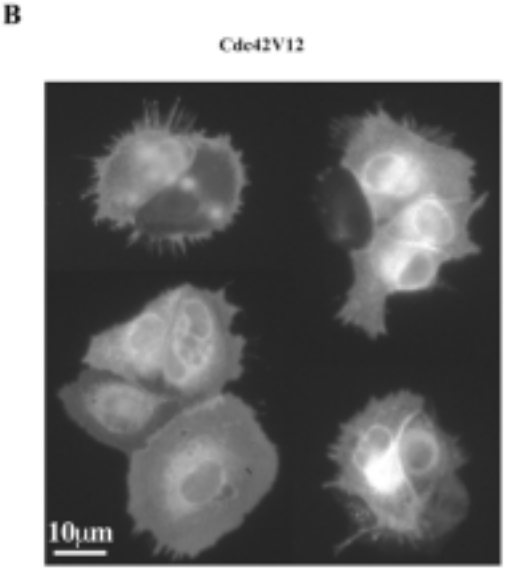
B
Cdc42V12
10μm

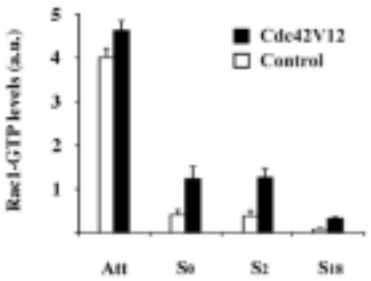
C
Rac1-GTP levels (a.u.)
Cdc42V12
Control
Att
S0
S2
S18

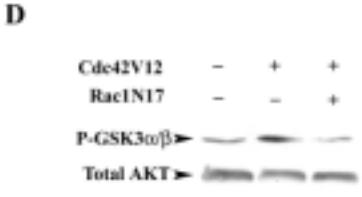
D
Cdc42V12 – + +
Rac1N17 – – +
P-GSK3α/β
Total AKT

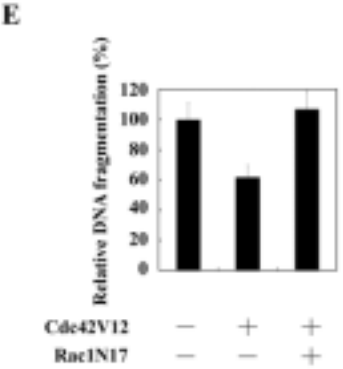
E
Relative DNA fragmentation (%)
Cdc42V12 – + +
Rac1N17 – – +

Figure 7

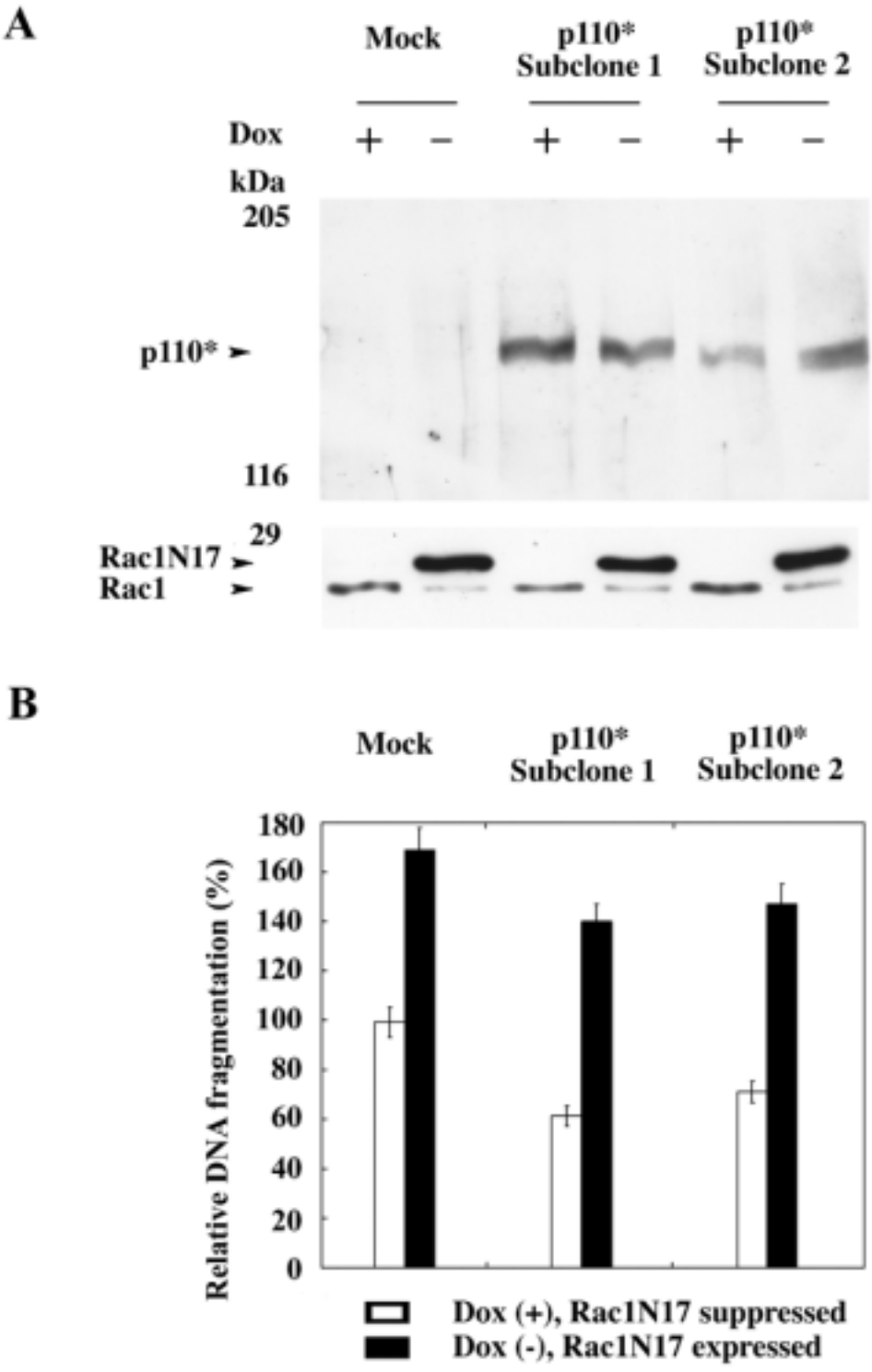
A
Mock
p110*
Subclone 1
p110*
Subclone 2
Dox
+ − + − + −
kDa
205
p110*
116
29
Rac1N17
Rac1
B
Mock
p110*
Subclone 1
p110*
Subclone 2
Relative DNA fragmentation (%)
180
160
140
120
100
80
60
40
20
0
Dox (+), Rac1N17 suppressed
Dox (-), Rac1N17 expressed

Figure 8

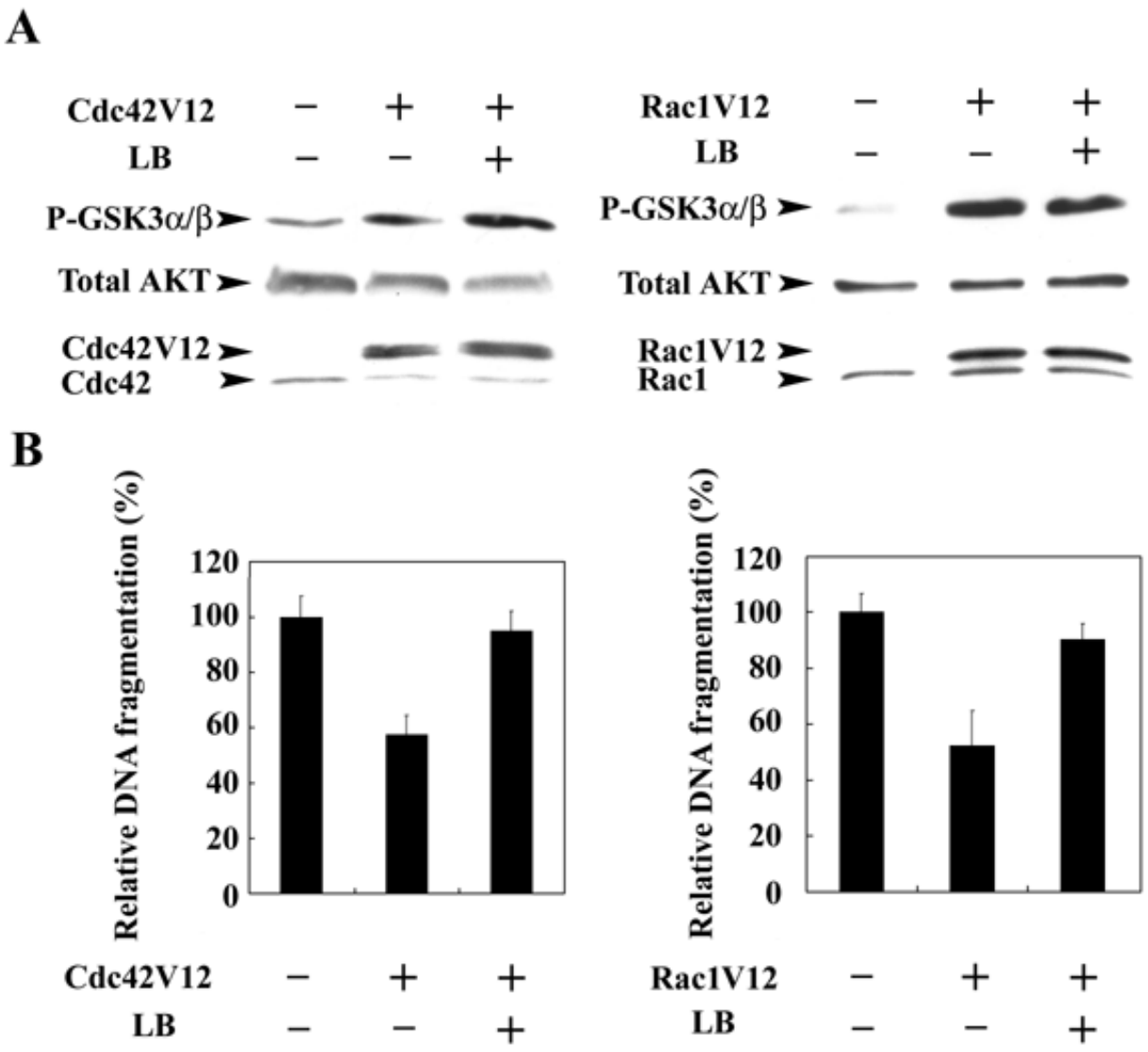
A
Cdc42V12 − + +
LB − − +
P-GSK3α/β
Total AKT
Cdc42V12
Cdc42
Rac1V12 − + +
LB − − +
P-GSK3α/β
Total AKT
Rac1V12
Rac1
B
Relative DNA fragmentation (%)
120
100
80
60
40
20
0
Cdc42V12 − + +
LB − − +
Relative DNA fragmentation (%)
120
100
80
60
40
20
0
Rac1V12 − + +
LB − − +

Appendix 3 (Submitted to Journal of Gene Medicine).

Doxycycline and Tetracycline Regulated Transcriptional Silencer Enhance the Expression Level and Transactivating Performance of rtTA

Jen-Feng Lai, Hsin-Yuan Cheng, Tzu-Ling Cheng, Yu-Yu Lin, Li-Chieh Chen, Mau-Ting Lin, Tzuu-Shuh Jou*

Department of Internal Medicine, National Taiwan University Hospital and National Taiwan University College of Medicine
No. 7, Chung-Shan S. Road
Taipei, 100 Taiwan

Running Head: tTS co-activates rtTA

*Address for reprint requests and other correspondence:
T.S. Jou
Tel: 8862-23123456 ext.7258
Fax: 8862-23709820
E-mail: jouts@med.mc.ntu.edu.tw

tetracycline regulated transcriptional silencer (tTS), reverse type tetracycline regulated transcriptional activator (rtTA), ubiquitin-proteasome pathway, ubiquitination, gene therapy

Abstract

Background- Tetracycline regulated transcriptional silencer (tTS) has been demonstrated to mitigate leaky expression of tetracycline inducible promoter under uninduced condition, and when conjugated with reverse type tetracycline controlled transactivator (rtTA), shows great promise for gene therapy. This effect was attributed to the effectiveness of tTS as a repressor of transcription at the tetracycline-regulated promoter. However, we observed an unexpected increase of transactivational activity by rtTA in the presence of tTS under inducible condition.

Methods- To explore the nature of this co-activational effect of tTS on rtTA, we examined the expression patterns of rtTA by Western blotting analysis of total cellular lysates or enriched ubiquitinated pool of proteins under various conditions, including the one when proteasomal degradation is inhibited.

Results- We demonstrate tTS, in addition to its established role as a transcriptional silencer, can enhance rtTA expression level by salvaging rtTA from ubiquitin-dependent proteasomal degradation pathway. Along with this finding, we also demonstrate doxycycline, a commonly used tetracycline analogue, inhibits the susceptibility of rtTA to ubiquitin-proteasome mediated degradation and enhances the expression level of rtTA.

Conclusions- Taken together, our data establish an unappreciated role of doxycyline and tTS in tetracycline regulated gene expression and the functionality of rtTA.

Introduction

Regulated gene expression offers great promise for experimental biologists as well as clinicians interested in gene therapy. Among many established regulatory gene expression systems, tetracycline regulated gene expression (Tet) system has withstood testing in many different cells and model organisms for more than a decade, and has been demonstrated to be capable of providing tight, dose-controllable expression at the expense of a simple, economic antibiotic [1-3]. The Tet system takes advantage of an artificial transcription factor, tetracycline regulated transactivator (tTA), which is a fusion between the bacterial Tet repressor (TetR) and the VP16 transcriptional activating domain of herpes simplex virus. Since the binding affinity between TetR and its cognate operator sequence is allosterically affected by tetracycline, tTA falls off the promoter and gene expression is shut down in the presence of tetracycline in a controllable way [4]. The original Tet system enjoys its popularity as Tet-Off system. The Tet-Off system later evolves into a new format by substituting four amino acids in tTA to generate reverse tTA (rtTA) which requires tetracycline for binding to the tetracycline regulated promoter (TRP) and subsequent activation of the downstream genes [5]. This transformed descendant is known as Tet-On system, and expected to be more useful than Tet-Off in developmental studies and gene therapy because of its favorable pharmacokinetics [6].

Though very tight regulation of gene expression may be achieved by the Tet system, which is demonstrated by the successful expression of the lethal diphtheria toxin gene in transgenic mice [7], it is sometimes difficult to establish cell lines or transgenic animals where genes encoding

potentially toxic products are under Tet control. These failures are mainly due to the episomal and multiple copied status of the transiently transferred DNA, a situation when chromatin suppression is lacking, and cumulated expression from multiple copies of the target gene may compromise the survival of candidate cells before long-term cell lines or stable transgenic animals could be established.

In order to circumvent the background expression, Tet-On system could be complemented with the tetracycline controlled transcriptional silencer (tTS) to mitigate the leaky expression associated with TRP. tTS is generated by fusion of TetR and the silencer domain derived from a transcriptional silencer [8-11]. By titrating the concentration of tetracycline or its analogue doxycycline, the experimenter could manipulate the association status of either tTS or rtTA with TRP. Accordingly, the gene activity is totally shutdown in the absence of inducer when tTS binds to TRP and actively shields the promoter from endogenous transcriptional machinery. Therefore, the combinatorial use of rtTA and tTS alleviates the leaky expression under uninduced condition, and offers promising opportunity for developing tightly controllable gene delivery systems for gene therapy. We propose that, in addition to the transcriptional suppressive effect targeted at TRP under uninduced condition, tTS potentiates the transcriptional activity of rtTA by protecting it from ubiquitin/proteasomal mediated degradation. This protective effect does not depend on association of rtTA and rTS and possibly depends on the conformational status of rtTA undergoing proteasomal degradation.

Materials and methods

Plasmids- Plasmids expressing rtTA (pTet-On), tTS^{kid-1} (pTet-tTS), enhanced green fluorescent protein (pEGFP-N1), and the tetracycline responsive luciferase reporter (pTRE-Luc) were purchased from Clontech (Palo Alto, CA, USA). Plasmids expressing tTA, tetracycline regulated silencers, tTS^{erbA} and tTS^{eve}, were generous gifts from Dr. Sabine Freundlieb and Dr. Hermann Bujard (University of Heidelberg). Plasmids expressing S2 (pUHrT10-1), M2 (pUHrT16-1) mutant of rtTA, or their synthetic (codon-humanized) variant $rtTA2^{S}$-S2 (pUHrT61-1), $rtTA2^{S}$-M2 (pUHrT62-1), and synthetic variant of tTA- $tTA2^{S}$ (pUHT61-1) were generous gifts from Dr. Wolfgang Hillen (University of Erlangen). Plasmids expressing myc tagged ubiquitin was a generous gift from Dr. Zee-Fen Chang (National Taiwan University). To construct TetR(B/E), we digested pTet-tTS with NheI and ClaI to release the KRAB transcriptional silencing domain from the TetR(B/E) moiety, and performed intra-molecular ligation after gel purifying the remaining DNA fragment. Amino terminal myc epitope tagged tTS^{kid-1} was constructed by standard molecular cloning procedure. The constructions of TetR(B/E) and myc epitope tagged tTS^{kid-1} expressing plasmids were verified by DNA nucleotide sequencing.

Cell Culture and Transfection- HEK293, Madin Darby canine kidney (MDCK), and LLC-PK1 cells were grown in DMEM containing 10% FBS and penicillin (10,000 units/ml), streptomycin (10 mg/ml), and amphotericin B (0.025 mg/ml) at 37^{o}C in a humidified atmosphere containing 5% CO_2. Cultures were routinely monitored for mycoplasma infection. Transfection was performed

using lipofectamine 2000 reagent (GIBCO BRL, Gaithersburg, MD). The cells were immediately trypsinized and split after 6 hours' incubation with the transfection mixture. The cells were plated with 1 μg/ml of doxycycline, if indicated, for 40 hours before being harvested for luciferase assay or immunoblotting analysis.

Chemicals and Antibodies- N-ethylmaleimide and cyclohexamide were from Sigma. Tumor necrosis factor and MG132 were purchased from CalBiochem. Ubiquitin C-terminal hydrolase (Isopeptidase-T) was from BIOMOL. Rabbit and mouse anti-VP16 antibodies were from Clontech (Palo Alto, CA, USA) and Santa Cruz Biotechnology (Santa Cruz, CA, USA), respectively. Rabbit anti-tetracycline represser antibody was from MoBiTec (Marco Island, FL, USA). Mouse anti-β-actin antibody was from Sigma (St. Louis, MO, USA). Mouse anti-ubiquitin antibody was from Santa Cruz Biotechnology (Santa Cruz, CA, USA). Mouse anti-myc epitope antibody was collected from the ascites of mice injected with the hybridoma cells (9E10).

Luciferase Assay- The assay was performed using Dual Firefly and Renilla Luciferase Reporter kit (Packard BioScience, Meriden, CT, U.S.A.) according to the manufacturer's instruction manual. pRL-TK (Promega, Madison, WI, USA), a renilla luciferase expressing construct driven by thymidine kinase promoter, is included in every transfection mixture as an internal control to normalize the transfection efficiency. For the luciferase assays, which did not involve tTS, the total amount of DNA used in each transfection was completed by the addition of pEGFP-N1, which was driven by a similar CMV promoter, in the transfection mixture to balance the promoter

effect and monitor the transfection efficiency. The cells were trypsinized after transfection and plated onto 24 well plates with half of the wells added with 1 μg/ml of doxycycline to activate the reporter (luciferase) gene. The cells were incubated for a further 40 hours before luciferase assays were performed. Promoter activities were measured by Wallac luminometer, and expressed by dividing the firefly luciferase activity with renilla luciferase activity; each value was the mean of a triplicated measurement. Every promoter assay was repeated for at least three times.

Northern analysis- Total RNA was extracted using RNAzol B (Tel-Test, Inc., Friendswood, TX). For assaying rtTA and GAPDH mRNA expression, 8 μg and 4 μg of total RNA were denatured by glyoxal and DMSO solution, and resolved on 1% agarose gel respectively. The separated nucleic acids were then transferred onto nylon membranes (Roche Molecular Biomedicals) and cross-linked by UV irradiation. The digoxigenin (DIG)-labeled DNA probes were generated by PCR DIG probe synthesis kit (Roche Molecular Biomedicals). The probe for detecting rtTA messenger corresponds to nt 1421-1790 of pTet-On vector (Clontech Laboratory, Inc.). This region is specific for the VP16 portion of rtTA, and therefore, does not cross-hybridize with the mRNA signal from pTet-tTS. The oligonucleotides for amplifying GAPDH probe are 5' ACCACAGTCCATGCCATCAT 3' and 5' TCCACCACCCTGTTGCTGTA 3'. The membranes were incubated overnight with the DIG labelled probes at 50^{o}C. Signals were detected using alkaline phosphatase conjugated anti-DIG- antibody as recommended by the manufacturer (Roche Molecular Biomedicals). Fluorographic images were quantified using Image Gauge V3.41

(Fujifilm).

Cell extraction, Immunoblotting and Immunoprecipitation analysis- Cells grown to 80% confluency were scraped on ice in 150 mM NaCl, 50 mM Tris-HCl, pH 7.5, 1% NP-40, and protease inhibitor cocktail (Complete, Roche Molecular Biomedicals). Twenty mM of N-ethylmaleimide (NEM) was also included to suppress the deubiquitinylating enzymes. Cell suspension was rocked at 4^{o}C for 10 minutes before being cleaned in pre-chilled centrifuge at 10000 G for another 10 minutes. The extracts were quantified by BCA protein assay kit (Pierce Chemical Co.). For Western blotting using total cellular extract, 50 μg lysate was loaded in each lane of SDS-PAGE. Equal loading was confirmed by probing the same blot with anti-β-actin antibody after stripping as the one shown in Figure 1. For the reason of clarity, similar control Western blotting results were not shown in other figures. For immunoprecipitation, 2 mg lysate was incubated with 1 μg of the specific antibody covalently linked to protein G-Sepharose (Amersham-Pharmacia Biotech) for 2 hours. The immunoprecipitates were washed with high stringency buffer (HS-B: 20 mM Tris-HCl, pH 7.5, 120 mM NaCl, 25 mM KCl, 5 mM EDTA, 5 mM EGTA, 0.1% SDS, 1% Na-deoxycholate, 0.5% Triton X-100), followed by wash in high salt wash buffer (HS-B containing 1M NaCl), and finally washed in 10 mM Tris-HCl, pH 7.5 and 2 mM EDTA. The washed immunoprecipitates were then resolved by SDS-PAGE, transferred electrophoretically to nitrocellulose filters, and processed for immunoblotting with specific antibodies. For Western blotting involving total lysate, it was developed using the ECL kit

(Amersham-Pharmacia Biotech). For Western blotting involving immunoprecipitated materials, the signal was developed using the SuperSignal West Femto Substrate kit (Pierce Chemical Co.). The data presented in the figures are representative of the results from at least three similar experiments.

Deubiquitination reaction- Isopeptidase T (the large molecular weight form of Ubiquitin C-terminal hydrolase, UCH) was pre-incubated for 15 minutes according to the instruction from the manufacturer (BIOMOL). Then, the immunoprecipitated materials were assayed in 100 μl of 25mM HEPES (pH 7.5), 10mM DTT, and 5nM isopeptidase T at 25^{o}C for one hour before being loaded onto SDS-PAGE.

Results

tTS^{kid-1} Potentiates the Transcriptional Activity of rtTA under Induced Condition

Previously, tTS had been shown to enhance the regulatory range of tetracycline expression system by circumventing the intrinsic basal activity associated with tetracycline responsive promoter under uninduced condition [9-11]. To test this possibility, we cotransfected pTet-TS with rtTA-expressing and the tetracycline regulated reporter plasmids into a variety of cell lines. In the absence of tTS^{kid-1}, rtTA displayed 22 folds of difference in its capability of activating the reporter under induced vs. uninduced condition in HEK293 cells (Table 1). In addition, rtTA-S2 and rtTA-M2, two new rtTA mutants selected by a yeast genetic screening strategy [12], and their synthetic variants also showed nice regulation of transactivating ability upon doxycycline induction. Surprisingly, the presence of tTS^{kid-1} not only suppressed 60% of the reporter activity under uninduced condition, but also bolstered the reporter activity under induced condition by three to eight folds, depending on which rtTA variant was conjugated in the transfection experiment (Table 1). This apparently co-activational effect of tTS^{kid-1} is quite unexpected since tTS^{kid-1} should be away from the promoter in the presence of doxycycline, which induces a conformational change in the tet repressor moiety of tTS^{kid-1} and causes it to fall off the promoter DNA according to the existing model [9-11]. Even if residual tTS^{kid-1} remains on the promoter in the presence of doxycycline, it should elicit a silencer function rather than the co-activating function as shown in the luciferase assay.

Besides HEK293, we also conducted similar experiments in MDCK and LLC-PK1 cell lines. In both cell lines, the augmenting effect of tTS^{kid-1} on the transactivating performance of rtTA and its variants under induced condition was again evident (Table 1). The ubiquitous finding of tTS^{kid-1} potentiating the transactivating capability of the prototypic rtTA and all the variants tested in three different cell lines indicates this phenomenon is not merely an exceptional event.

tTS^{kid-1} and Doxycycline Increase the Expression Levels of rtTA and Various rtTA Mutants

The intriguing luciferase assay results prompted us to examine the status of rtTA expression under the transfection condition. Western blot analysis using a polyclonal antibody recognizing the VP16 moiety revealed that the expression levels of rtTA and its mutants rtTA-S2 and rtTA-M2 were affected by both doxycycline and tTS^{kid-1} (Fig. 1A). Whether tTS^{kid-1} was present or not, doxycyline increased rtTA expression. Similarly, tTS^{kid-1} also increased rtTA level, and this enhancing effect on rtTA expression was especially notable in the presence of doxycycline. Doxycycline and tTS^{kid-1} synergistically increased the expression level of rtTA by about 20 folds. Western blot analysis of the rtTA-S2 and rtTA-M2 variants disclosed the same trend. Because the synthetic rtTA variants $rtTA2^{S}$-S2 and $rtTA2^{S}$-M2 were engineered with a shorter version of VP16 activation domain [12], which precluded recognition by the VP16 anti-sera, the rabbit anti-TetR sera were used instead to detect the expression status of these two synthetic variants. Anti-TetR sera are supposed to recognize also the TetR moiety in tTS^{kid-1}; however, we cannot detect any specific signal for tTS^{kid-1} unless the fluorographs were developed after a prolonged exposure time

(Fig. 5B). Therefore, the signals shown in Fig. 1A literally reflected the expression levels of rtTA and its mutants, but not those for tTS^{kid-1}. Indeed, the expression patterns revealed by anti-TetR sera in Fig. 1A demonstrated both $rtTA2^{S}$-S2 and $rtTA2^{S}$-M2 were up-regulated by doxycycline and tTS^{kid-1}. To exclude the possibility that the increased rtTA level in the presence of doxycycline was due to sequestration of rtTA by the promoter DNA and also avoid the possible confounding signal from tTS^{kid-1} by using anti-TetR sera, we checked the expression of rtTA and the other rtTA mutants in the absence of tetracycline regulated reporter plasmids and tTS^{kid-1}. Western blot analysis showed rtTA expression was augmented by doxycycline alone (Fig. 1B). This finding strongly indicates that sequestration of rtTA at the promoter cannot be the cause of a higher rtTA expression level under induced condition. Similarly, rtTA-S2 and rtTA-M2 expression levels were increased in the presence of doxycycline (Fig. 1B). To definitively assess the level of the synthetic mutants, we performed another Western blotting analysis using the anti-TetR antisera. This again showed the expression levels of all different Tet-On type transcriptional regulators were up-regulated by doxycycline alone (Fig. 1B). Surprisingly, doxycycline has no effect on the expression levels of Tet-Off type transcriptional regulators, tTA and its synthetic mutant $tTA2^{S}$ (Fig. 1B).

tTS^{kid-1} Affects Post-translational Processing of rtTA

To understand the mechanistic basis for the up-regulating effect of doxycycline and tTS^{kid-1} on rtTA, we analyzed the effect of doxycycline and tTS^{kid-1} on rtTA transcriptional levels by

Northern blot analysis. The result showed neither doxycycline (Fig. 2A) nor tTS^{kid-1} (Fig. 2B) had any effect on rtTA mRNA expression. In order to determine whether the accumulation of rtTA was due to increased protein synthesis, we examined the effect of tTS^{kid-1} on rtTA translation in the presence of protein synthesis inhibitor cyclohexamide. While rtTA decreased by ~70% during the eight hour tracing under the control condition, its level changed only modestly in the presence of tTS^{kid-1} during the same period (Fig. 2C). Interestingly, the total cellular protein level declined at a similar rate after cyclohexamide treatment for either the control or the cells expressing tTS^{kid-1} (data not shown), implying the effect of tTS^{kid-1} on rtTA is rather selective. The finding that tTS^{kid-1} affected rtTA protein degradation coupled with the Northern blot analysis result (Fig. 2B) demonstrates the effect of tTS^{kid-1} is directed at post-translational modification of rtTA.

TetR Is the Critical Domain Responsible for the Enhancing Effect of tTS^{kid-1} on rtTA

To examine whether the up-regulating effect on rtTA is a unique property for tTS^{kid-1} or a common phenomenon for other tTSs, we cotransfected tTS^{eve} and tTS^{erbB}, constructs expressing TetR fused with the silencing domains of eve and erbA [10], respectively with rtTA expressing plasmid in the luciferase reporter assay. Although the silencing domains from different transcriptional repressors differed in their abilities to repress the reporter activity under uninduced condition, they unanimously increased the transactivating ability of rtTA under induced condition (Table 2). Interestingly, the TetR by itself, although unable to suppress the promoter under uninduced condition presumably due to its lack of transcriptional silencing domain, could

cooperatively activate the promoter with rtTA (Table 2). This result indicates that the TetR moiety in these transcriptional repressors is responsible for enhancing the transactivating effect of rtTA.

The Enhancing Effect of tTS^{kid-1} on rtTA is Independent of Direct Interaction

Although tTS^{kid-1} has been deliberately engineered with a chimeric TetR composed of dimerisation domains from different classes of TetRs to prevent heterodimerisation between rtTA and tTS^{kid-1} [9, 10], it is pertinent to examine whether the degradation-saving and transcriptional co-activating effect of tTS^{kid-1} on rtTA is through a stable and functional complex formed by tTS^{kid-1} and rtTA. Therefore, we performed a co-immunoprecipitation study to question this possibility. The anti-TetR antibody was the only way for us to recognize tTS^{kid-1}, which also reacted with rtTA. In order to trace the behavior of tTS^{kid-1} and to distinguish it from rtTA, we generate an amino myc-tagged tTS^{kid-1} (Myc-tTS). Although with a slightly decrease in potency, Myc-tTS could suppress the luciferase reporter activity under non-inducible condition and in the meantime potentiate the effect of rtTA as a transcriptional activator under inducible condition (data not shown). This demonstrated Myc-tTS possessed a functional trait similar to tTS^{kid-1}. By immunoprecipitating rtTA using anti-VP16 antibody, we did not detect any associated Myc-tTS in the immunocomplex (Supplementary figure 1). The fact rtTA and tTS do not form a complex excludes direct protein-protein interaction as the cause for the stabilizing effect of tTS on rtTA.

rtTA is Ubiquitinated and Degraded by Proteasome

While we were examining the effect of doxycycline and tTS on rtTA level, we noticed there were both high and low molecular weight forms of rtTA signals in the Western blots, especially for the over-expressed synthetic tTA and rtTA mutants (Fig. 1B). This laddering pattern is in line with the possibility of rtTA being regulated by the ubiquitin-proteasome pathway. It is well established that ubiquitin-dependent proteasomal proteolysis plays a pervasive role in protein destruction [13]. Therefore, we used quantitative immunoprecipitation and various proteolysis inhibitors to examine the expression pattern of rtTA. The rtTA expression increased after inhibition of proteasomal function by MG132 (Figure 3A) and a higher molecular form of rtTA was evident in the immunoprecipitates from MG132 treated cells, but not in the cells treated with 50 mM ammonium chloride which inhibited lysosomal function (Figure 3B). This result shows proteasomal but not lysosomal pathway plays a role in rtTA degradation. The higher molecular weight variant of rtTA is also recognized by anti-ubiquitin antibody, indicating rtTA is ubiquinated (Figure 3C). The higher molecular weight form of rtTA diminished after ubiquitin C-terminal hydrolase treatment further confirming rtTA was ubiquitinated (Figure 3B and 3C). Accordingly, these results demonstrate rtTA is spontaneously ubiquitinated and subsequently degraded by proteasome. The appearance of ubiquitinated rtTA only after inhibition of the proteasomal function implies it is a normally unstable intermediate targeted for proteasomal degradation. We also examined the effect of tTS^{kid-1} on rtTA ubiquitination by replacing half amount of rtTA expressing plasmid with tTS^{kid-1} expressing plasmid. Please note halfing the amount of rtTA

expressing plasmids generally resulted in lower expression level, but in the presence of tTS^{kid-1}, the expression level of rtTA was restored and furthermore (Figure 3D), there was also increasingly ubiquinated rtTA in the presence of tTS^{kid-1} (Figure 3E).

tTS^{kid-1} is Ubiquitinated and Degraded by Proteasome

Having established rtTA as an ubiquitinated protein undergoing proteasomal degradation and repeatedly found the signal of tTS^{kid-1}, which shares partial homology with rtTA, could barely be detected by Western blotting analysis only after prolonged exposure of the fluorography (Fig. 5B), we suspect tTS^{kid-1} is also ubiquitinated and fast degraded by proteasomal pathway. Indeed, examination of the amino acid sequences of rtTA and tTS^{kid-1} reveals a high percentage of lysines, which are the target residues of ubiquitination, in both proteins (4.18% for rtTA and 6.74% for tTS^{kid-1} as supposed to the 2/61 possible codon usage frequency). Because we were unable to use the rabbit anti-TetR antisera to perform immunoprecipitation, we immunoprecipitated the tTS^{kid-1} expressing lysates with ubiquitin antibody. After resolving the immune complex by SDS-PAGE, Western blot analysis identified a higher molecular weight variant of tTS^{kid-1} which was even more pronounced after treatment of MG132 (Fig. 4A). The intensity of this variant decreased after UCH treatment. Similar to rtTA, the level of tTS^{kid-1} was not affected by 50 mM ammonium chloride treatment (Fig. 4A). Taken together, these data indicate tTS^{kid-1} is significantly ubiquitinated and undergoes proteasomal degradation. The fact that the general ubiquitinated status is not affected by the expression of tTS^{kid-1} (Fig. 4B) indicates the effect of tTS^{kid-1} on rtTA ubiquitination (Fig.

3D and 3E) is very selective, rather than a general event.

Doxycycline Increases Ubiquitinated rtTA and tTS^{kid-1} While Increasing Degradation of tTS^{kid-1} and Decreasing rtTA Degradation.

Since both rtTA and tTS^{kid-1} are ubiquitinated and undergo proteasomal degradation, it is intriguing to examine whether doxycycline, as a conformational inducer for both trans-regulators, would affect their modification. Interestingly, doxycycline apparently has differential effect on rtTA and tTS^{kid-1}. Western blotting analysis of total lysate revealed doxycycline increased expression level of the un-modified form of rtTA while decreased that of tTS^{kid-1} (Fig. 5A and 5B, upper panels). Immunoblotting analysis of ubiquitinated proteins showed doxycycline increased the ubiquitination of both rtTA and tTS^{kid-1} (Fig. 5A and 5B, lower panels). Assessment of the general ubiquitination status by immunoblotting analysis of total cell lysates did not disclose any significant change of ubiquitin signals implying the effect of doxycycline on enhancing rtTA and tTS^{kid-1} ubiquitination is specific (Fig. 5C).

Having demonstrated tTS^{kid-1} could increase the post-translational stability of rtTA (Fig. 2) and the presence of tTS^{kid-1} could enhance the ubiquination of rtTA (Fig. 3D and 3E), we hypothesize tTS^{kid-1} increases rtTA expression through an interfering effect on proteasomal degradation. Therefore, it is of concern that other proteins, which normally undergo proteasomal degradation, would be affected by the expression of tTS^{kid-1} as well. We set up to examine whether IκB, whose dependence on ubiquitin/proteasomal pathway has been well documented [14-17], would be affected by tTS^{kid-1}. Western blotting analysis showed the expression levels of IκB,

whether under basal condition or stimulated by TNFα, was neither affected by doxycycline nor by tTS^{kid-1} (Fig. 6).

Discussion

Regulated gene expression has attracted the interest of many researchers in last decade thanks to the emergence of tight and efficient gene expression systems. Among the regulated gene expression systems, the advantages of tetracycline regulated gene expression system have been well documented both in cell lines and in whole organisms [4, 6, 18]. The combined use of both tetracycline regulated transcriptional activator and silencer is especially useful for transient transfection condition when chromatin repression is absent and high copy number of the plasmid templates permit leaky expression under uninduced condition. Previously, the target of this bipartite system was thought to be the promoter DNA. Tetracycline regulated transcriptional silencer (tTS) was demonstrated to actively shield the promoter and suppress the residual activity under uninduced condition. In addition to this established effect, we demonstrate tTS could enhance rtTA activity under induced condition, and this effect is through protection of rtTA from proteasomal degradation. Our data indicate both tTS and rtTA are ubiquitinated proteins, which undergo proteasome-mediated degradation. However, the steady state levels of tTS and rtTA are inversely affected by doxycycline with doxycyline increasing the level of rtTA while tTS level is decreased by doxycycline. Interestingly, both proteins are increasingly ubiquitinated in the presence of doxycycline. Based upon these findings, we propose the following model (Fig. 7). The proteolysis of rtTA and tTS via ubiquitin-proteasome pathway is probably represented by two different processes: (a) the identification of a substrate and its ubiquitination by ubiquitination machinery (ubiquitin activating, conjugating, and ligating enzymes) (b) the recognition of

ubiquitinated substrate and its digestion by the 26S proteasome. Although doxycycline affects the ubiquitinated status of both rtTA and tTS, the ubiquitin-conjugating and -ligating machinery doesn't seem to distinguish these two transcriptional regulators in light of the finding that both rtTA and tTS are increasingly ubiquitinated in the presence of doxycycline. In contrast, the ubiquitinated rtTA seems to be protected from the proteasomal degradation at the sacrifice of ubiquitinated tTS. This finding implies that the proteasomal machinery could distinguish the difference between tTS and rtTA, presumably due to the allosteric effect of tetracycline or its analogue on the TetR moiety in these two chimeric proteins. The finding that other tetracycline regulated silencers, such as tTS^{erbA} and tTS^{eve}, as well as TetR itself could enhance the transcriptional activating effect of rtTA makes the VP16 moiety in rtTA and the Kid-1 moiety in tTS unlikely candidates for determining the proteasomal susceptibility. Thus, tetracycline or its analogues has at least three roles in modulating tetracycline regulated gene expression systems: (1) affects the binding efficiency of rtTA and tTS for tetracycline regulated promoter, (2) increases the ubiquitination of both rtTA and tTS, and (3) affects the adaptability of rtTA and tTS for proteasome presumably through its effect on the conformation of TetR moiety in rtTA and tTS.

The dependence of rtTA expression level on doxycycline is another surprising finding and raises the concern that the activation of tetracycline responsive promoter by rtTA actually relies solely on the protein level of rtTA, but is not a conformation dependent phenomenon as in the case of its analogous molecule, tTA. The observation that tTA and its synthetic variant $tTA2^{S}$ exhibit pronounced range of transactivating ability while protein levels remain about the same between

induced and uninduced conditions (Fig. 1B) implies Tet-On and Tet-Off types transactivators could be regulated differently by tetracycline or its analogues. Nevertheless, we think the conformational effect of doxycycline on Tet-On type transactivators is still the primary determinant of the tetracycline responsive promoter activity because the protein levels of Tet-On type transactivators in the absence or presence of doxycycline are not always proportional to the measured luciferase reporter activities. For example, in HEK293 cells, rtTA2^{S}-S2 displayed a 347 folds difference in transactivating power between uninduced and induced condition when the transfection mixture contains tTS (Table 1). However, the expression levels of rtTA2^{S}-S2 were about the same under these conditions (Fig. 1A). We also noted rtTA-S2 and rtTA-M2 expression levels in the presence of Dox and tTS^{kid-1} were slightly more than those in the presence of Dox but without tTS^{kid-1} (Fig. 1A), while there was an eight fold difference in promoter activities between these two conditions (Table 1). The discrepancy between the expression levels of rtTA or its variants and the promoter activities implies factors other than quantitative changes of transactivators must be taken into consideration to explain the effect of tTS and doxycycline. As we have demonstrated, tTS and doxycycline modulate post-translational modification of rtTA. Thus, qualitative effects such as different protein-protein interaction and subcellular compartmentalization together with the quantitative effects on the dynamics of protein degradation might be the overall contributions of post-translational modification upon rtTA by tTS and doxycycline.

The finding of modulated expression of rtTA by doxycycline and tTS has practical implication for the users of tetracycline regulated gene expression system. The VP16 moiety in the rtTA has been thought to be associated with a squelching effect, which presumably reflects titration of endogenous transcription factors by a strong trannsactivator [4, 19]. Therefore, the fact that rtTA levels are different under uninduced vs. induced situation certainly raises a concern about the specificity of the tetracycline promoter driven target gene. This must be taken into consideration when researchers interpret the phenotypic difference under experimental conditions when target gene is uninduced and induced.

Acknowledgements: We would like to express our gratitudes to Dr. Hermann Bujard and Sabine Freundlieb for sending us the plasmids encoding tTA, $tTS^{B/E}$erA and $tTS^{B/E}$eve, to Dr. Wolfgang Hillen for sending us plasmids encoding the rtTA mutants, S_2, M_2, synthetic S_2, and synthetic M_2. Our work was supported by National Science Council, Taiwan, R.O.C.. (NSC 90-2323-B-002-009 & NSC 92-3112-B-002-003)

References

1 Baron U., Bujard H. Tet repressor-based system for regulated gene expression in eukaryotic cells: principles and advances. *Methods Enzymol* 2000;**327:** 401-421.

2 Berens C., Hillen W. Gene regulation by tetracyclines. Constraints of resistance regulation in bacteria shape TetR for application in eukaryotes. *Eur J Biochem* 2003;**270:** 3109-3121.

3 Gossen M., Bujard H. Studying gene function in eukaryotes by conditional gene inactivation. *Annu Rev Genet* 2002;**36:** 153-173.

4 Gossen M., Bujard H. Tight control of gene expression in mammalian cells by tetracycline-responsive promoters. *Proc Natl Acad Sci U S A* 1992;**89:** 5547-5551.

5 Gossen M., Freundlieb S., Bender G., Muller G., Hillen W., Bujard H. Transcriptional activation by tetracyclines in mammalian cells. *Science* 1995;**268:** 1766-1769.

6 Furth P.A., St Onge L., Boger H., *et al.* Temporal control of gene expression in transgenic mice by a tetracycline-responsive promoter. *Proc Natl Acad Sci U S A* 1994;**91:** 9302-9306.

7 Lee P., Morley G., Huang Q., *et al.* Conditional lineage ablation to model human diseases. *Proc Natl Acad Sci U S A* 1998;**95:** 11371-11376.

8 Deuschle U., Meyer W.K., Thiesen H.J. Tetracycline-reversible silencing of eukaryotic promoters. *Mol Cell Biol* 1995;**15:** 1907-1914.

9 Forster K., Helbl V., Lederer T., Urlinger S., Wittenburg N., Hillen W. Tetracycline-inducible expression systems with reduced basal activity in mammalian cells.

Nucleic Acids Res 1999;**27:** 708-710.

10 Freundlieb S., Schirra-Muller C., Bujard H. A tetracycline controlled activation/repression system with increased potential for gene transfer into mammalian cells. *J Gene Med* 1999;**1:** 4-12.

11 Rossi F.M., Guicherit O.M., Spicher A., *et al.* Tetracycline-regulatable factors with distinct dimerization domains allow reversible growth inhibition by p16. *Nat Genet* 1998;**20:** 389-393.

12 Urlinger S., Baron U., Thellmann M., Hasan M.T., Bujard H., Hillen W. Exploring the sequence space for tetracycline-dependent transcriptional activators: novel mutations yield expanded range and sensitivity. *Proc Natl Acad Sci U S A* 2000;**97:** 7963-7968.

13 Glickman M.H., Ciechanover A. The ubiquitin-proteasome proteolytic pathway: destruction for the sake of construction. *Physiol Rev* 2002;**82:** 373-428.

14 Alkalay I., Yaron A., Hatzubai A., Orian A., Ciechanover A., Ben-Neriah Y. Stimulation-dependent I kappa B alpha phosphorylation marks the NF-kappa B inhibitor for degradation via the ubiquitin-proteasome pathway. *Proc Natl Acad Sci U S A* 1995;**92:** 10599-10603.

15 Chen Z., Hagler J., Palombella V.J., *et al.* Signal-induced site-specific phosphorylation targets I kappa B alpha to the ubiquitin-proteasome pathway. *Genes Dev* 1995;**9:** 1586-1597.

16 DiDonato J.A., Mercurio F., Karin M., *et al.* Phosphorylation of I kappa B alpha precedes

but is not sufficient for its dissociation from NF-kappa B. *Mol Cell Biol* 1995;**15:** 1302-1311.

17 Scherer D.C., Brockman J.A., Chen Z., Maniatis T., Ballard D.W. Signal-induced degradation of I kappa B alpha requires site-specific ubiquitination. *Proc Natl Acad Sci U S A* 1995;**92:** 11259-11263.

18 Lamartina S., Roscilli G., Rinaudo C.D., *et al.* Stringent control of gene expression in vivo by using novel doxycycline-dependent trans-activators. *Hum Gene Ther* 2002;**13:** 199-210.

19 Gill G., Ptashne M. Negative effect of the transcriptional activator GAL4. *Nature* 1988;**334:** 721-724.

Table 1. Effect of tTS^{kid-1} expression on the transactivating activities of rtTA and its variants.

Promoter activities by luciferase reporter assay

	(-) tTS^{kid-1}			(+) tTS^{kid-1}		
	-Dox	+Dox	Activation factors	-Dox	+Dox	Activation factors
HEK293						
rtTA	**171 ± 1**	**3683 ± 233**	**22**	**69 ± 3**	**10507 ± 304**	**152**
rtTA-S2	**133 ± 8**	**1376 ± 98**	**10**	**86 ± 3**	**11052 ± 590**	**129**
rtTA-M2	**105 ± 4**	**1966 ± 222**	**19**	**45 ± 6**	**15227 ± 369**	**338**
$rtTA2^S$-S2	**218 ± 5**	**8752 ± 943**	**40**	**65 ± 2**	**22578 ± 110**	**347**
$rtTA2^S$-M2	**260 ± 25**	**8221 ± 754**	**32**	**111 ±15**	**30657 ± 170**	**276**
MDCK						
rtTA	**78 ± 5**	**1681 ± 189**	**22**	**16 ± 1**	**7415 ± 583**	**463**
rtTA-S2	**61 ± 2**	**896 ± 29**	**15**	**14 ± 1**	**6143 ± 266**	**439**
rtTA-M2	**71 ± 2**	**2652 ± 65**	**37**	**13 ± 1**	**7455 ± 378**	**573**
$rtTA2^S$-S2	**53 ± 3**	**2191 ± 75**	**41**	**9 ± 1**	**6125 ± 339**	**680**
$rtTA2^S$-M2	**74 ± 1**	**3680 ± 109**	**50**	**11 ± 1**	**5065 ± 107**	**460**
LLC-PK1						
rtTA	**45 ± 7**	**1192 ± 14**	**26**	**11 ± 1**	**3448 ± 39**	**313**
rtTA-S2	**39 ± 2**	**1074 ± 98**	**27**	**15 ± 2**	**4004 ± 133**	**267**
rtTA-M2	**42 ± 5**	**3981 ± 191**	**95**	**15 ± 1**	**4455 ± 43**	**297**
$rtTA2^S$-S2	**36 ± 7**	**2780 ± 234**	**77**	**14 ± 1**	**3639 ± 146**	**260**
$rtTA2^S$-M2	**76 ± 11**	**4210 ± 92**	**55**	**17 ± 1**	**4390 ± 521**	**258**

1.2 μg of the plasmid expressing rtTA or various rtTA mutants was co-transfected with 1.2 μg pTRE-Luc and 0.4 μg pRL-TK in the presence of mock or 1.2 μg pTet-tTS (tTS^{kid-1} expressing plasmid) into one million HEK293, MDCK, or LLC-PK1 cells. Luciferase activities were quantified in the absence (-Dox) and presence (+Dox) of 1μg/ml doxycycline. Values are the arithmetic means ± S.E. of three independent determinations.

Table 2. Effect of tetracycline regulated transcriptional silencers on the transactivating activities of rtTA.

	Promoter activities by luciferase reporter assay		
	-Dox	**+Dox**	**Activation factors**
rtTA + EGFP*	**206 ± 6**	**3617 ± 153**	**18**
rtTA + tTS^{kid-1}	**60 ± 2**	**7701 ± 105**	**128**
rtTA + tTS^{erbA}	**20 ± 1**	**6317 ± 147**	**315**
rtTA + tTS^{eve}	**225 ± 8**	**6864 ± 155**	**31**
rtTA + Tet R(B/E)**	**192 ± 4**	**7718 ± 30**	**40**

1.2 μg of the plasmid expressing rtTA was co-transfected with 1.2 μg pTRE-Luc and 0.4 μg pRL-TK in the presence of 1.2 μg plasmid expressing various tetracycline regulated silencers into one million HEK293 cells. Luciferase activities were quantified in the absence (-Dox) and presence (+Dox) of 1μg/ml doxycycline. Values are the arithmetic means of three independent determinations with S.E. shown. *****pEGFP was included to equalize the total amount of plasmids used in each transfection. **The tetracycline repressor moiety of tTS^{kid-1} is a hybrid between the class B DNA binding domain and the class E dimerization domain of TetR, and therefore TetR(B/E) is used in this experiment.

Figure Legends

FIG. 1. **tTS^{kid-1} and doxycycline enhance expression levels of rtTA and its mutants.** *A.* HEK 293 cells were transfected under the condition as described in table 1. The expression patterns of rtTA and its mutants were examined by immunoblotting analysis using either rabbit anti-VP16 or anti-TetR sera. *B.* HEK 293 cells (2 x 10^6) were transfected with 4 μg of the plasmids expressing tTA, rtTA, or their various mutnats whose expression patterns in the absence or presence of doxycycline (Dox) were detected by immunoblotting analysis 40 hours later using either rabbit anti-VP16 or anti-TetR sera. Please note the synthetic variants- tTA2^S, rtTA2^S-S2, and rtTA2^S-M2 were engineered with three repeats of VP16 minimal activation domain which rendered them migrate as a lower molecular weight variant (double arrowheads) than the other tetracycline regulators (arrowheads) on SDS-PAGE. Please also note that the signals of rtTA2^S-S2 and rtTA2^S-M2 were stronger in Fig. 1B than Fig. 1A due to larger amount of plasmids used in the transfection (4 μg vs 1.2 μg) and a longer exposure time of fluorography in order to augment the weak signals from rtTA and the other variants. Fifty μg of total cellular lysate was loaded per lane; equal loading was confirmed by the β-actin signal. The positions of molecular weight markers, in kilodalton, are labeled on the left of each blot.

FIG. 2. **tTS^{kid-1} enhances rtTA protein stability.** *A.* Two million HEK 293 cells were transfected with 4 μg pTet-ON. The cells were splitted onto two halves either with or without 1 μg/ml of doxycycline (Dox) after transfection. Forty hours later, RNA was extracted from the cells, and

rtTA mRNA level was assessed by Northern blot analysis. *B.* Two million HEK 293 cells were transfected with 2 μg pTet-ON with 2 μg of pTet-TS (+tTS^{kid-1}) or 2 μg of pEGFP (-tTS^{kid-1}) to complete the total amount of plasmids used in each transfection. Forty hours later, rtTA mRNA level was assessed by Northern blotting analysis. GAPDH mRNA levels were also examined to ensure equal loading. *C.* Two million HEK 293 cells were transfected with 2 μg pTet-ON with either 2 μg of pEGFP (-tTS^{kid-1}) or 2 μg of pTet-TS (+tTS^{kid-1}). Forty hours later, cells were incubated in the presence of 25 μM cyclohexamide (CHX) for the indicated period before rtTA level in the cell lysates were assessed by Western blot analysis using rabbit anti-VP16 antibody. rtTA signals on the fluorography in the absence (empty square) or presence (filled square) of tTS^{kid-1} expression were quantified and plotted against the time.

FIG. 3. **rtTA is ubiquitinated and a proteasomal substrate.** *A-C*, Two million HEK 293 cells were transfected with the indicated plasmids and cell extracts were prepared 40 hours after transfection. Fifty mM ammonium chloride and 25 μM MG132 pre-treatment for 3 hr were used to inhibit lysosomal and proteasomal degradation respectively. Ubiquitin C-terminal hydrolase (UCH) was used to treat an aliquot of the MG132-pretreated immunoprecipitate as indicated. The expression patterns of rtTA were detected by immunoblotting analysis using rabbit anti-VP16 sera (A). Two milligrams cell lysate was immunoprecipitated with 1 μg mouse anti-VP16 antibody, and the immunoprecipitates were separated by SDS-PAGE. Two identically processed blots were immunoblotted with rabbit anti-TetR sera (B) and mouse anti-ubiquitin antibody (C) to disclose

the nature of the higher molecular weight variant of rtTA. *D-E*, Two million HEK 293 cells were transfected with the indicated plasmids and cell extracts were prepared 40 hours after transfection. Two mg cell lysate was immunoprecipitated with 1 μg mouse anti-VP16 antibody. The immunoprecipitated cell extracts were then processed for Western blot analysis using rabbit anti-VP16 (D) antibody or mouse anti-ubiquitin antibody (E). LC and HC denote the presence of the immunoglobulin light and heavy chains associated with the immunoprecipitates. The positions of molecular weight markers, in kilodalton, are labeled on the left of each blot.

FIG. 4. **tTS^{kid-1} is ubiquinated and a proteasomal substrate.** *A-B*, Two million HEK 293 cells were transfected with the indicated plasmids and cell extracts were prepared 40 hours after transfection. Fifty mM ammonium chloride and 25 μM MG132 pre-treatment for 3 hr were used to inhibit lysosomal and proteasomal degradation respectively. UCH was used to treat an aliquot of the MG132-pretreated immunoprecipitate as indicated. Two milligrams cell lysate was immunoprecipitated with 1 μg mouse anti-ubiquitin antibody. The immunoprecipitates were separated by SDS-PAGE, and immunoblotted with rabbit anti-TetR sera (A). The general ubiquitination status was examined by immunoblotting analysis of 50 μg total cell lysate using mouse anti-ubiquitin antibody (B). The positions of molecular weight markers, in kilodalton, are labeled on the left of each blot.

FIG. 5. **Doxycycline increases ubiquinated rtTA and tTS^{kid-1}.** Two million HEK 293 cells were transfected with the indicated plasmids and cell extracts were prepared 40 hours after transfection. *A*, Fifty μg of total cell lysate was separated by SDS-PAGE and the expression patterns of rtTA were detected by rabbit anti-VP16 antibody. Two milligrams cell lysate was immunoprecipitated with 1 μg mouse anti-ubiquitin antibody, and the immune complex was resolved by SDS-PAGE followed by Western blotting analysis using rabbit anti-TetR antibody. *B*, Fifty μg of total cell lysate was separated by SDS-PAGE and the expression patterns of tTS^{kid-1} were detected by rabbit anti-TetR antibody. Two milligrams cell lysate was immunoprecipitated with 1 μg mouse anti-ubiquitin antibody, and the immune complex was resolved by SDS-PAGE followed by Western blotting analysis using rabbit anti-TetR antibody. An arrow denotes the position of the un-modified tTS^{kid-1}, which is visible only after prolonged exposure of the fluorography. *C*, The general ubiquitination status was examined by immunoblotting analysis of 50 μg total cell lysate using mouse anti-ubiquitin antibody. The positions of molecular weight markers, in kilodalton, are labeled on the left of each blot.

FIG. 6. **tTS^{kid-1} could not stabilize IκBα under either basal or TNFα treated condition.** Two million HEK 293 cells were transfected with 4 μg pTet-TS (+tTS^{kid-1}) or mock plasmid (-tTS^{kid-1}) and the transfected cells were splitted in the absence or presence of Doxycycline (Dox) immediately after transfection. The cells were pre-treated with 25 μM MG132 for 3 hr followed by 10ng/ml treatment of TNFα for 30 minutes as indicated before cell extracts were prepared 40

hours after transfection. Fifty μg of total cell lysate was separated by SDS-PAGE and the expression patterns of IκBα were detected by immunoblotting analysis. The positions of molecular weight markers, in kilodalton, are labeled on the left of each blot.

FIG. 7. **Proposed model for the regulation of rtTA by tTS, ubiquitination, and sumoylation.** Dox-doxycycline, rTetR- reverse type tetracycline repressor, TetR[B/E]-chimeric TetR derived from fusion of class B and E tetracycline repressors, VP16- transactivation domain from Herpes Simplex virus, kid-1- transcriptional silencing domain, KRAB, from Kid-1 protein, and TRP, tetracycline regulated promoter. Please see discussion section for details.

Figure 1

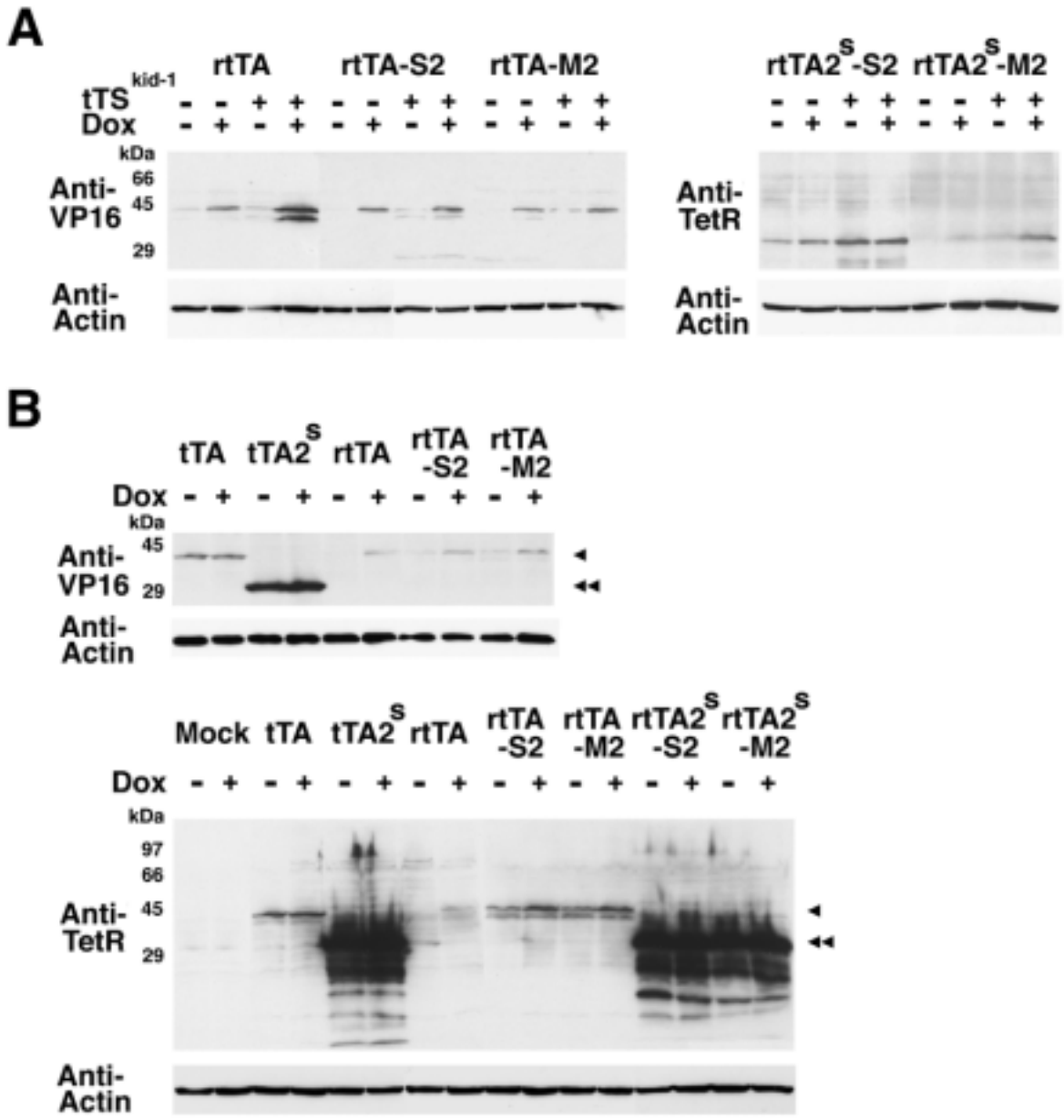
A
rtTA
rtTA-S2
rtTA-M2
rtTA2S-S2
rtTA2S-M2
kid-1
tTS
Dox
kDa
66
45
29
Anti-VP16
Anti-TetR
Anti-Actin
B
tTA
tTA2S
rtTA
rtTA-S2
rtTA-M2
Dox
kDa
45
29
Anti-VP16
Anti-Actin
Mock
tTA
tTA2S
rtTA
rtTA-S2
rtTA-M2
rtTA2S-S2
rtTA2S-M2
Dox
kDa
97
66
45
29
Anti-TetR
Anti-Actin

Figure 2

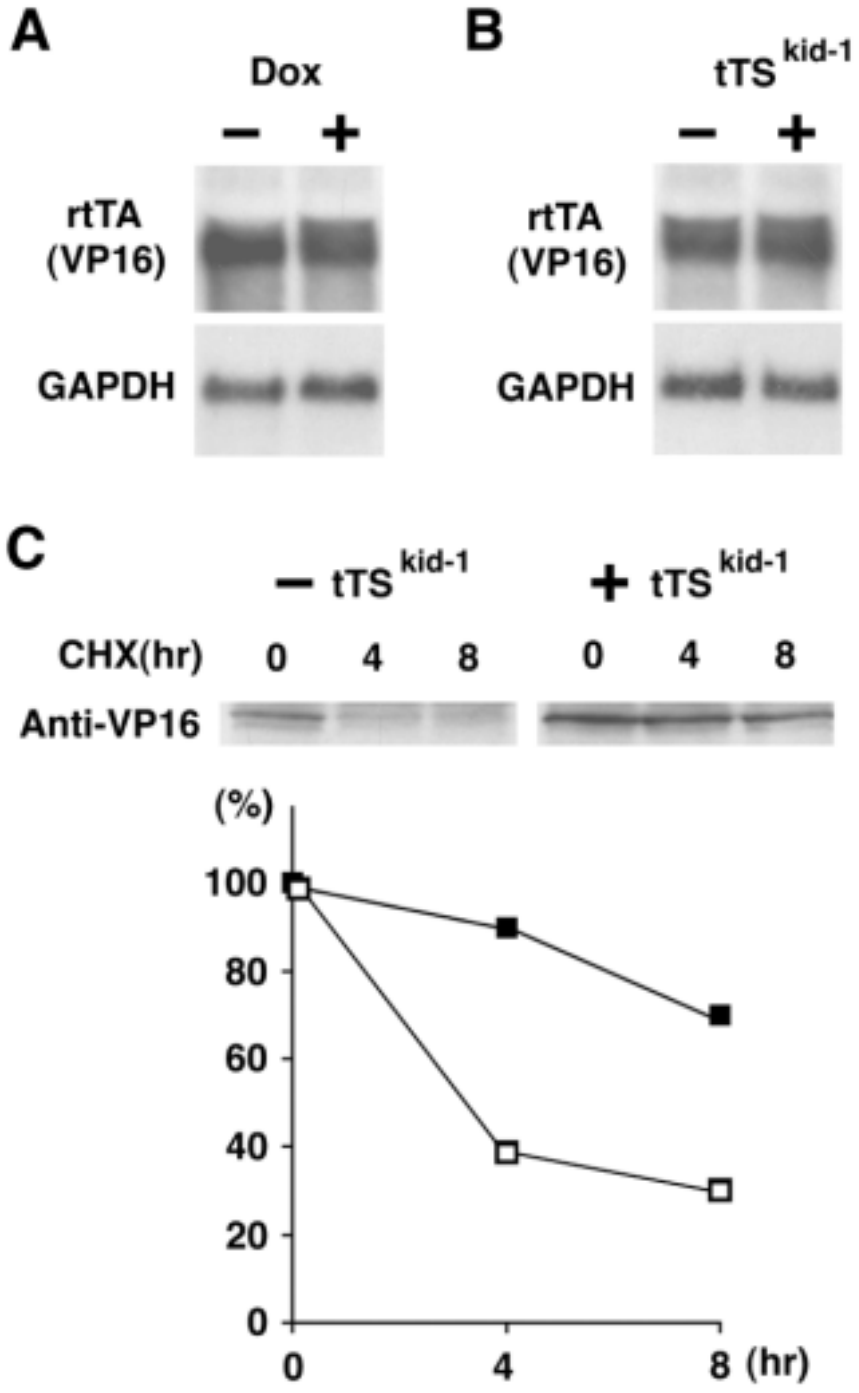
A
Dox
–
+
rtTA
(VP16)
GAPDH
B
tTS kid-1
–
+
rtTA
(VP16)
GAPDH
C
– tTS kid-1
+ tTS kid-1
CHX(hr)
0
4
8
0
4
8
Anti-VP16
(%)
100
80
60
40
20
0
0
4
8 (hr)

Figure 3

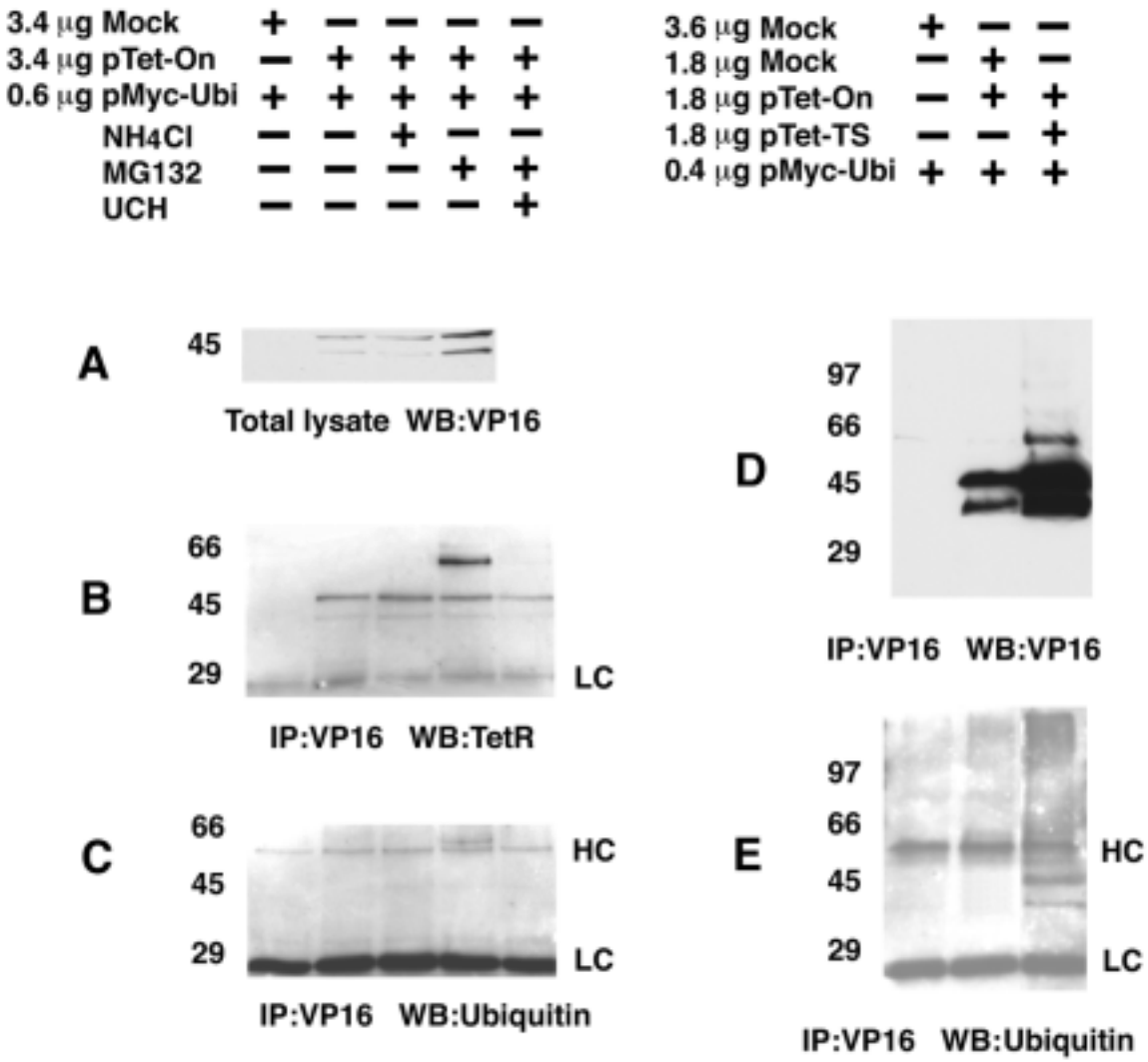
3.4 μg Mock + − − − −
3.4 μg pTet-On − + + + +
0.6 μg pMyc-Ubi + + + + +
NH4Cl − − + − −
MG132 − − − + +
UCH − − − − +
3.6 μg Mock + − −
1.8 μg Mock − + −
1.8 μg pTet-On − + +
1.8 μg pTet-TS − − +
0.4 μg pMyc-Ubi + + +
A
45
Total lysate WB:VP16
B
66
45
29
LC
IP:VP16 WB:TetR
C
66
45
29
HC
LC
IP:VP16 WB:Ubiquitin
D
97
66
45
29
IP:VP16 WB:VP16
E
97
66
45
29
HC
LC
IP:VP16 WB:Ubiquitin

Figure 4

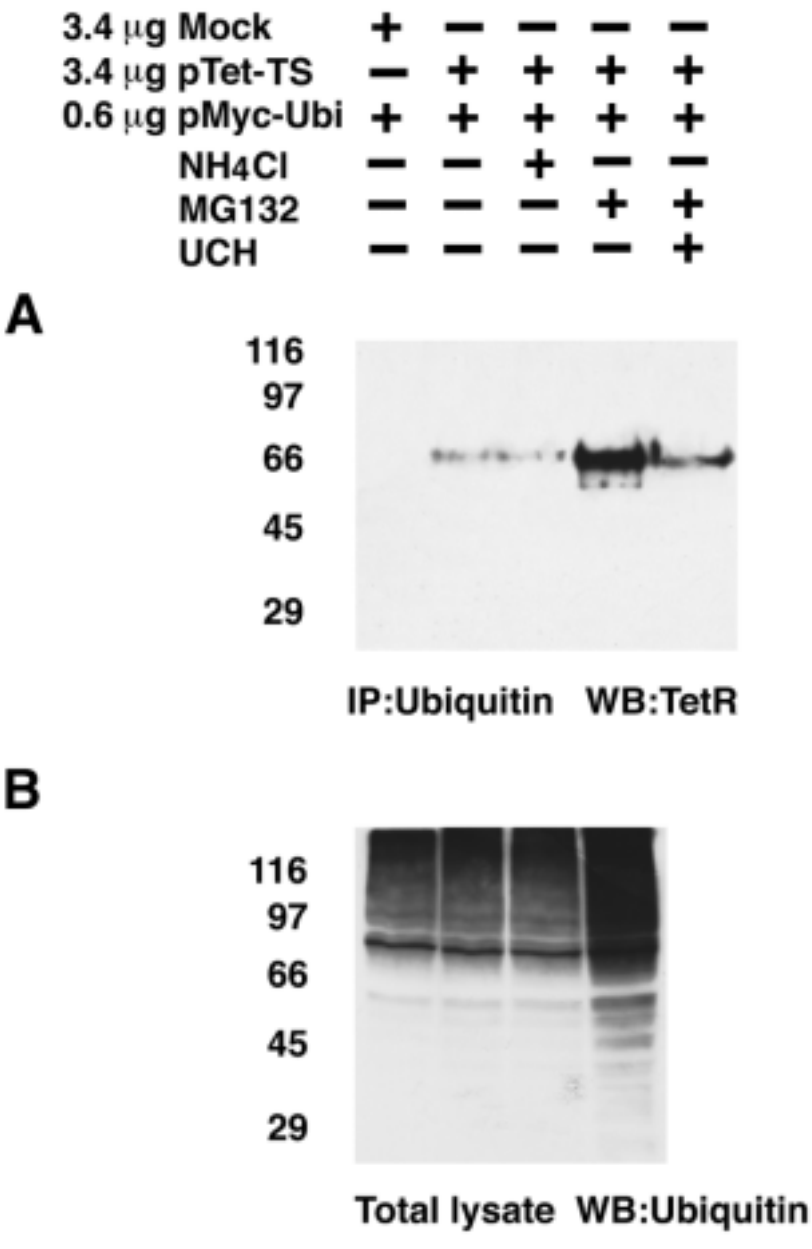
3.4 μg Mock + − − − −
3.4 μg pTet-TS − + + + +
0.6 μg pMyc-Ubi + + + + +
NH4Cl − − + − −
MG132 − − − + +
UCH − − − − +
A
116
97
66
45
29
IP:Ubiquitin WB:TetR
B
116
97
66
45
29
Total lysate WB:Ubiquitin

Figure 5

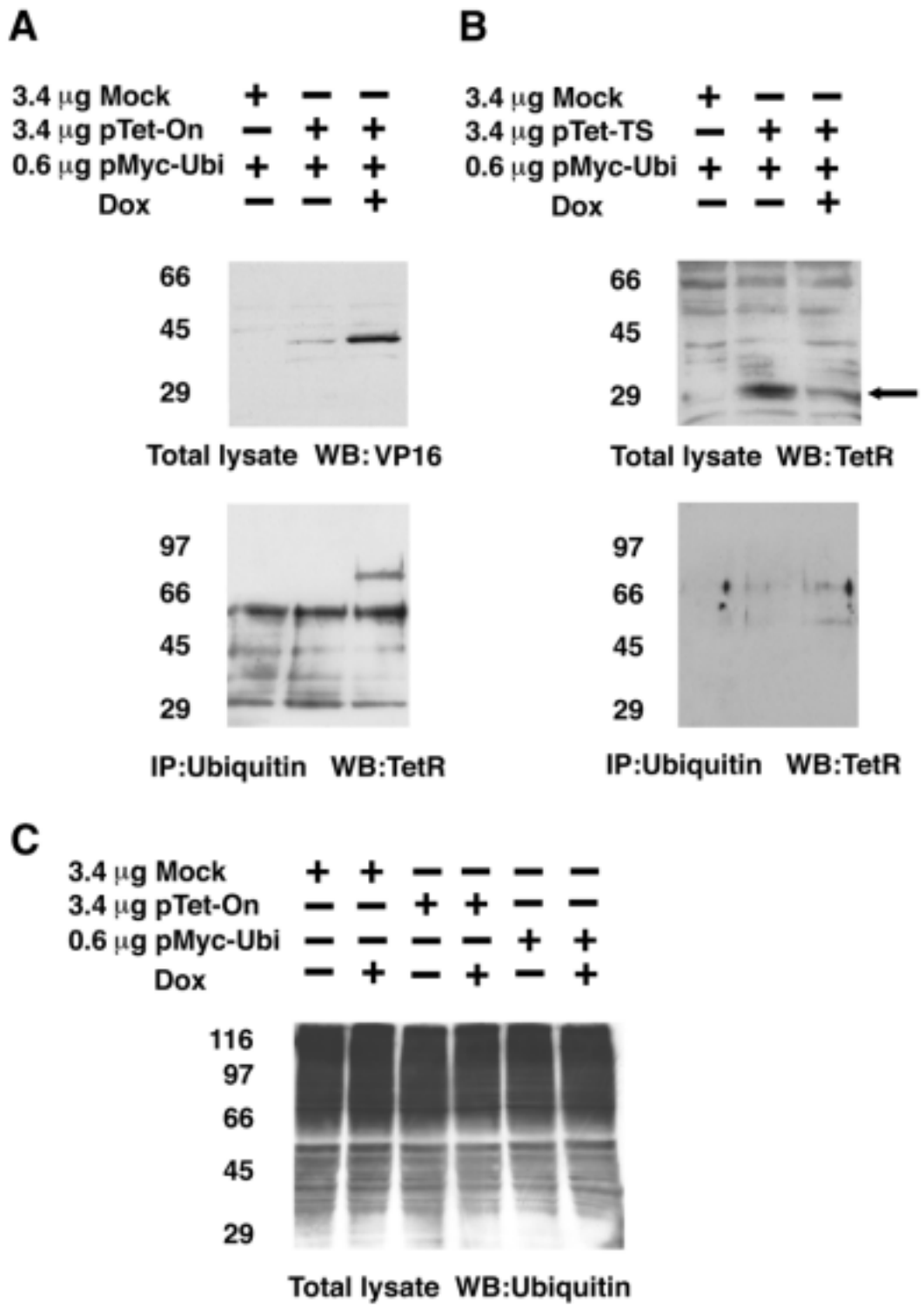
A
3.4 μg Mock + − −
3.4 μg pTet-On − + +
0.6 μg pMyc-Ubi + + +
Dox − − +
66
45
29
Total lysate WB: VP16
97
66
45
29
IP:Ubiquitin WB:TetR
B
3.4 μg Mock + − −
3.4 μg pTet-TS − + +
0.6 μg pMyc-Ubi + + +
Dox − − +
66
45
29
Total lysate WB:TetR
97
66
45
29
IP:Ubiquitin WB:TetR
C
3.4 μg Mock + + − − − −
3.4 μg pTet-On − − + + − −
0.6 μg pMyc-Ubi − − − − + +
Dox − + − + − +
116
97
66
45
29
Total lysate WB:Ubiquitin

Figure 6

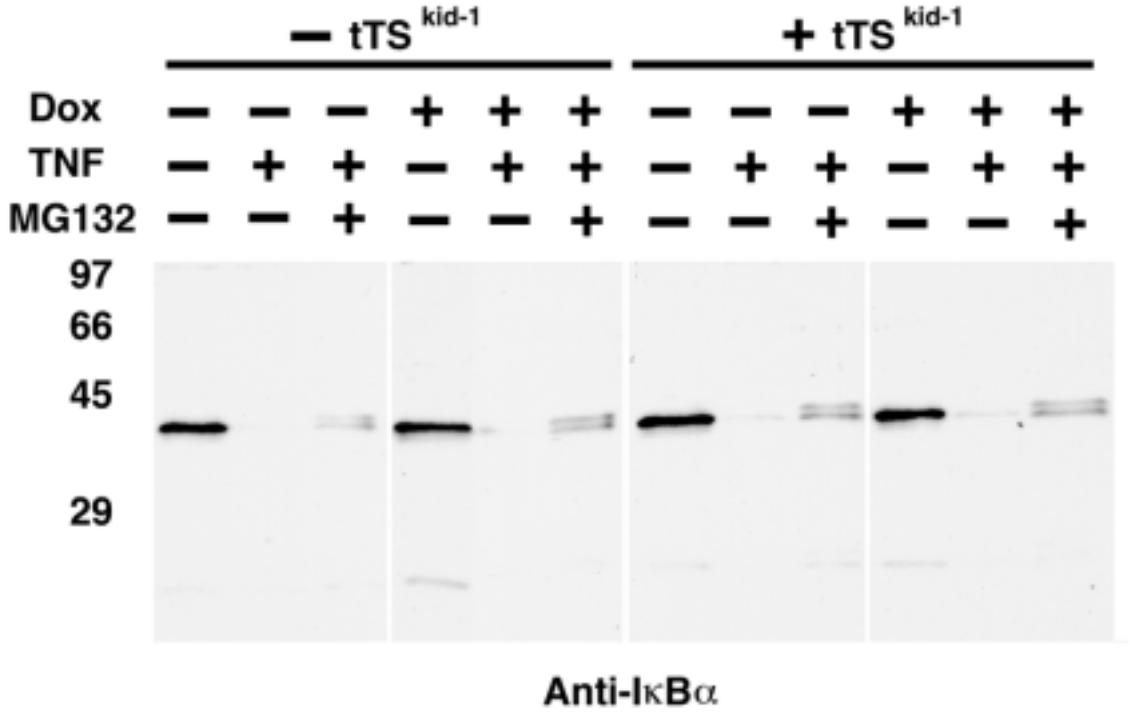

Figure 7

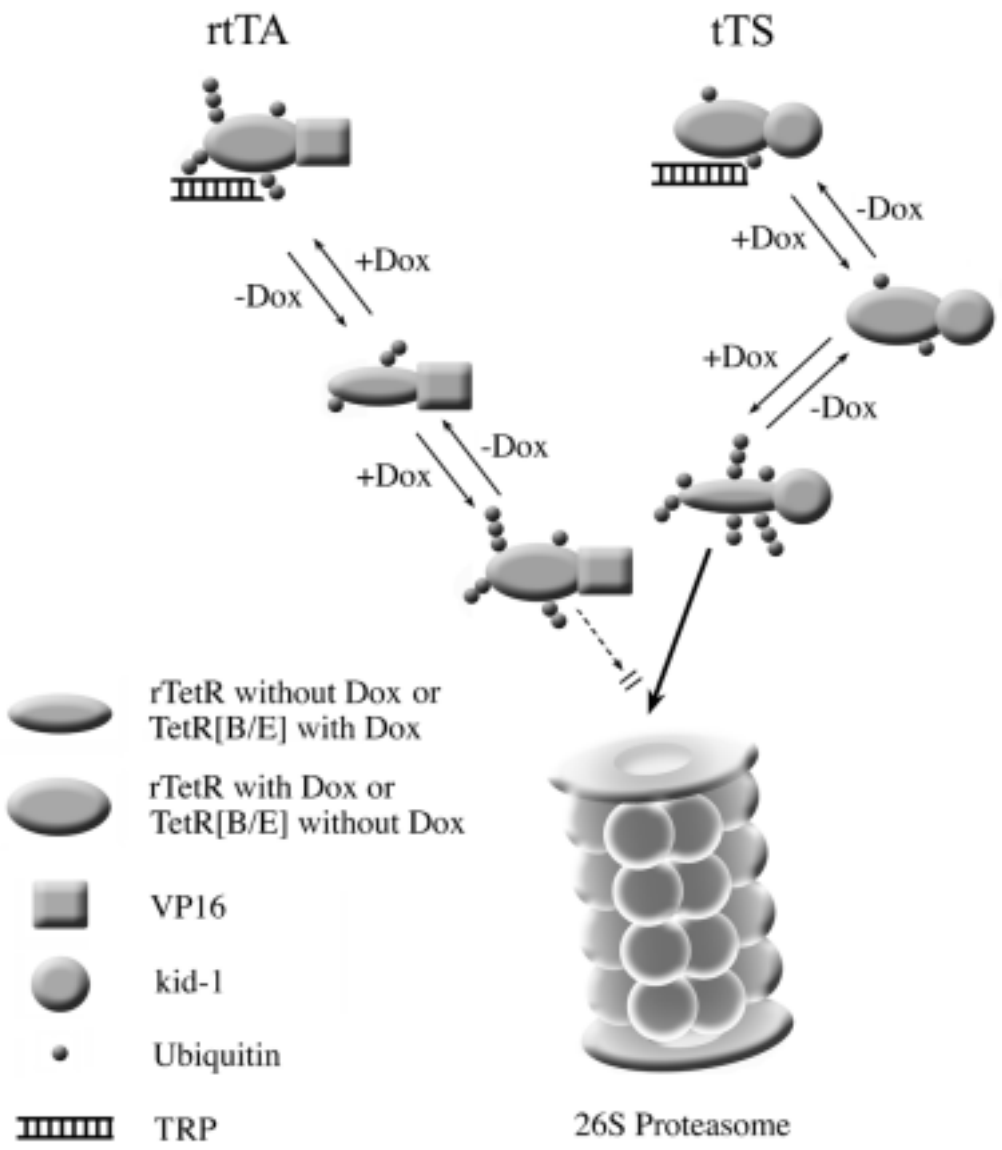
rtTA
tTS
+Dox
-Dox
+Dox
-Dox
+Dox
-Dox
+Dox
-Dox
+Dox
-Dox
rTetR without Dox or
TetR[B/E] with Dox
rTetR with Dox or
TetR[B/E] without Dox
VP16
kid-1
Ubiquitin
TRP
26S Proteasome

Supplementary Figure, Supporting Information

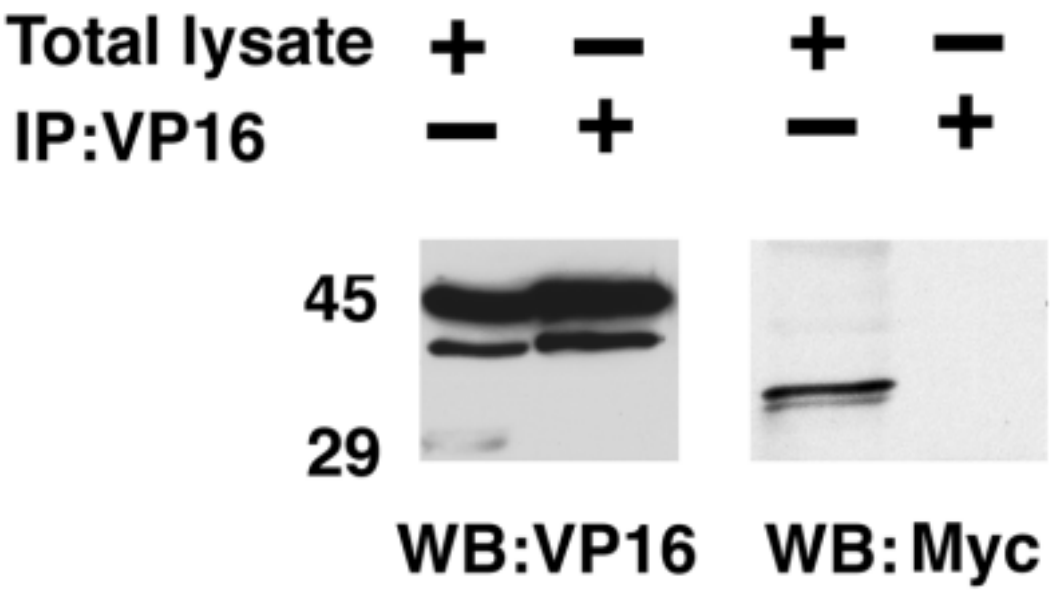

rtTA and myc-epitope tagged tTS^{kid-1} do not dimerize. Two μg of the plasmid expressing rtTA was co-transfected with 2 μg of plasmid expressing myc-epitope tagged tTS^{kid-1} into two million HEK293 cells. Cell extracts were prepared 40 hours after transfection. Fifty μg total cell lysate and immunoprecipitated material from 2 mg lysate by 1 μg mouse anti-VP16 antibody were separated by SDS-PAGE. Two identically processed blots were immunoblotted with rabbit anti-VP16 sera and mouse anti-myc antibody respectively. The positions of molecular weight markers, in kilodalton, are labeled on the left of each blot.